NASA TM X-812

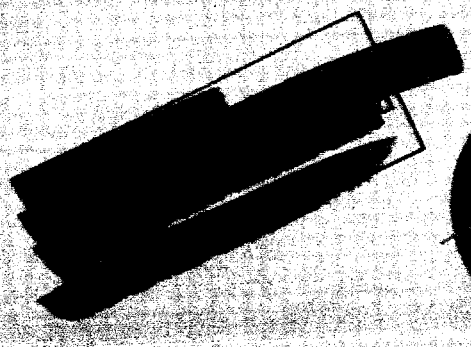

TECHNICAL MEMORANDUM

X-812

STABILITY AND CONTROL CHARACTERISTICS AT MACH NUMBERS OF 1.41 AND 2.20 OF A MULTIMISSION STOL AIRPLANE CONFIGURATION WITH A VARIABLE-SKEW WING

By Gerald V. Foster

Langley Research Center
Langley Station, Hampton, Va.

NATIONAL AERONAUTICS AND SPACE ADMINISTRATION

WASHINGTON

May 1963

TECHNICAL MEMORANDUM X-812

STABILITY AND CONTROL CHARACTERISTICS AT MACH NUMBERS OF 1.41 AND 2.20 OF A MULTIMISSION STOL AIRPLANE CONFIGURATION WITH A VARIABLE-SKEW WING*

By Gerald V. Foster

SUMMARY

An investigation has been made to determine the stability and control characteristics at Mach numbers of 1.41 and 2.20 of a multimission STOL airplane configuration having a skewed wing fixed at skew angles of 0°, 30°, 60°, and 90°. The results indicated a nonlinear variation of longitudinal stability with wing skew angle such that the stability level decreased with increasing skew angle to 60° and then increased again. Increasing the wing skew angle resulted in a decrease in minimum drag but had little effect on maximum lift-drag ratio because of an increase in drag due to lift. The yawing-moment variation with sideslip angle was generally linear at wing skew angles of either 0° or 90° whereas at intermediate skew angles a nonlinear variation occurred. Unlike either 0° or 90° skew angles, intermediate skew angles introduced both yaw and rolling moments at an angle of sideslip of 0°.

INTRODUCTION

The National Aeronautics and Space Administration is currently conducting studies to develop a multimission airplane configuration capable of short-field operation combined with maximum possible range at low altitude, and the ability to accelerate to supersonic speeds for short durations. In order to achieve the efficiency required throughout the speed range, efforts of this study have been directed largely toward configurations incorporating variable sweep of the wing outboard panels. Some of the available results of this study are presented in references 1 to 15. In addition to the variable-sweep wing panel concept, references 14 and 15 also include a limited amount of results obtained at transonic and supersonic speeds for an airplane configuration having a trapezoidal wing which could be set at various skew angles by rotating the entire wing about a pivot at the 50-percent wing root chord. The purpose of the present investigation was to determine the aerodynamic characteristics of a configuration having

*Title, Unclassified.

a skewed wing design similar to that of references 14 and 15, but differing markedly in fuselage, inlet, and tail design. The results of the investigation presented herein show the effects of wing skew angle, horizontal-tail deflection, and various components on the longitudinal and lateral aerodynamic characteristics of the configuration for Mach numbers of 1.41 and 2.20.

SYMBOLS

The data have been reduced to coefficient form based on the wing at a skew angle of 0°. The moments are referred to a point corresponding to the quarter-chord point of the mean geometric chord. The results are referred to the body-axis system except for the lift and drag coefficients which are referred to the wing-axis system. The symbols used are as follows:

b	wing span, in.
C_D	drag coefficient, Drag/qS
C_L	lift coefficient, Lift/qS
C_{L_α}	lift-curve slope
C_l	rolling-moment coefficient, Rolling moment/qSb
C_{l_β}	lateral stability derivative
C_m	pitching-moment coefficient, Pitching moment/qS$\bar{c}$
$\partial C_m/\partial C_L$	longitudinal stability derivative
$C_{m,0}$	pitching-moment coefficient at $C_L = 0$
C_{m_δ}	horizontal-tail effectiveness
C_n	yawing-moment coefficient, Yawing moment/qSb
C_{n_β}	directional stability derivative
C_Y	side-force coefficient, Side force/qS
C_{Y_β}	side-force derivative
$\bar{c}$	mean geometric chord, in.
L/D	lift-drag ratio

M	Mach number
q	free-stream dynamic pressure, lb/sq ft
S	wing area, sq ft
α	angle of attack, deg
β	angle of sideslip, deg
δ_h	deflection angle of horizontal tail, positive when trailing edge is down, deg
Λ	angle of sweep of 50-percent chord line, deg

Subscripts:

max	maximum
min	minimum
L	left
R	right

Model components:

B	body
W	wing
H	horizontal tail
V	vertical tail

MODEL AND APPARATUS

Details of the model are presented in figure 1. A photograph of the model is presented in figure 2. Some additional geometric details of various components of the model are presented in table I. The body of the model was representative of current high-speed fighter configurations having a high-fineness-ratio forebody and twin ramp-type inlets connected to separate exits at the base of the body. The wing was trapezoidal in planform and had a 5-percent-thick airfoil section having a flat lower surface. Except for the region of leading edge the airfoil profile was defined by coordinates of NACA 64A010 airfoil. The leading-edge radius of NACA 64A005 airfoil section was fitted to this airfoil section. The wing was attached to the top of the body in a manner which permitted rotation of the wing about the 50-percent root-chord point. Wing skew angles

tested were 0°, 30° (left tip forward), -60°, and -90° (right tip forward). The horizontal tail was an all-movable surface having symmetrical NACA 64A series sections which were 4.35 percent thick at the root and 2 percent thick at the tip. These panels were attached to the upper part of the body with a fixed dihedral angle of -20° with respect to the wing-chord plane. The vertical tail was composed of two elements which were attached to the body at an angle of 30° with respect to the vertical.

TESTS, CORRECTIONS, AND ACCURACY

The tests were conducted in the Langley 4- by 4-foot supersonic pressure tunnel at Mach numbers of 1.41 and 2.20. The conditions of the tests were as follows:

Mach number	1.41	2.20
Stagnation pressure, lb/sq in. abs	12	12
Stagnation temperature, °F	100	110
Reynolds number based on $\bar{c}$	1.75×10^6	1.32×10^6

The stagnation dewpoint was maintained sufficiently low (-25° F or less) so that no significant condensation effects were encountered in the test section. Flow transition was fixed by the use of 1/8-inch-wide band of No. 80 grit carborundum located at 5-percent local chord of wing and tail surfaces, a strip around the body 1 inch behind the nose of the body, and 3/8 inch behind the outboard leading edge of the outboard lip of the inlet. The angles of attack and sideslip were corrected for deflection of the balance and sting under load. Pressure at the base and in the balance chamber were measured relative to free-stream static pressure to determine the influence on the drag of the model. The internal drag was determined from the change in momentum from free-stream conditions to the measured conditions at the duct exit. The net external drag was obtained by subtracting the base drag, balance chamber drag, and internal drag from the total drag measurements. The drag corrections for the complete model (BWVH) are as follows:

	Drag correction for -	
	M = 1.41	M = 2.20
Balance chamber	0.0015	0.0004
Base drag	0.0019	0.0015
Internal drag	0.0021	0.0062

The estimated accuracy of the measured quantities is as follows:

	Accuracy for -	
	M = 1.41	M = 2.20
C_L	±0.0056	0.0077
C_D	0.0004	0.0006
C_m	0.0022	0.0030
C_n	0.0007	0.0010
C_l	0.0002	0.0003
C_Y	0.0056	0.0077
α, β, δ_h, deg	0.1	0.1

PRESENTATION OF RESULTS

The results of the investigation are presented in the following figures:

Longitudinal Characteristics

Lateral Characteristics

RESULTS AND DISCUSSION

Longitudinal Characteristics

The results indicate a large nonlinear variation in longitudinal stability with wing skew angle for both Mach numbers (fig. 9) such that the stability level decreases with increasing skew angle to 60° and then increases again. The level of longitudinal stability for all skew angles however is relatively high. Varying the wing skew angle from 0° to 90° resulted in a progressive decrease in minimum drag and lift-curve slope. (See fig. 9.) The drag due to lift increases with skew angle, however, and the resulting maximum values of L/D are essentially invariant with wing skew angle. Relatively low values of maximum L/D (about 4) were obtained because of the high ratio of volume to wing area. Deflection of the horizontal tail provided linear pitch effectiveness C_{m_δ} at both Mach numbers (figs. 4 and 7) that was essentially unaffected by wing skew angle. Because of the generally high stability level and the negative $C_{m,0}$ large deflections of the tail are required for trimming with attendant decreases in L/D.

Lateral Characteristics

The results indicating the effect of change in wing skew angle on the lateral aerodynamic characteristics are presented in figures 10 and 13. A summary of these results is presented in figure 16. It should be pointed out that in considering the effects of wing skew angle the results obtained with negative wing skew angles and positive sideslip angles should be compared with results obtained with positive skew angles and negative sideslip angles. In general, the yawing moments of the configuration with the wing at a skew angle of either 0° or 90° varied linearly with β through the angle-of-attack range, whereas at intermediate skew angles a nonlinear variation of yawing moment with β occurs with increasing angle of attack. (See figs. 10 and 13.) Unlike either 0° or 90° skew angles, intermediate skew angles introduced both yaw and rolling moments at $\beta = 0^\circ$.

There is a general tendency for the directional stability to decrease with increasing α for the 0° and intermediate wing-skew positions with large regions of instability occurring above about $\alpha = 8^\circ$ at $M = 2.20$. (See fig. 16.) For a skew angle of 90°, however, C_{n_β} initially decreases with increasing α and then increases again so that at $\alpha = 13^\circ$ and $M = 2.20$ the configuration is directionally stable. The configuration maintained a positive dihedral effect $\left(-C_{l_\beta}\right)$ throughout the angle-of-attack range for all wing skew angles tested. Differentially deflecting the horizontal tail provides positive lateral control and a favorable yawing moment throughout the angle-of-attack range with the wing at either 0° or 90° skew angle. (See fig. 17.)

CONCLUDING REMARKS

The results of an investigation of the stability and control characteristics of a multimission STOL airplane configuration with skewed wings at supersonic speeds indicated a nonlinear variation of longitudinal stability with wing skew angle such that the stability level decreased with increasing skew angles to 60° and then increased again. Increasing the wing skew angle resulted in a decrease in minimum drag but had little effect on maximum lift-drag ratio because of an increase in drag due to lift. The yawing-moment variation with sideslip angle was generally linear at wing skew angles of either 0° or 90° whereas at intermediate skew angles a nonlinear variation occurred. Unlike either 0° or 90° skew angles, intermediate skew angles introduced both yaw and rolling moments at an angle of sideslip of 0°.

Langley Research Center,
National Aeronautics and Space Administration,
Langley Station, Hampton, Va., February 21, 1963.

REFERENCES

1. Alford, William J., Jr., and Henderson, William P.: An Exploratory Investigation of the Low-Speed Aerodynamic Characteristics of Variable-Wing-Sweep Airplane Configurations. NASA TM X-142, 1959.

2. Alford, William J., Jr., Luoma, Arvo A., and Henderson, William P.: Wind-Tunnel Studies at Subsonic and Transonic Speeds of a Multiple-Mission Variable-Wing-Sweep Airplane Configuration. NASA TM X-206, 1959.

3. Spearman, M. Leroy, and Foster, Gerald V.: Stability and Control Characteristics at a Mach Number of 2.01 of a Variable-Wing-Sweep Configuration With Outboard Wing Panels Swept Back 75°. NASA TM X-32, 1959.

4. Spearman, M. Leroy, and Foster, Gerald V.: Effects of Various Modifications on the Supersonic Stability Characteristics of a Variable-Wing-Sweep Configuration at a Mach Number of 2.01. NASA TM X-260, 1960.

5. Foster, Gerald V.: Stability and Control Characteristics at Mach Numbers of 2.50, 3.00, and 3.71 of a Variable-Wing-Sweep Configuration With Outboard Wing Panels Swept Back 75°. NASA TM X-267, 1960.

6. Foster, Gerald V.: Effects of Spoiler-Slot-Deflector Control on the Aerodynamic Characteristics at a Mach Number of 2.01 of a Variable-Wing-Sweep Configuration With the Outer Wing Panels Swept Back 75°. NASA TM X-273, 1960.

7. Spencer, Bernard, Jr.: Stability and Control Characteristics at Low Subsonic Speeds of an Airplane Configuration Having Two Types of Variable-Sweep Wings. NASA TM X-303, 1960.

8. Bielat, Ralph P., Robins, A. Warner, and Alford, William J., Jr.: The Transonic Aerodynamic Characteristics of Two Variable-Sweep Airplane Configurations Capable of Low-Level Supersonic Attack. NASA TM X-304, 1960.

9. Spearman, M. Leroy, and Robinson, Ross B.: Stability and Control Characteristics at a Mach Number of 2.01 of a Variable-Sweep Airplane Configuration Capable of Low-Level Supersonic Attack – Outer Wing Swept 75°. NASA TM X-310, 1960.

10. Foster, Gerald V., and Morris, Odell A.: Aerodynamic Characteristics in Pitch at a Mach Number of 1.97 of Two Variable-Wing-Sweep V/STOL Configurations With Outboard Wing Panels Swept Back 75°. NASA TM X-322, 1960.

11. Luoma, Arvo A., and Alford, William J., Jr.: Performance, Stability, and Control Characteristics at Transonic Speeds of Three V/STOL Airplane Configurations With Wings of Variable Sweep. NASA TM X-321, 1960.

12. Foster, Gerald V., and Morris, Odell A.: Stability and Control Characteristics at a Mach Number of 1.97 of an Airplane Configuration Having Two Types of Variable-Sweep Wings. NASA TM X-323, 1960.

13. Foster, Gerald V. and Morris, Odell A.: Static Longitudinal and Lateral Aerodynamic Characteristics at a Mach Number of 2.20 of a Variable-Wing-Sweep STOL Configuration. NASA TM X-329, 1960.

14. Morris, Odell A., and Foster, Gerald V.: Static Longitudinal and Lateral Aerodynamic Characteristics at a Mach Number of 2.20 of a V/STOL Configuration With a Variable-Sweep Wing and With a Skewed Wing Design. NASA TM X-521, 1961.

15. Luoma, Arvo A.: Longitudinal Aerodynamic Characteristics at Transonic Speeds of Two V/STOL Airplane Configurations With Skewed and Variable-Sweep Wings. NASA TM X-527, 1961.

TABLE I.- GEOMETRIC CHARACTERISTICS OF MODEL

Wing (skew angle of 0°):

Area, sq ft	1.000
Span, in.	22.50
Mean geometric chord, in.	7.20
Aspect ratio	3.535
Taper ratio	0.257
Sweep of 50-percent chord line, deg	0
Dihedral, deg	0
Twist, deg	0
Airfoil section	Modified upper half of NACA 64A010
Root chord, in.	9.20
Tip chord, in.	2.36

Horizontal tail:

Area, sq ft	0.226
Span, in.	13.42
Taper ratio	0.339
Sweep of leading edge, deg	32
Sweep of trailing edge, deg	15
Root airfoil section	64A004.35
Tip airfoil section	64A002
Root chord, in.	5.75
Tip chord, in.	1.95
Dihedral (from horizontal), deg	-20

Vertical tail:

Area (total), sq ft	0.212
Span, in.	3.71
Taper ratio	0.248
Sweep of leading edge, deg	45
Sweep of trailing edge, deg	0
Dihedral (from vertical), deg	30
Root airfoil section	64A004
Tip airfoil section	64A002
Root chord, in.	5.70
Tip chord, in.	1.415

Body:

Length, in.	42.60
Balance chamber area, sq ft	0.0218
Base rim area, sq ft	0.0158

[redacted]

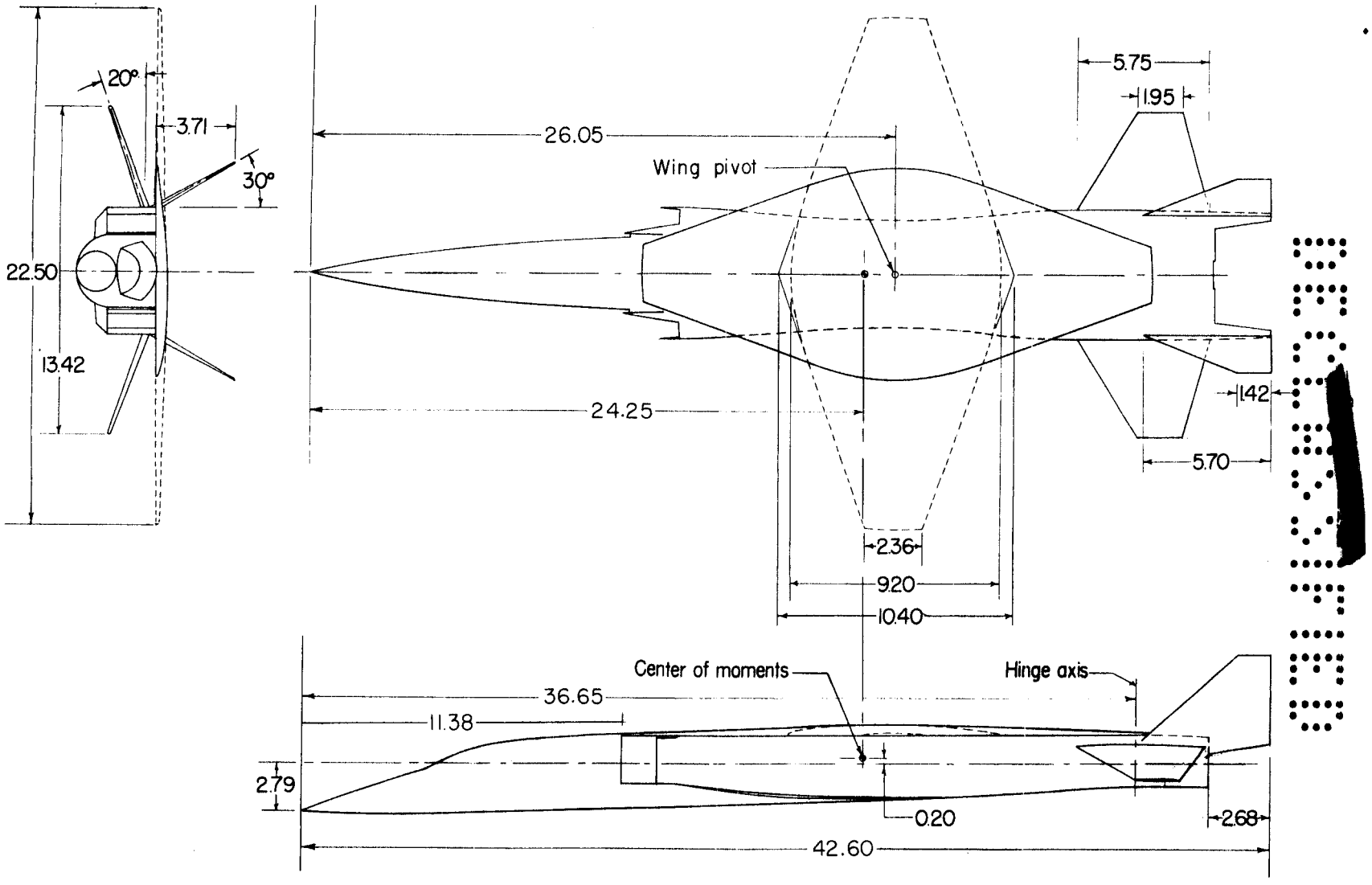

Figure 1.- Details of model. All dimensions are in inches unless otherwise noted.

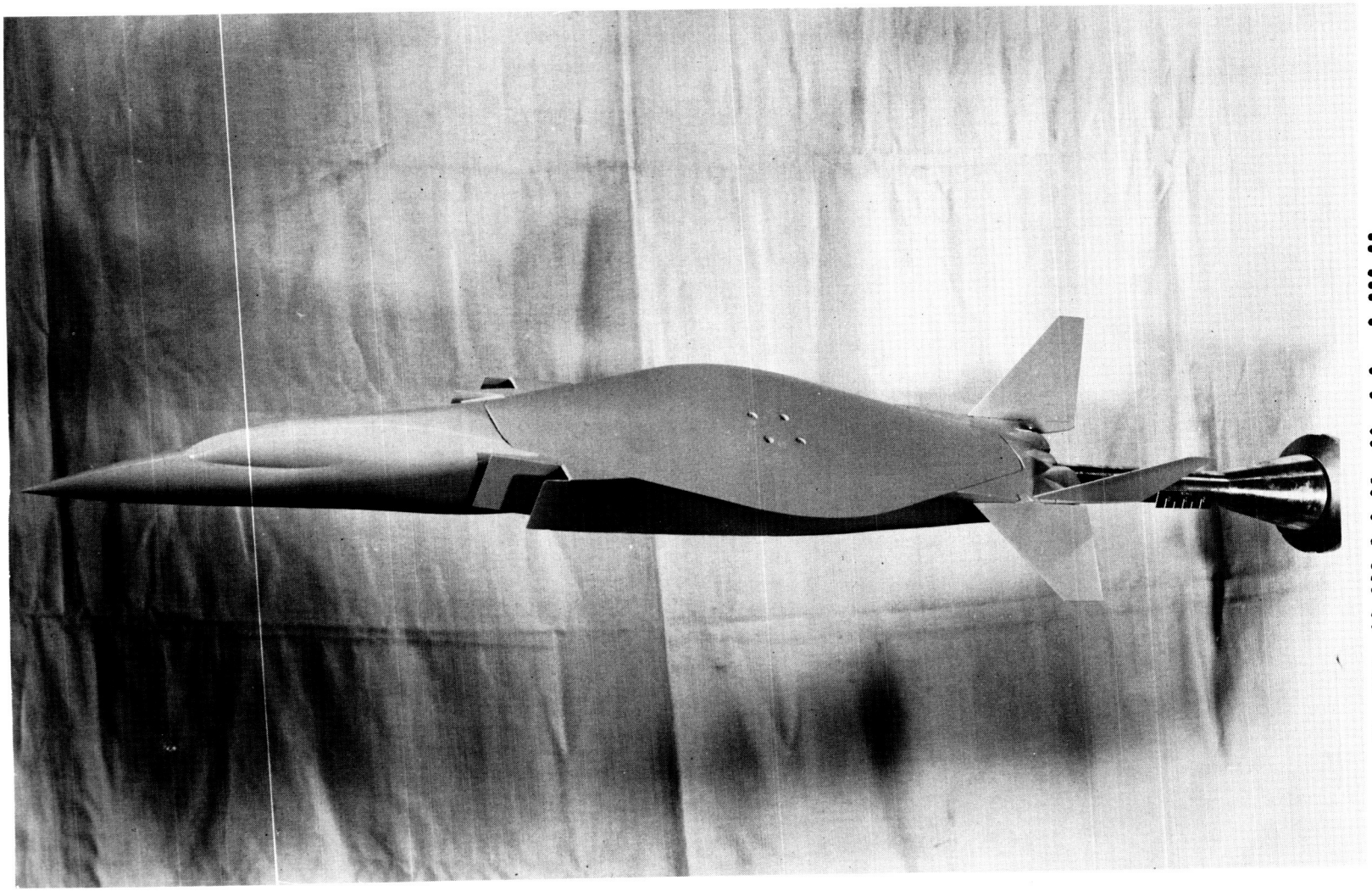

Figure 2.- Photograph of a model with wing skew of 90°.

L-60-6859

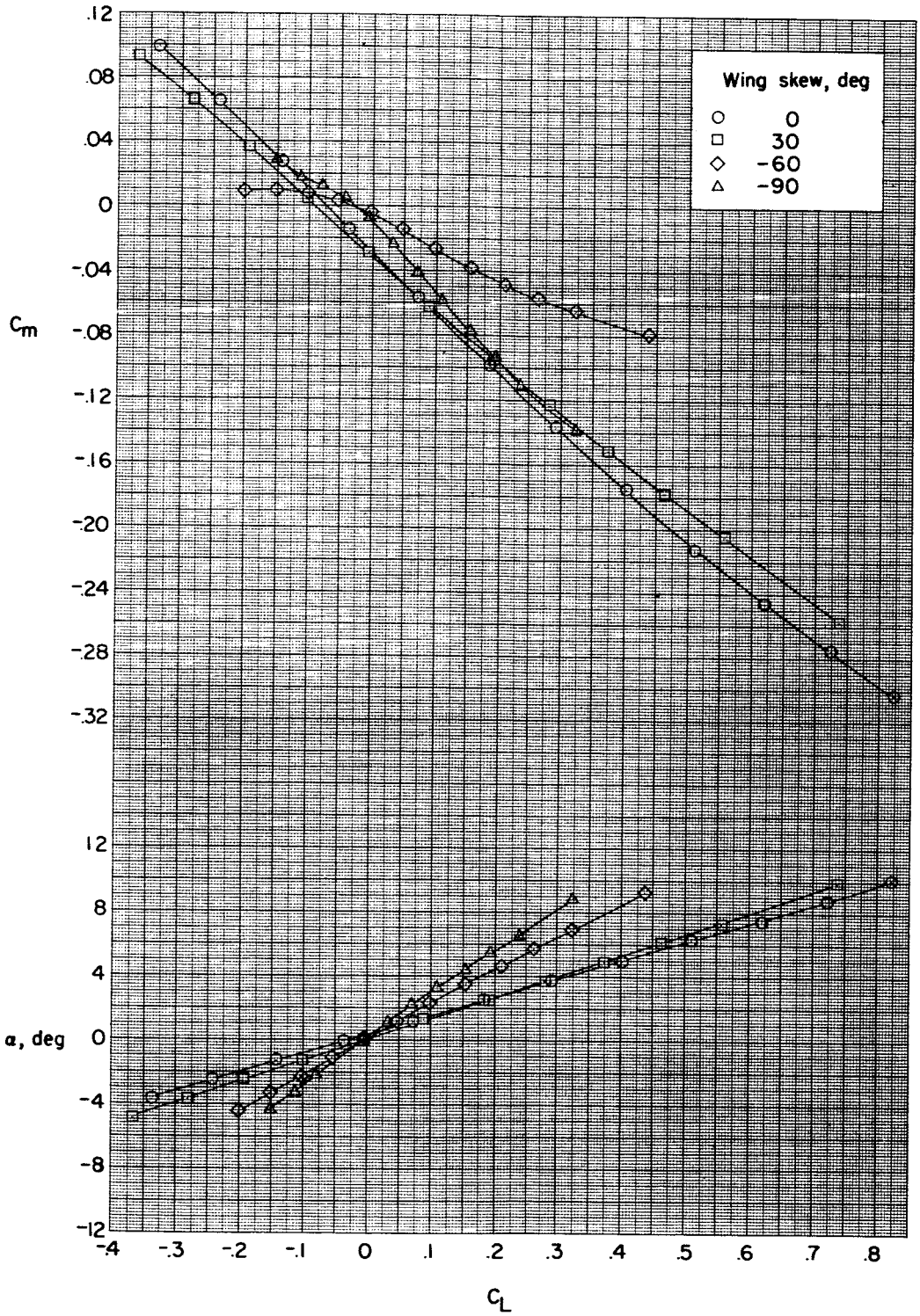

Figure 3.- Effect of change of wing skew angle on the longitudinal aerodynamic characteristics of the complete configuration. $\delta_h = 0^o$; M = 1.41.

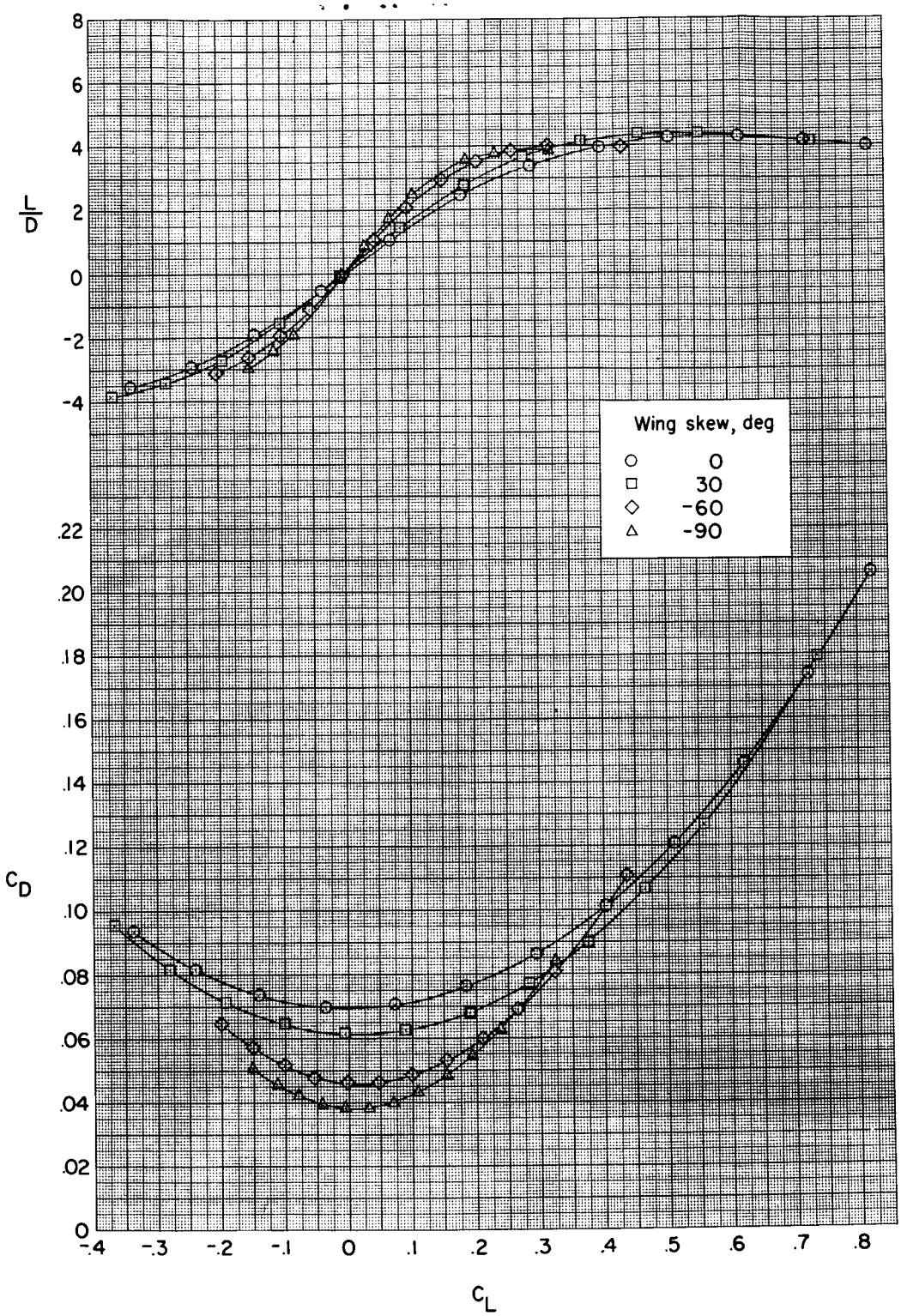

Figure 3.- Concluded.

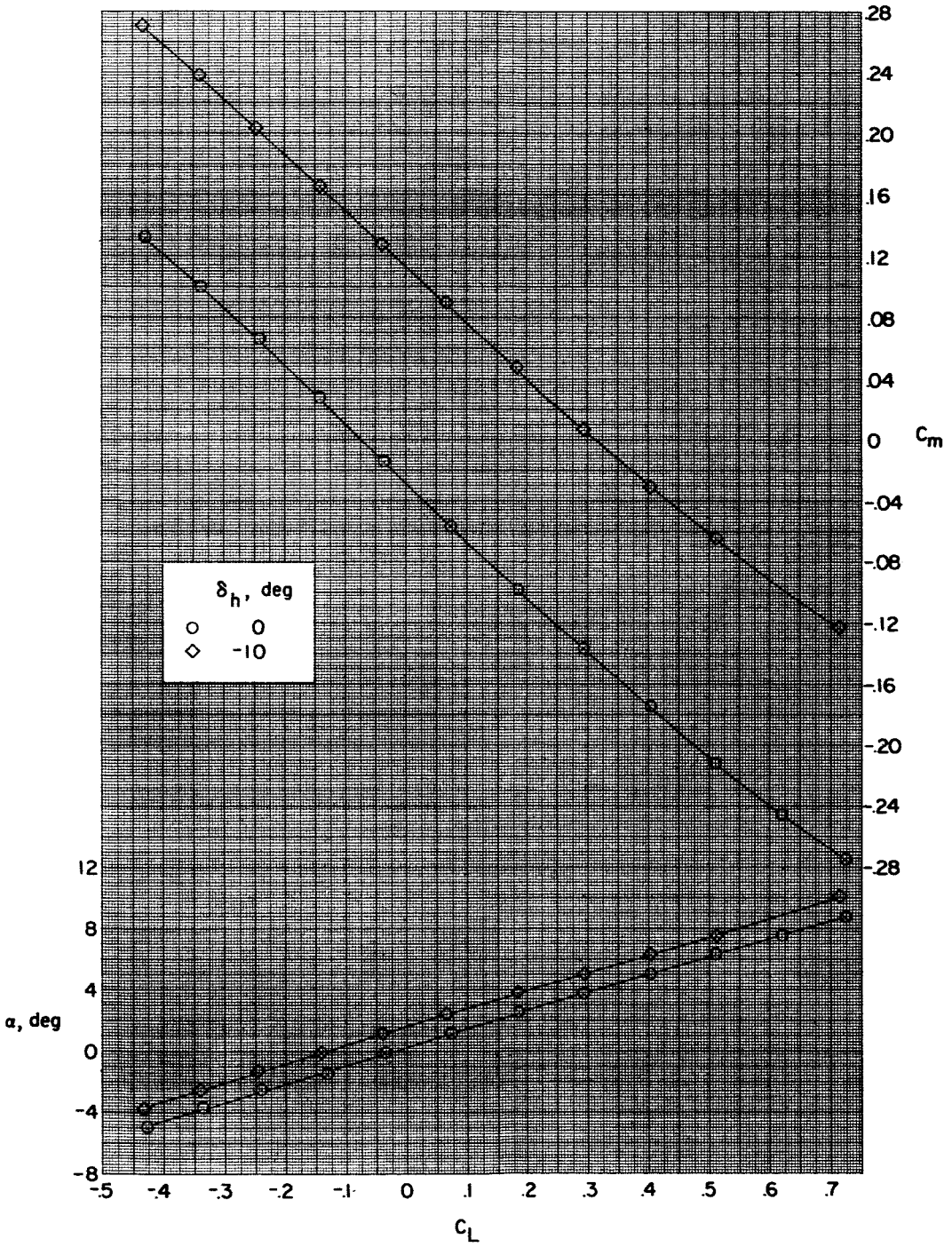

(a) Wing skew, 0°.

Figure 4.- Effect of horizontal-tail deflection on the aerodynamic characteristics in pitch for the complete configuration. M = 1.41.

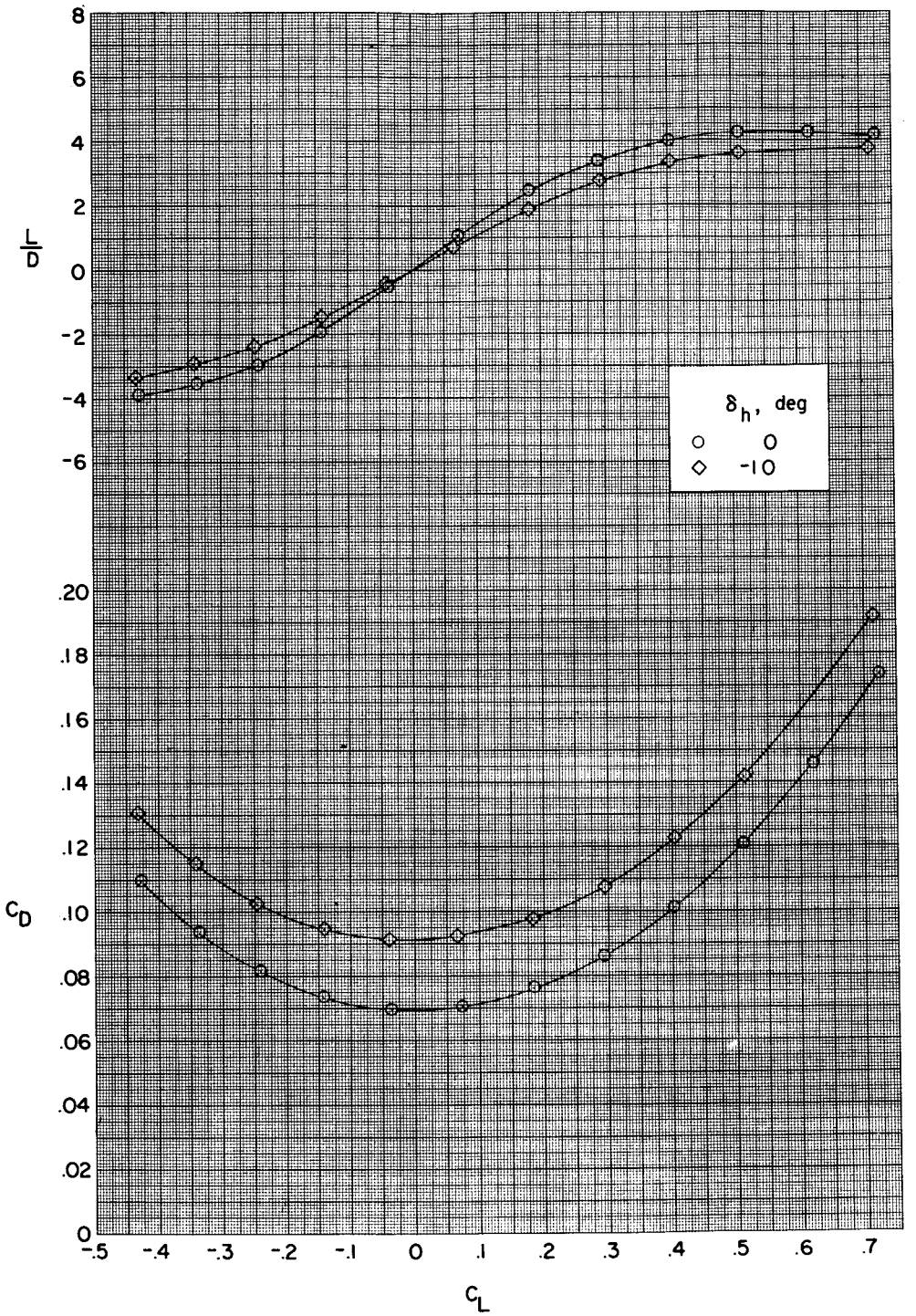

(a) Wing skew, 0°. Concluded.

Figure 4.- Continued.

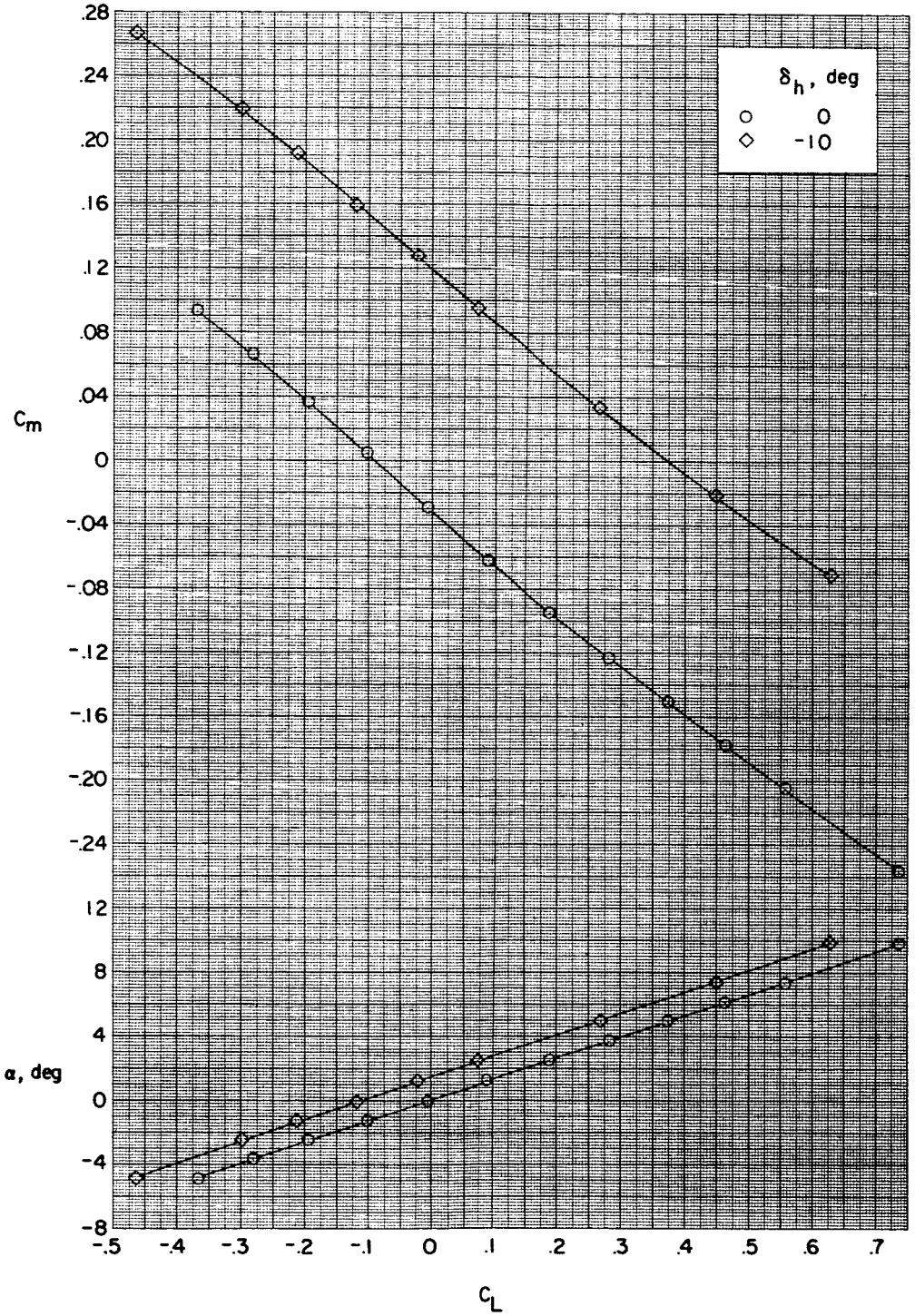

(b) Wing skew, 30°.

Figure 4.- Continued.

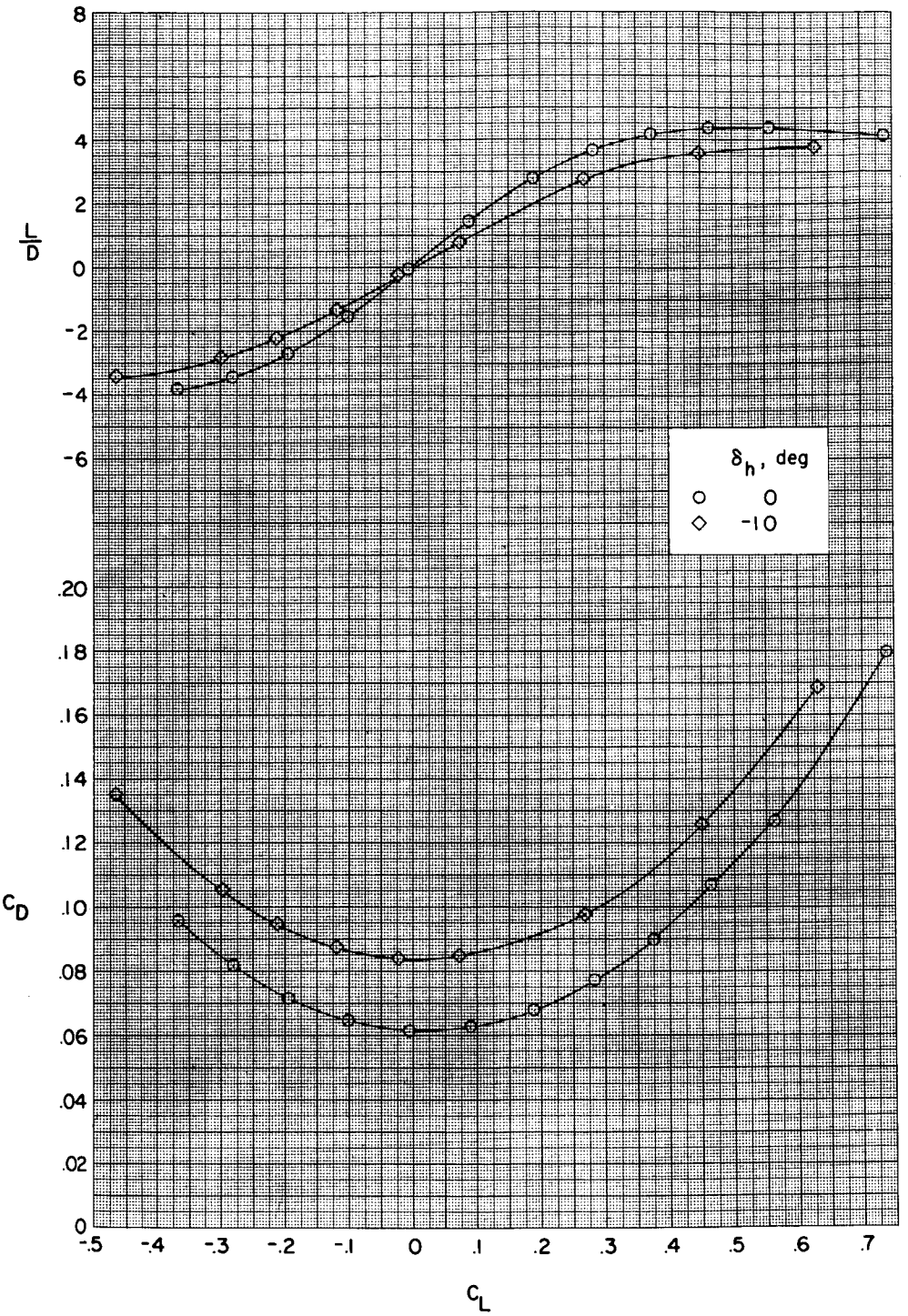

(b) Wing skew, 30°. Concluded.

Figure 4.- Continued.

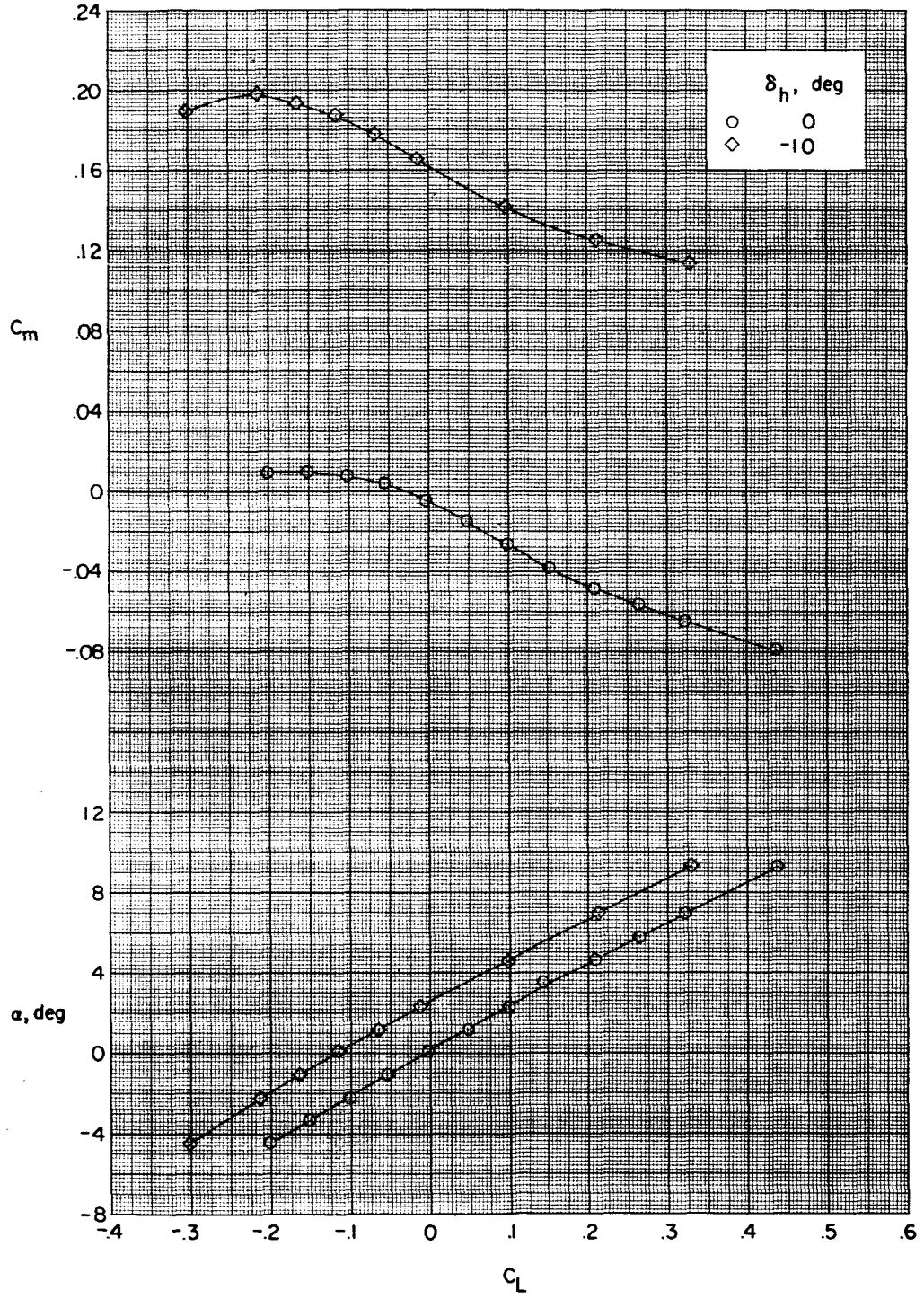

(c) Wing skew, -60°.

Figure 4.- Continued.

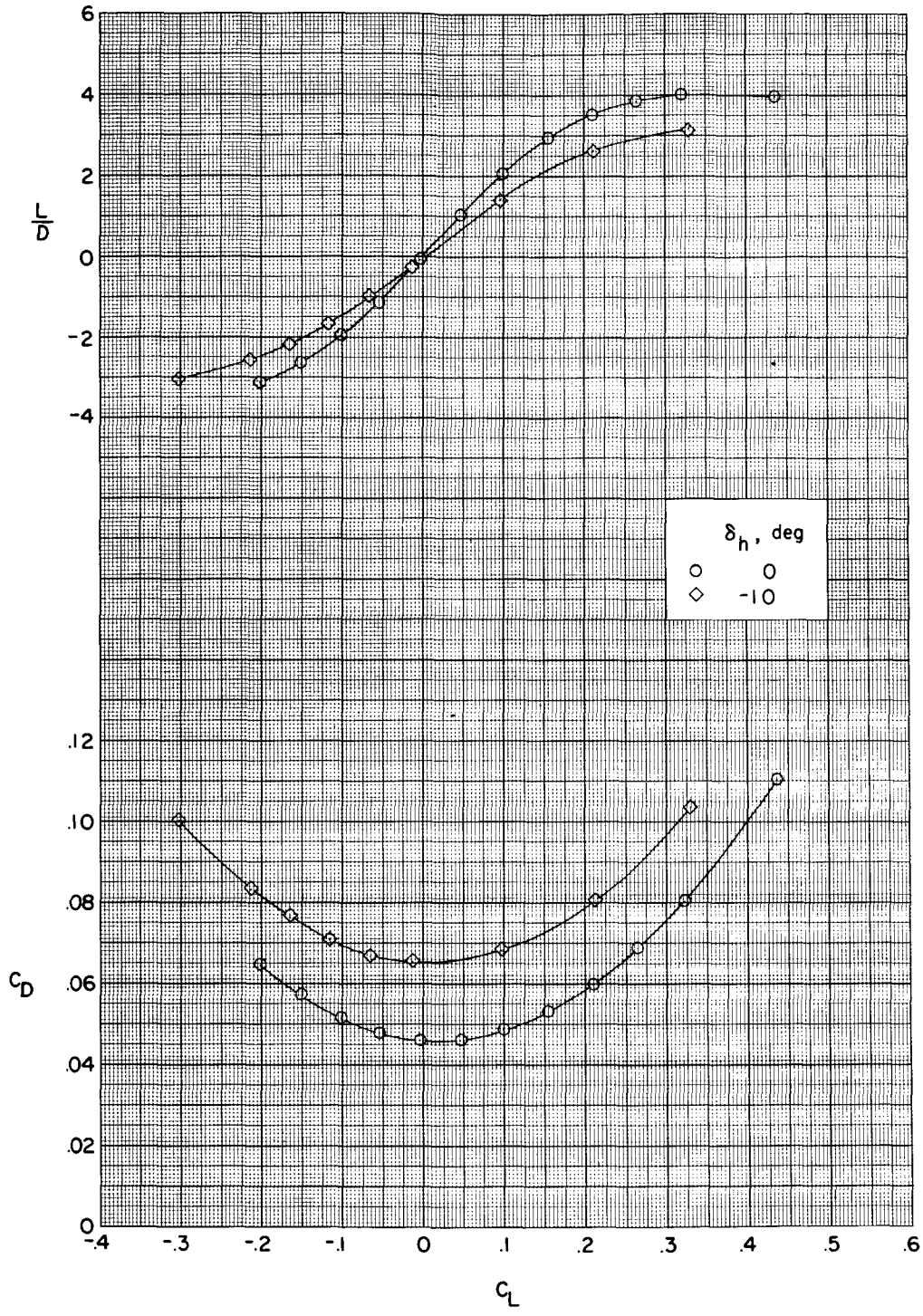

(c) Wing skew, -60°. Concluded.

Figure 4.- Continued.

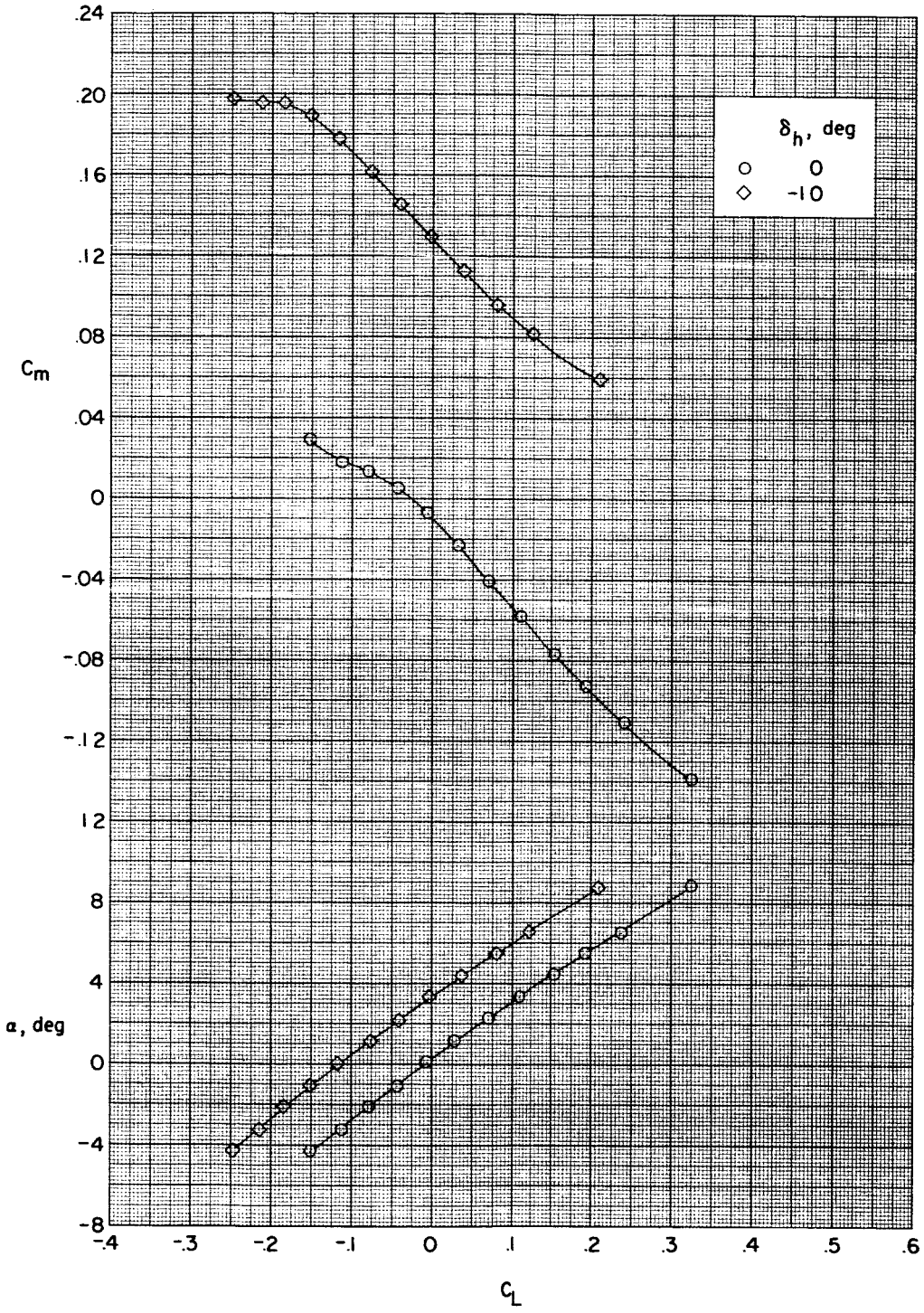

(d) Wing skew, -90°.

Figure 4.- Continued.

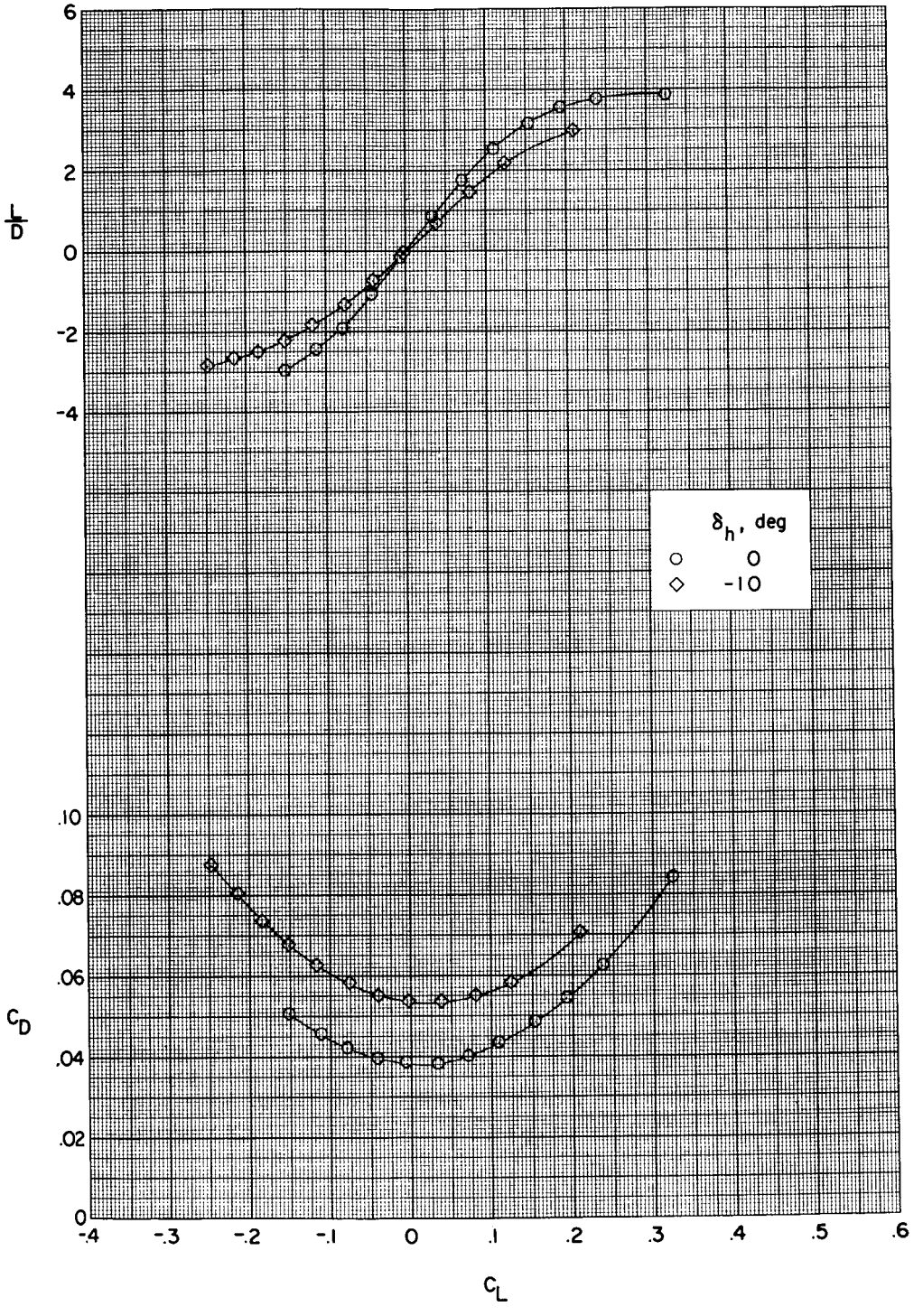

(d) Wing skew, -90°. Concluded.

Figure 4.- Concluded.

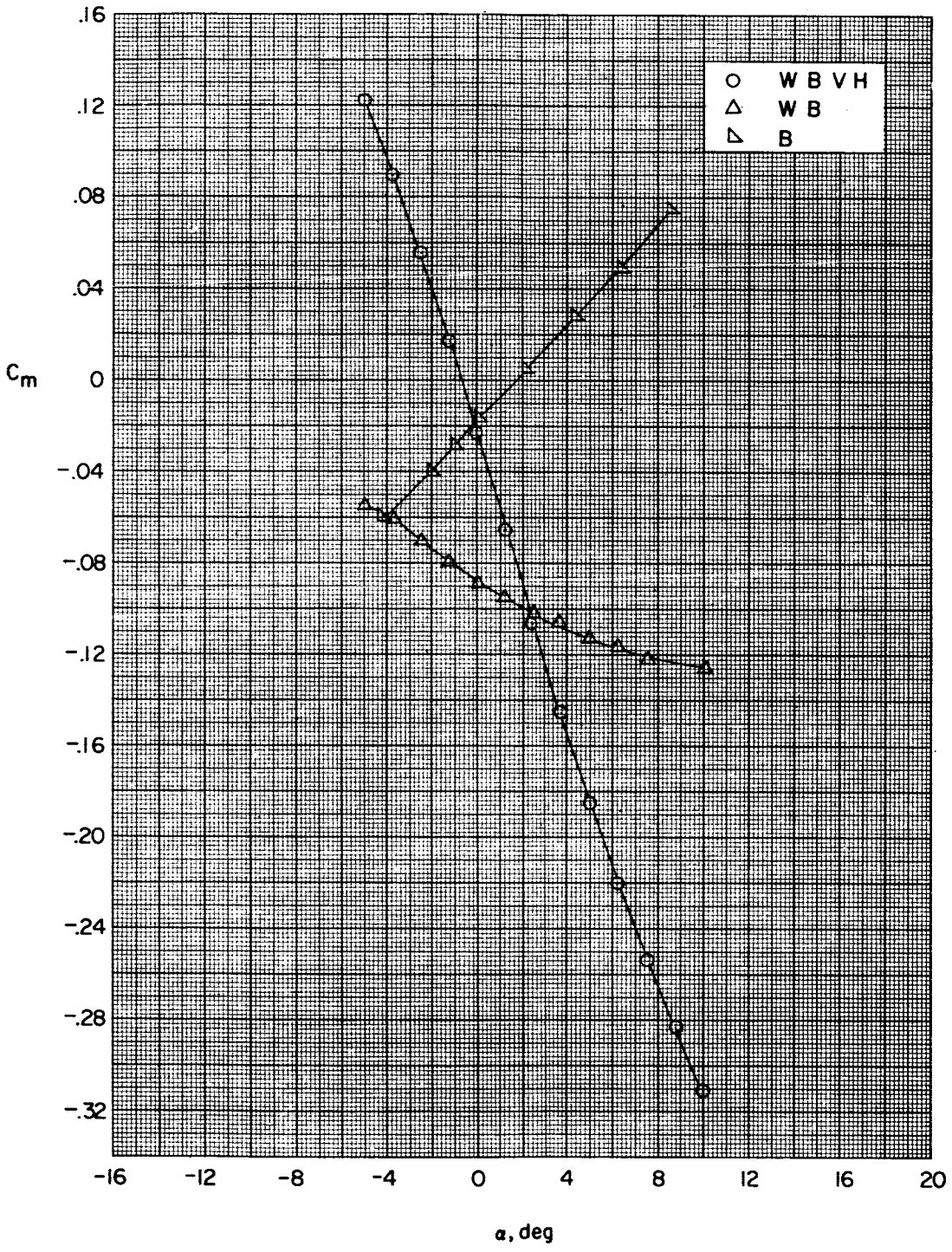

(a) Wing skew, 0°.

Figure 5.- Effects of various components on the longitudinal aerodynamic characteristics of the model. M = 1.41.

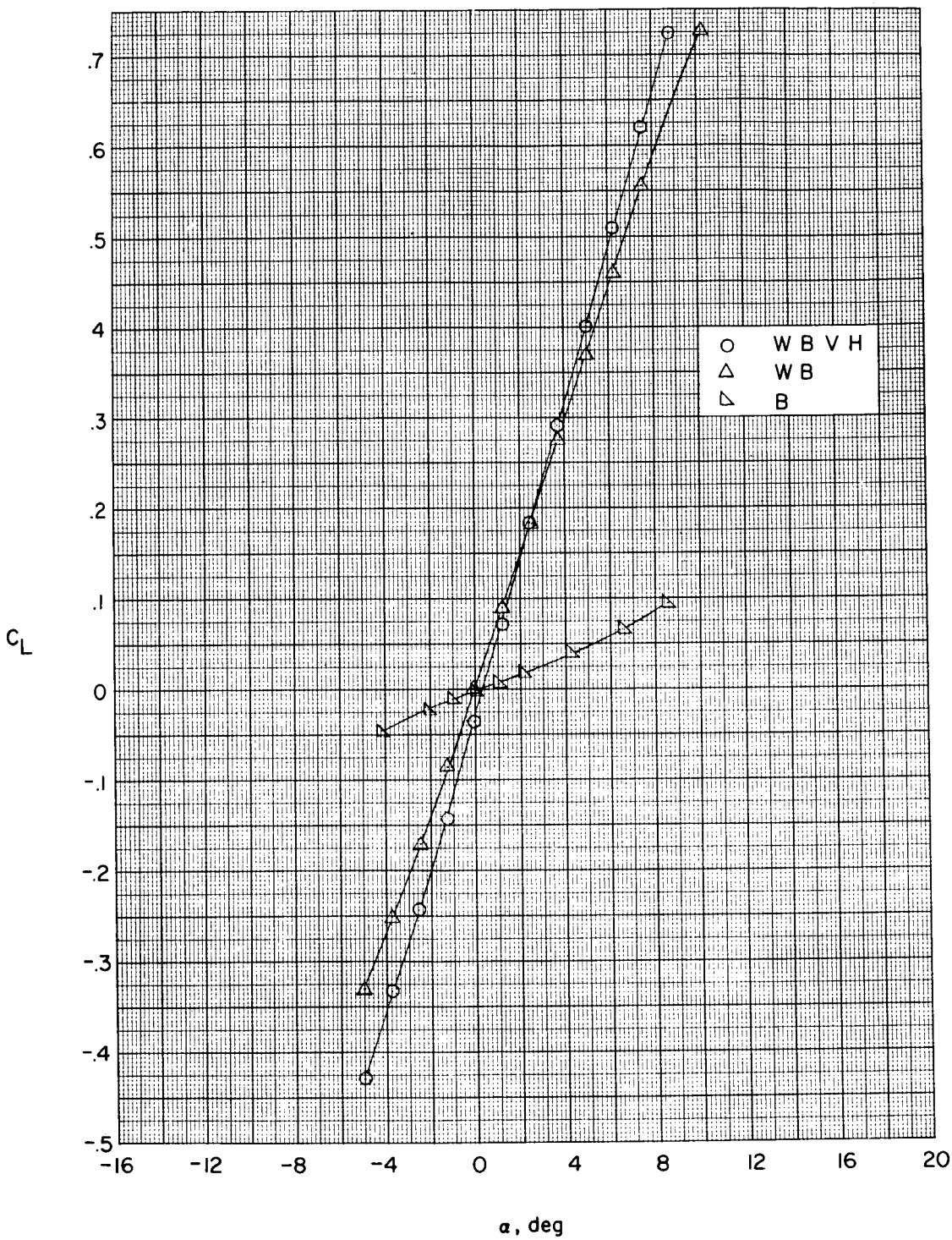

(a) Wing skew, 0°. Continued.

Figure 5.- Continued.

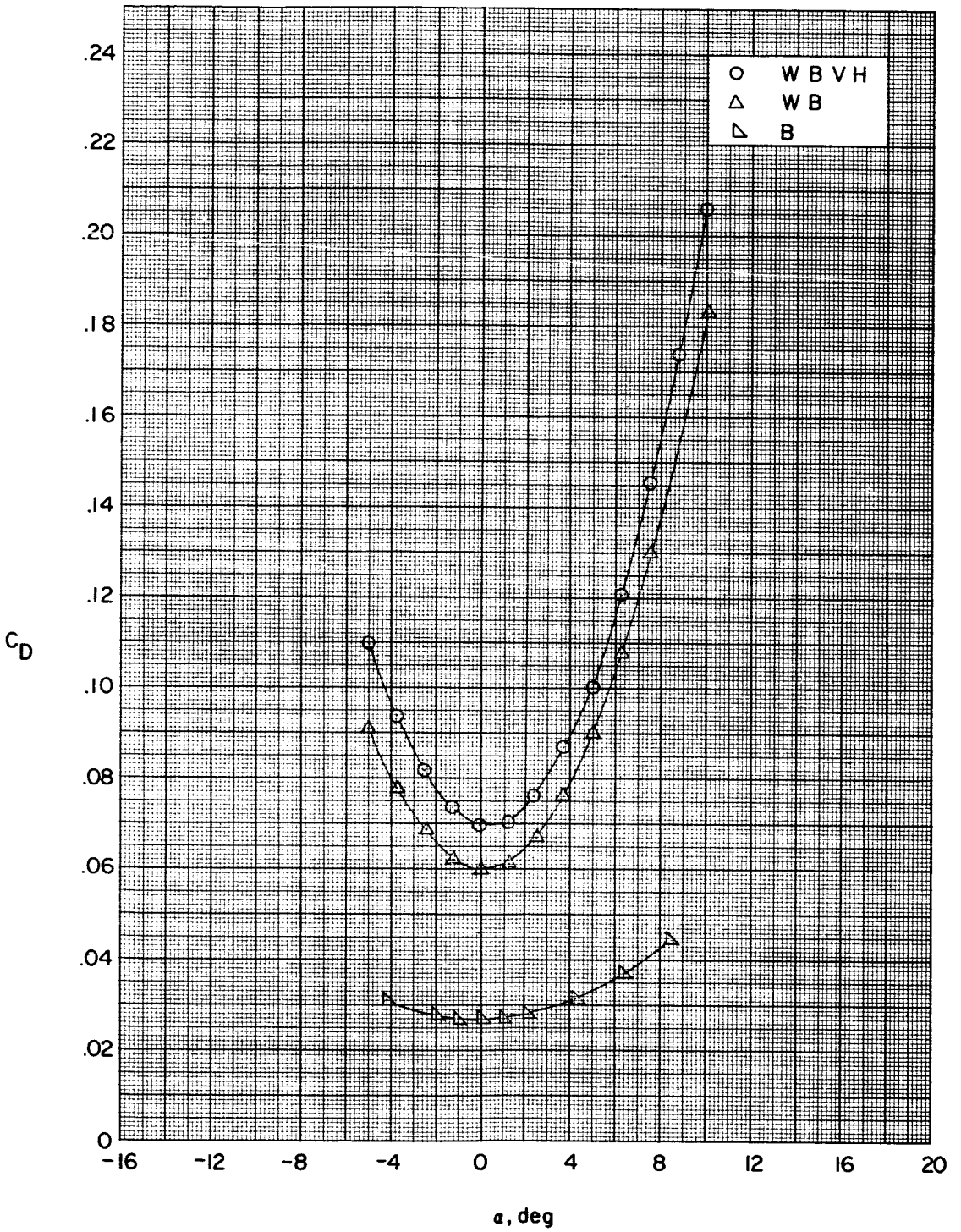

(a) Wing skew, 0°. Concluded.

Figure 5.- Continued.

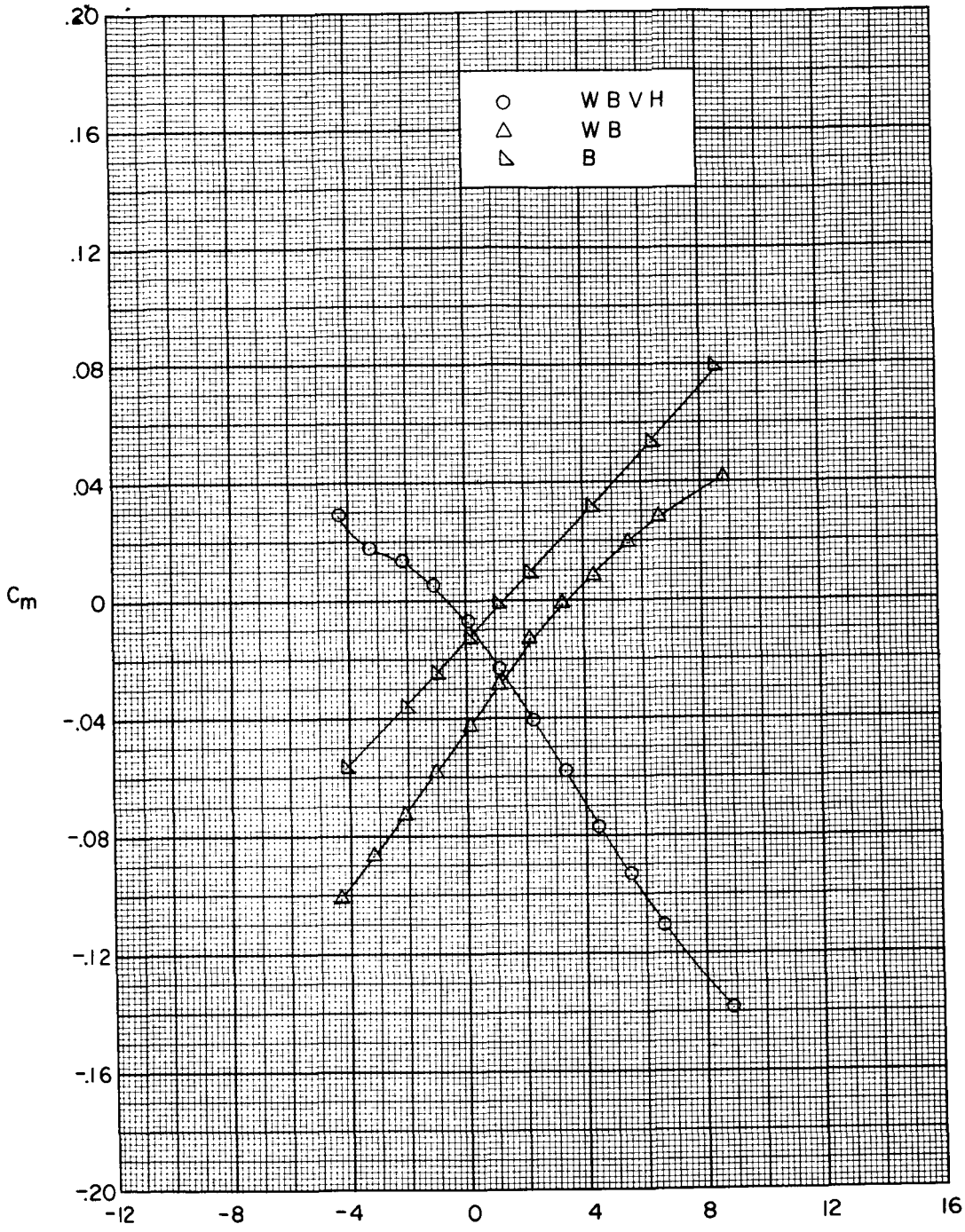

(b) Wing skew, -90°.

Figure 5.- Continued.

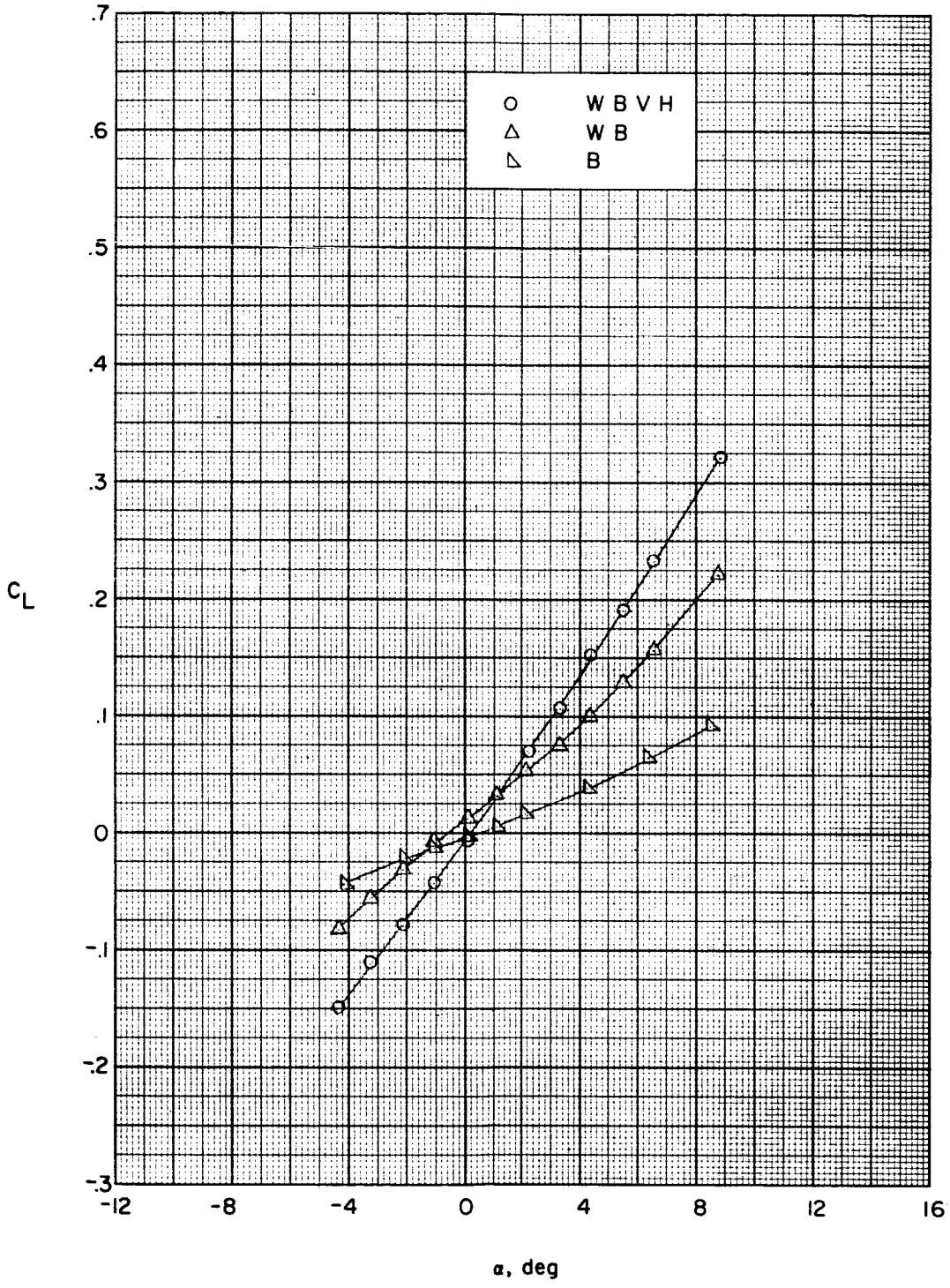

(b) Wing skew, -90°. Continued.

Figure 5.- Continued.

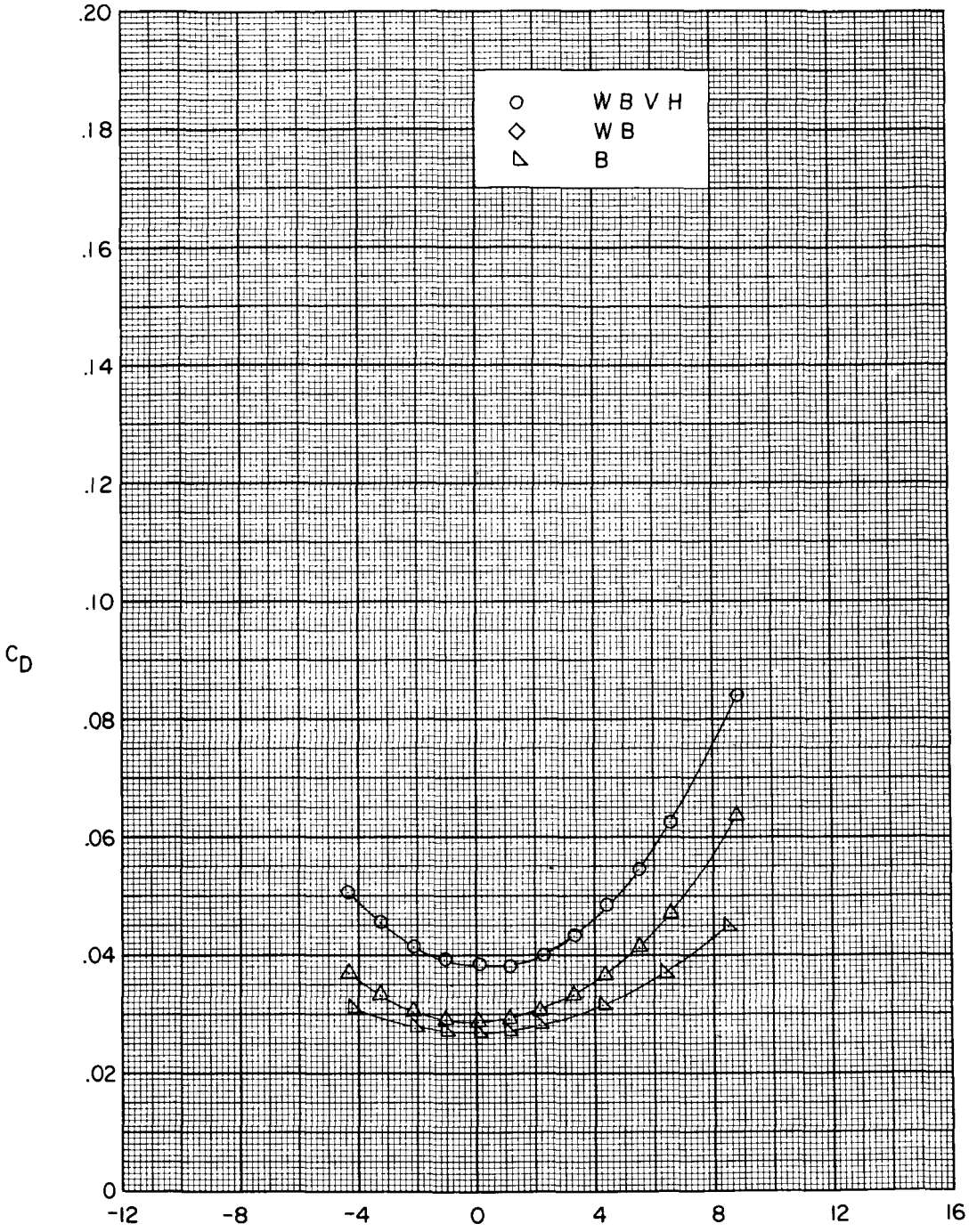

(b) Wing skew, -90°. Concluded.

Figure 5.- Concluded.

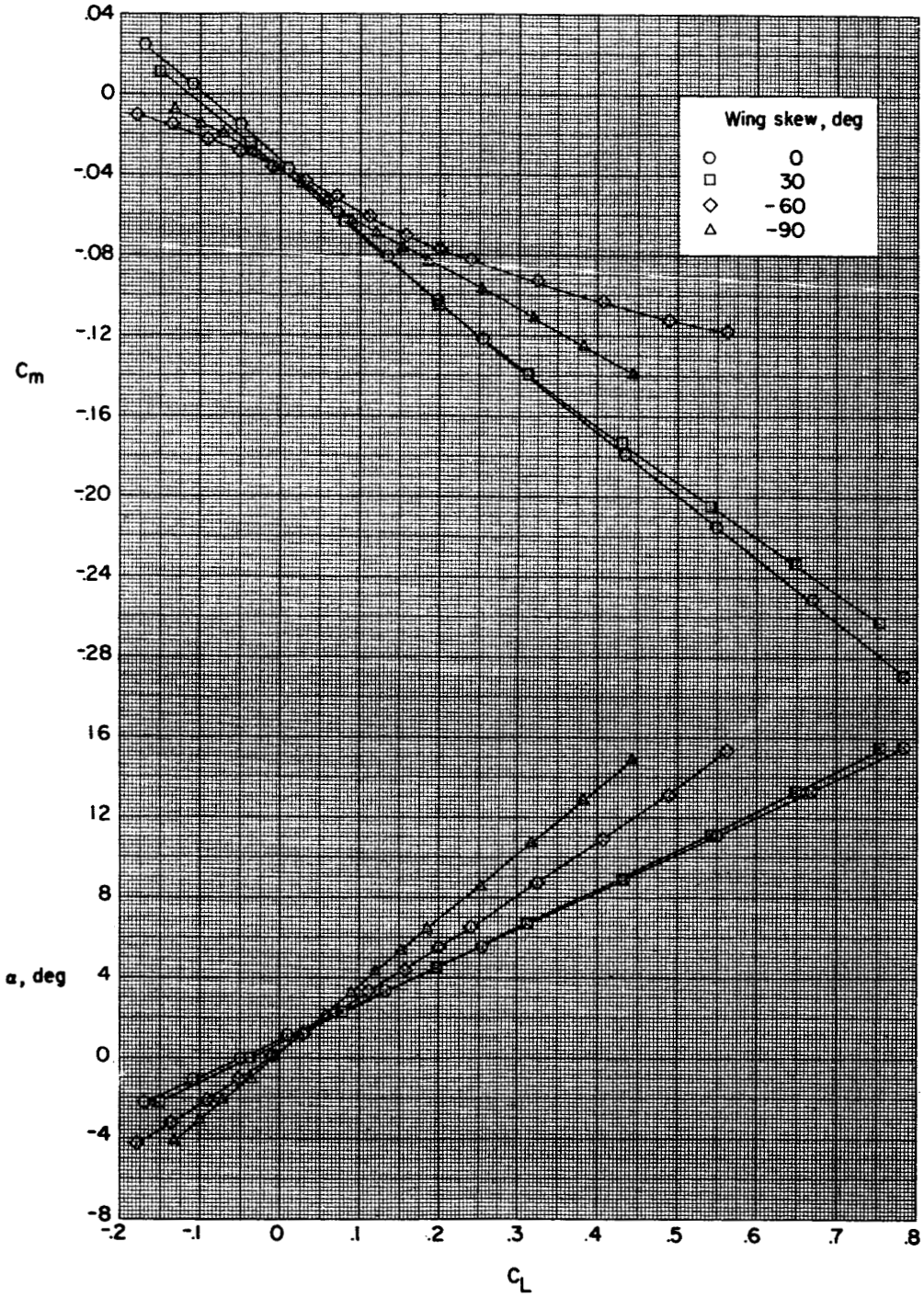

Figure 6.- Effect of variation of wing skew angle on the longitudinal aerodynamic characteristics of the complete configuration. $\delta_h = 0^o$; M = 2.20.

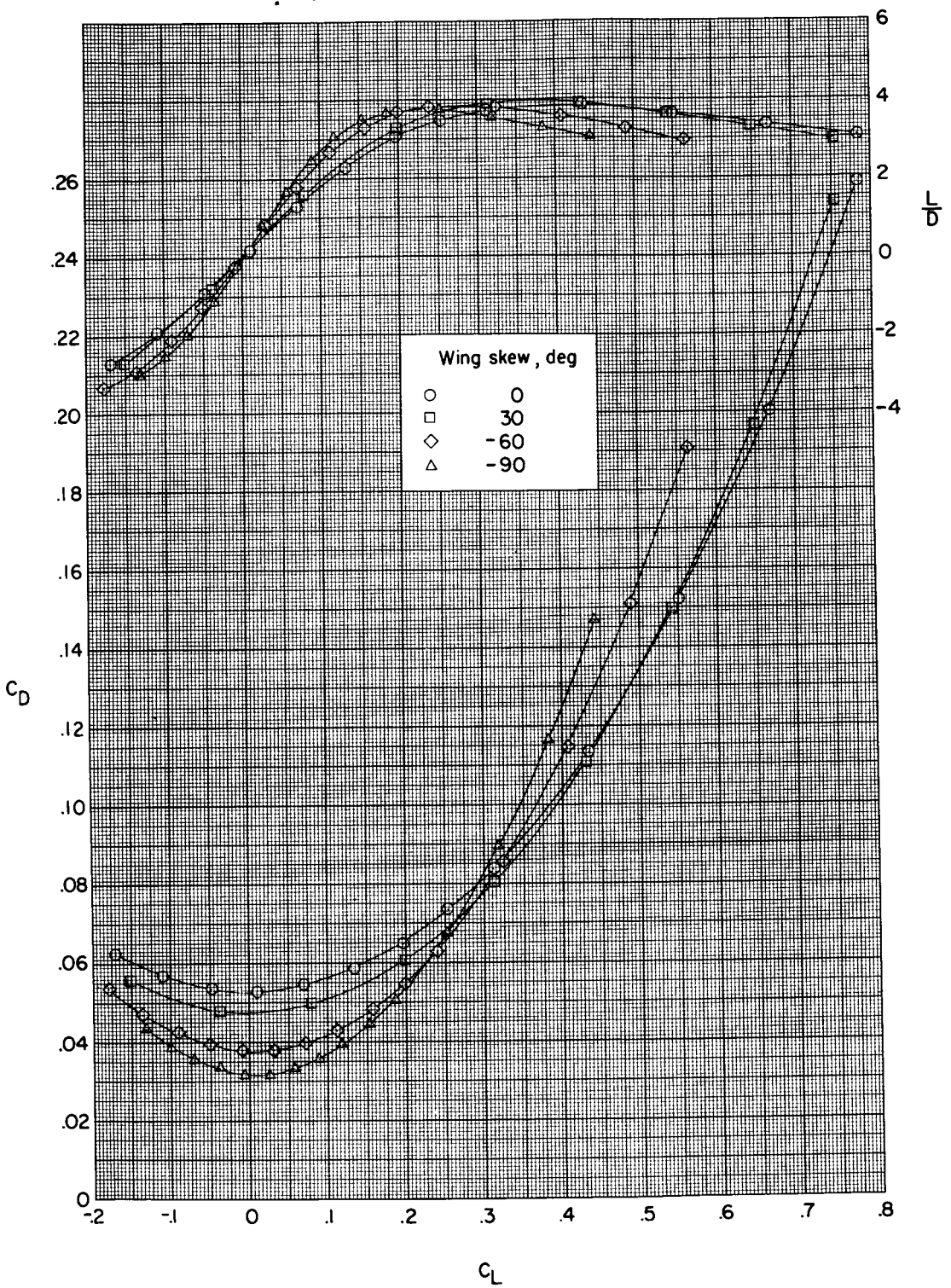

Figure 6.- Concluded.

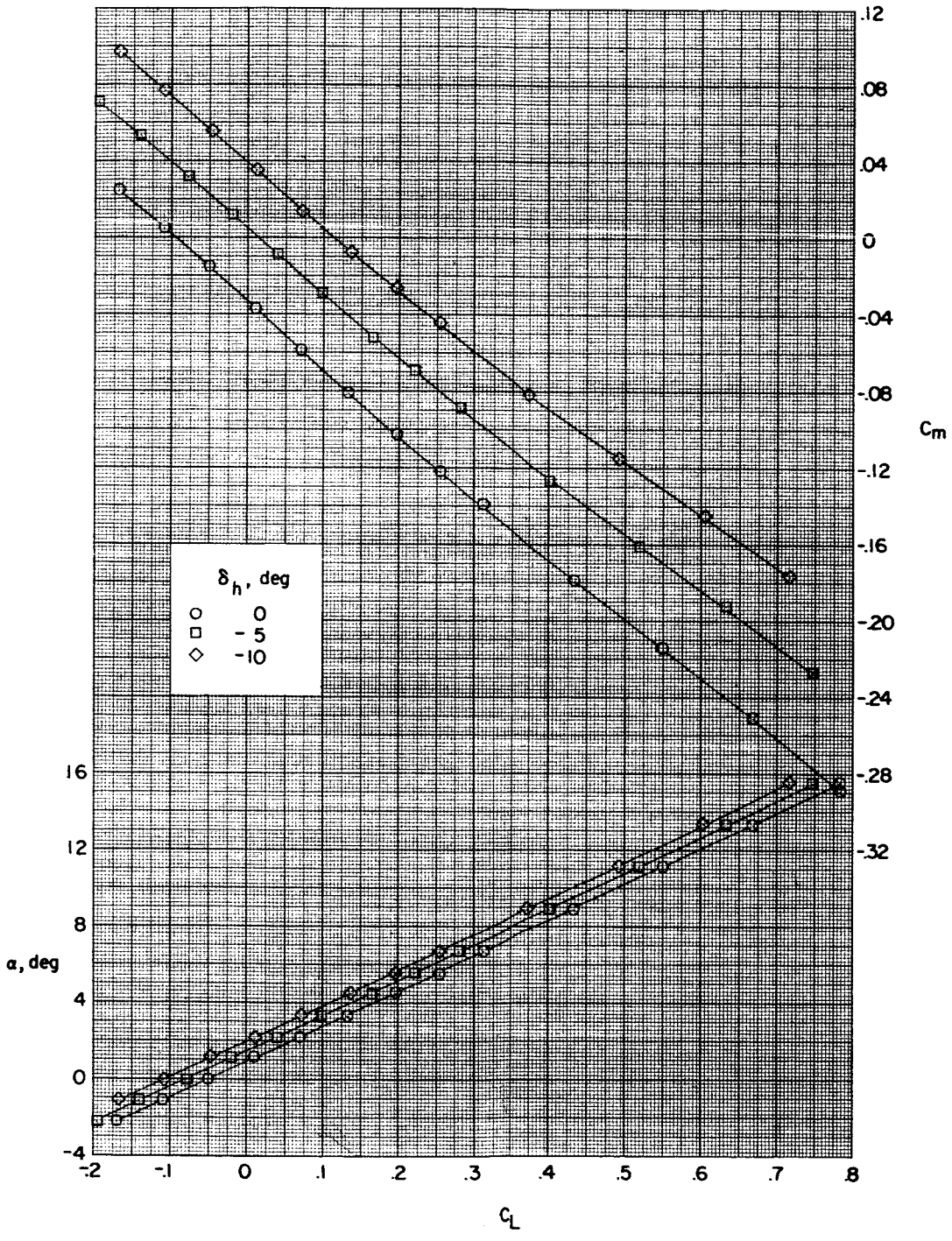

(a) Wing skew, 0°.

Figure 7.- Effect of horizontal-tail deflection on the aerodynamic characteristics in pitch for the complete configuration. M = 2.20.

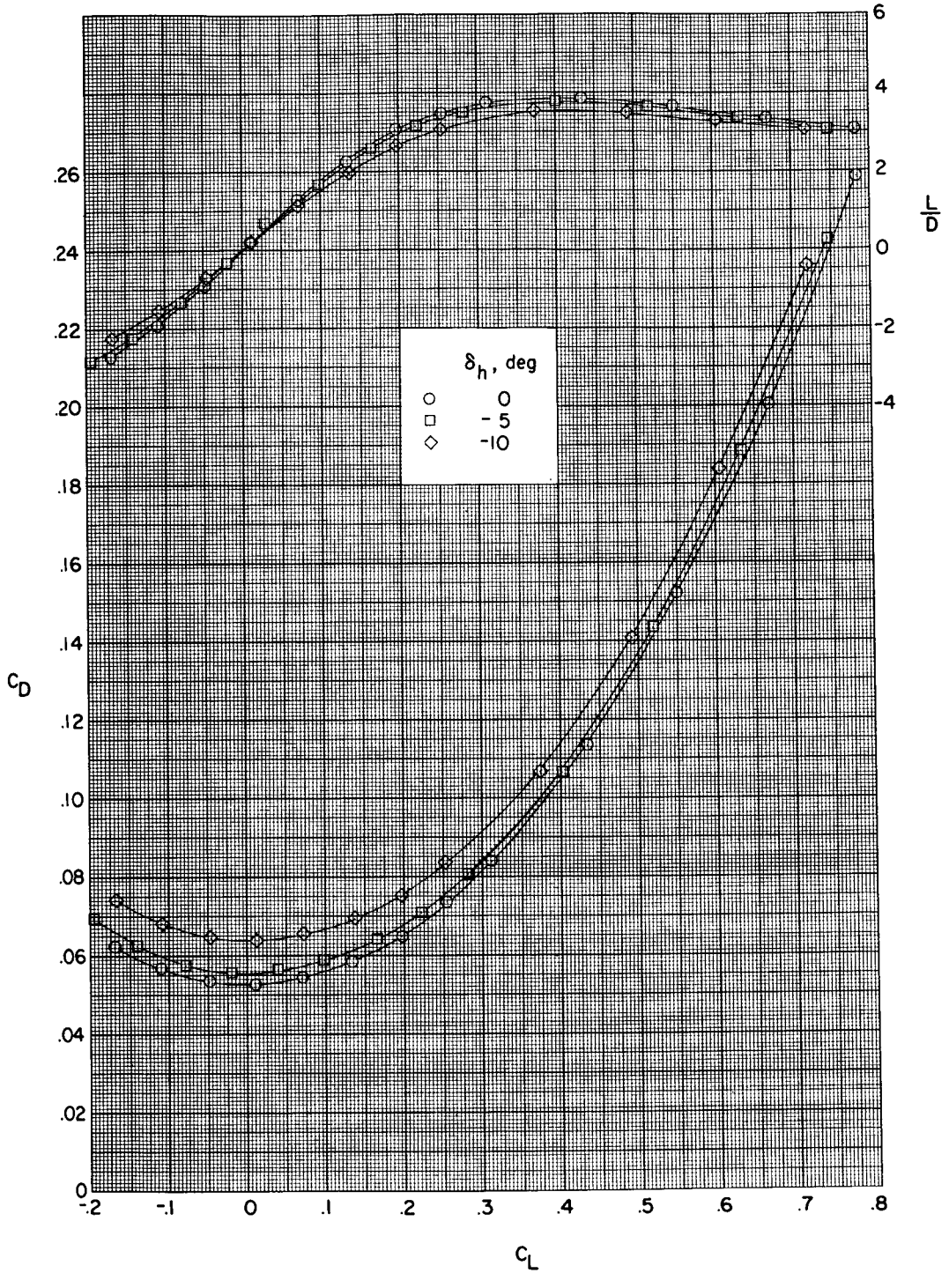

(a) Wing skew, 0°. Concluded.

Figure 7.- Continued.

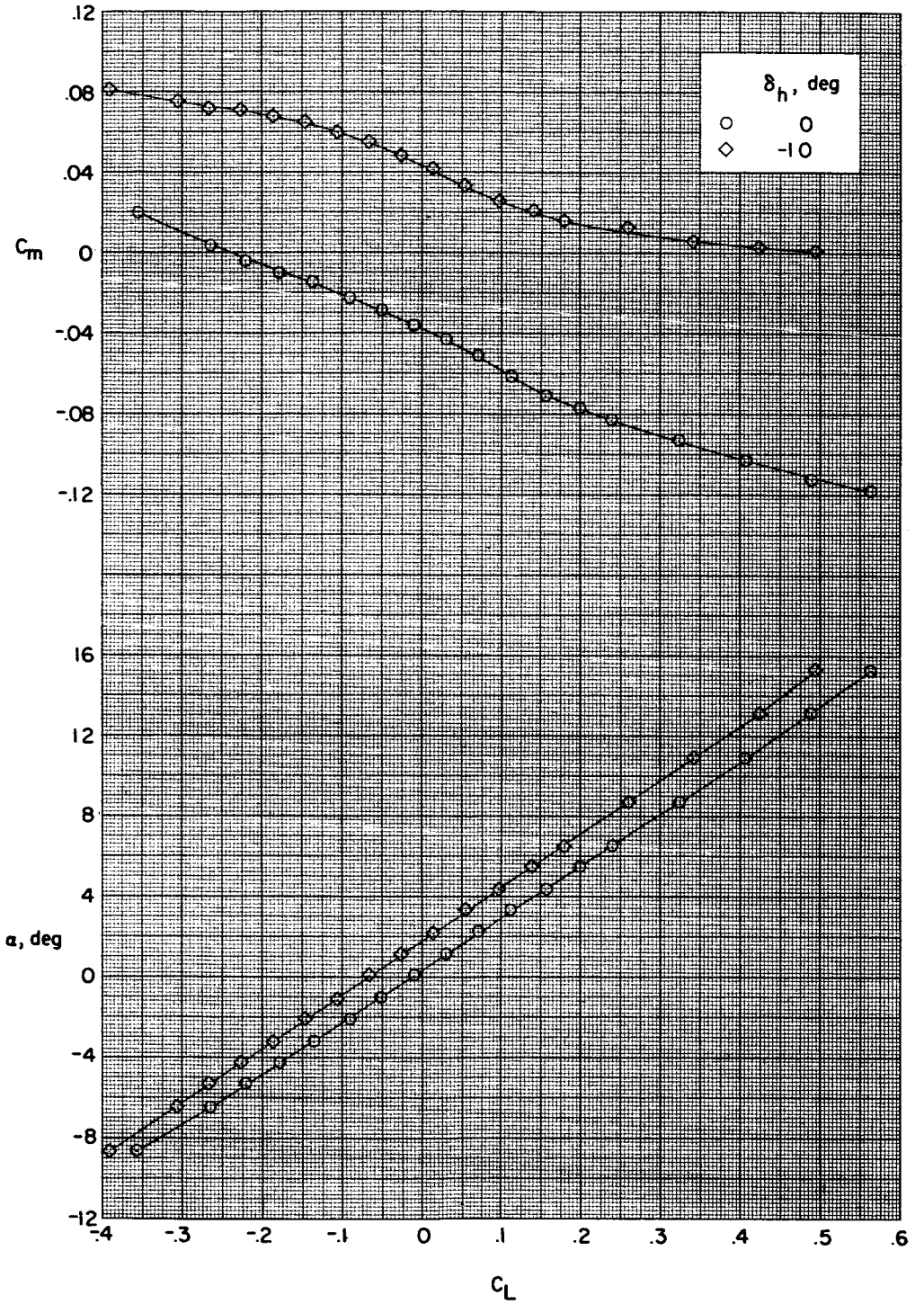

(b) Wing skew, -60°.

Figure 7.- Continued.

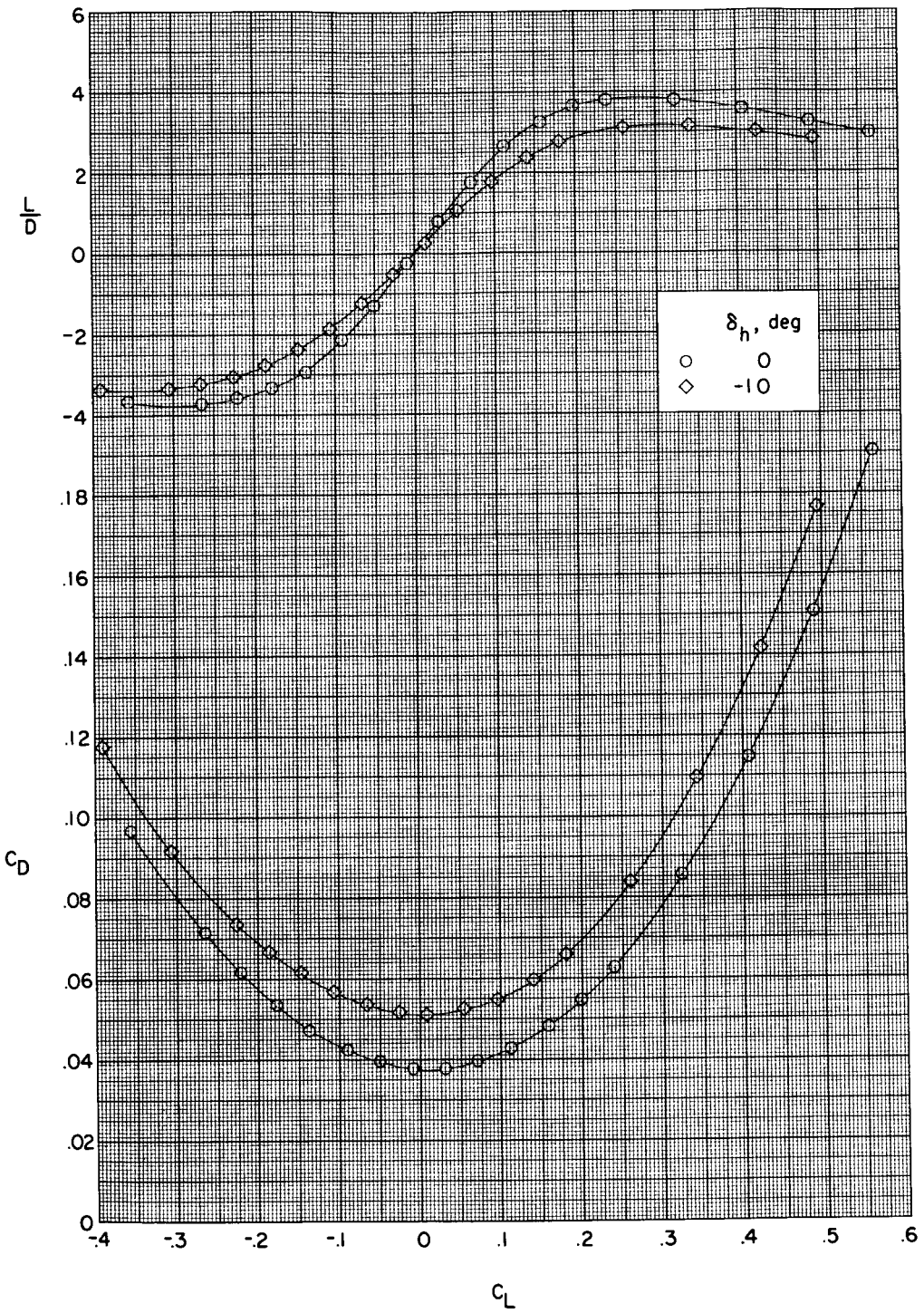

(b) Wing skew, -60°. Concluded.

Figure 7.- Continued.

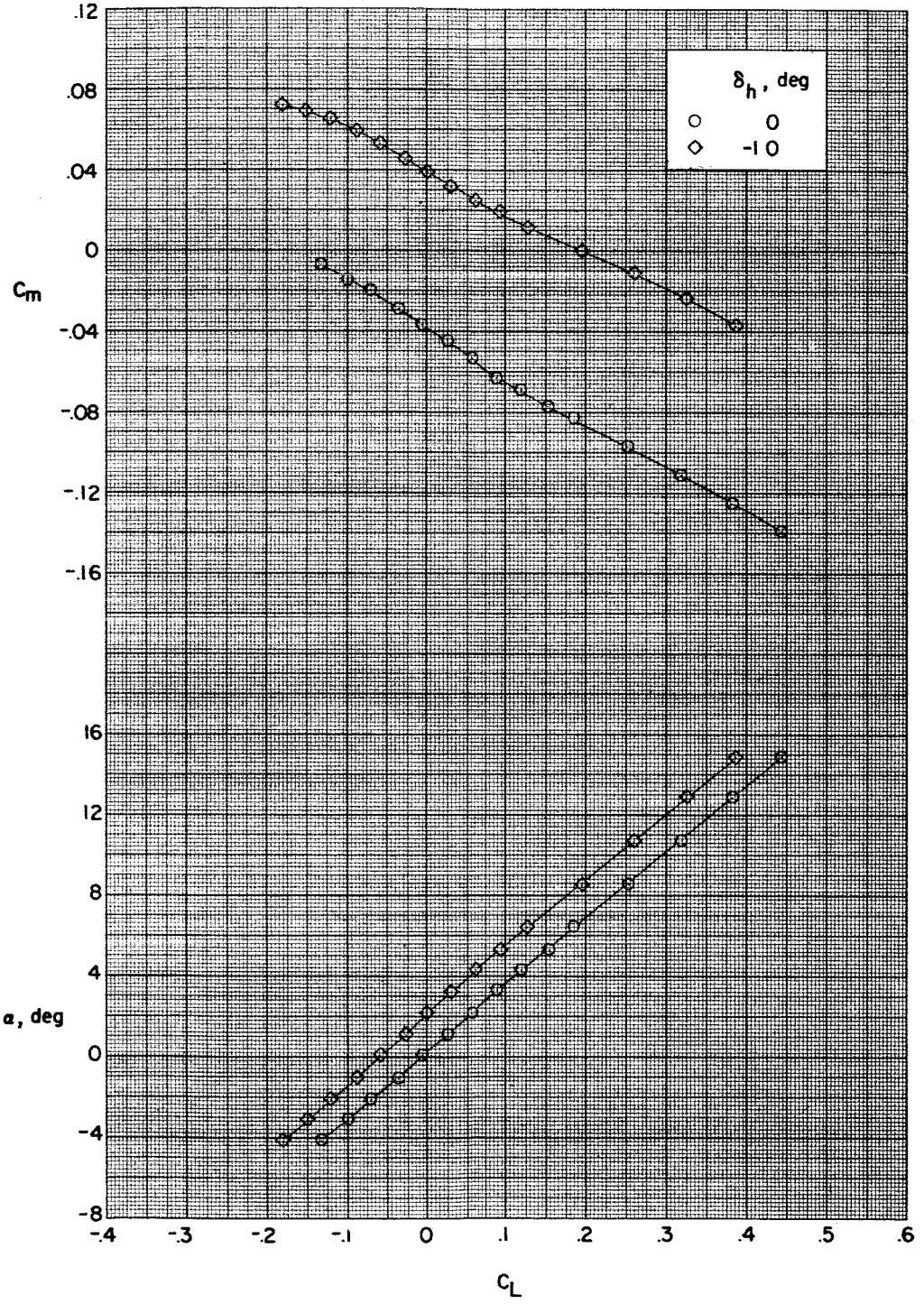

(c) Wing skew, -90°.

Figure 7.- Continued.

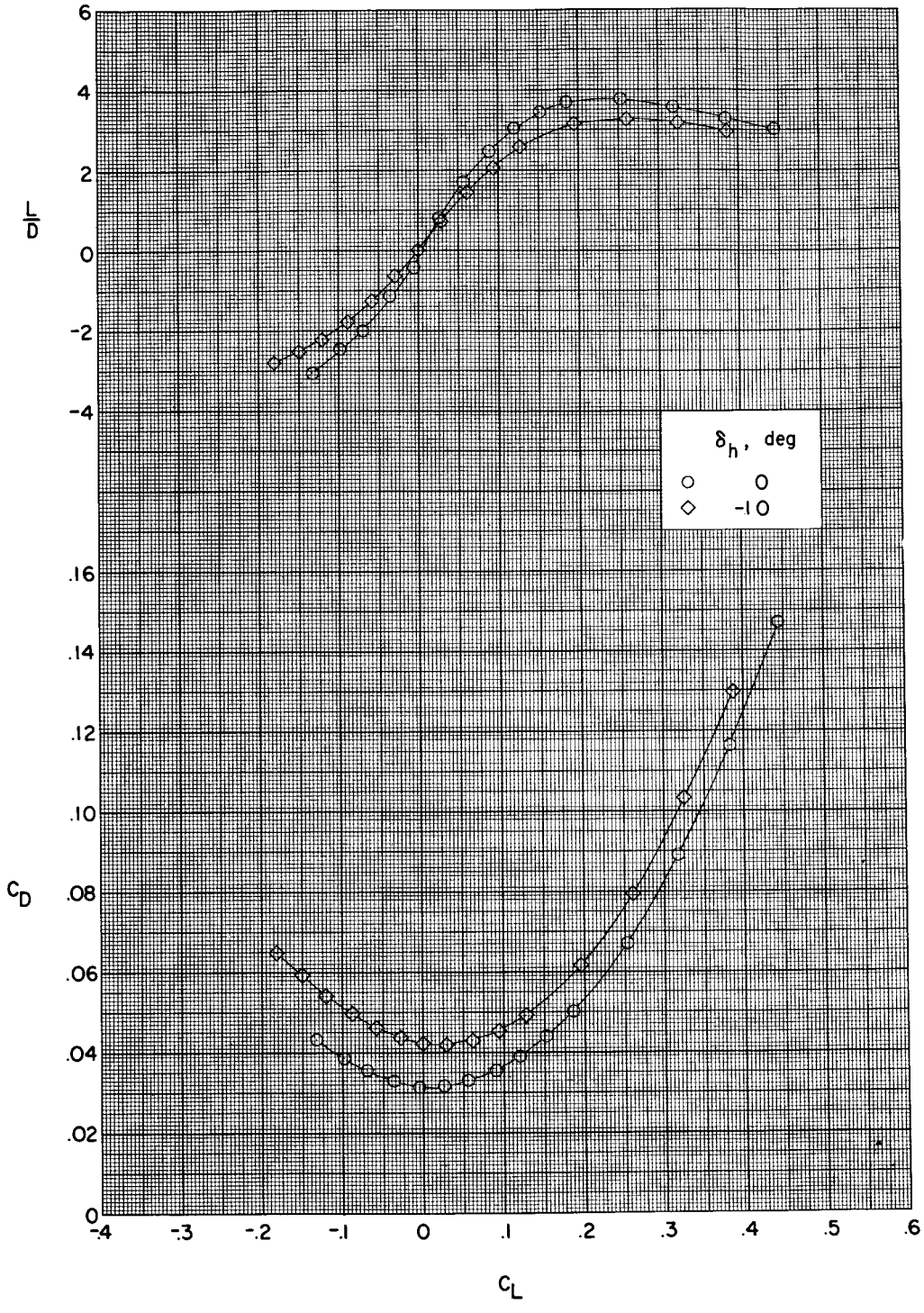

(c) Wing skew, -90°. Concluded.

Figure 7.- Concluded.

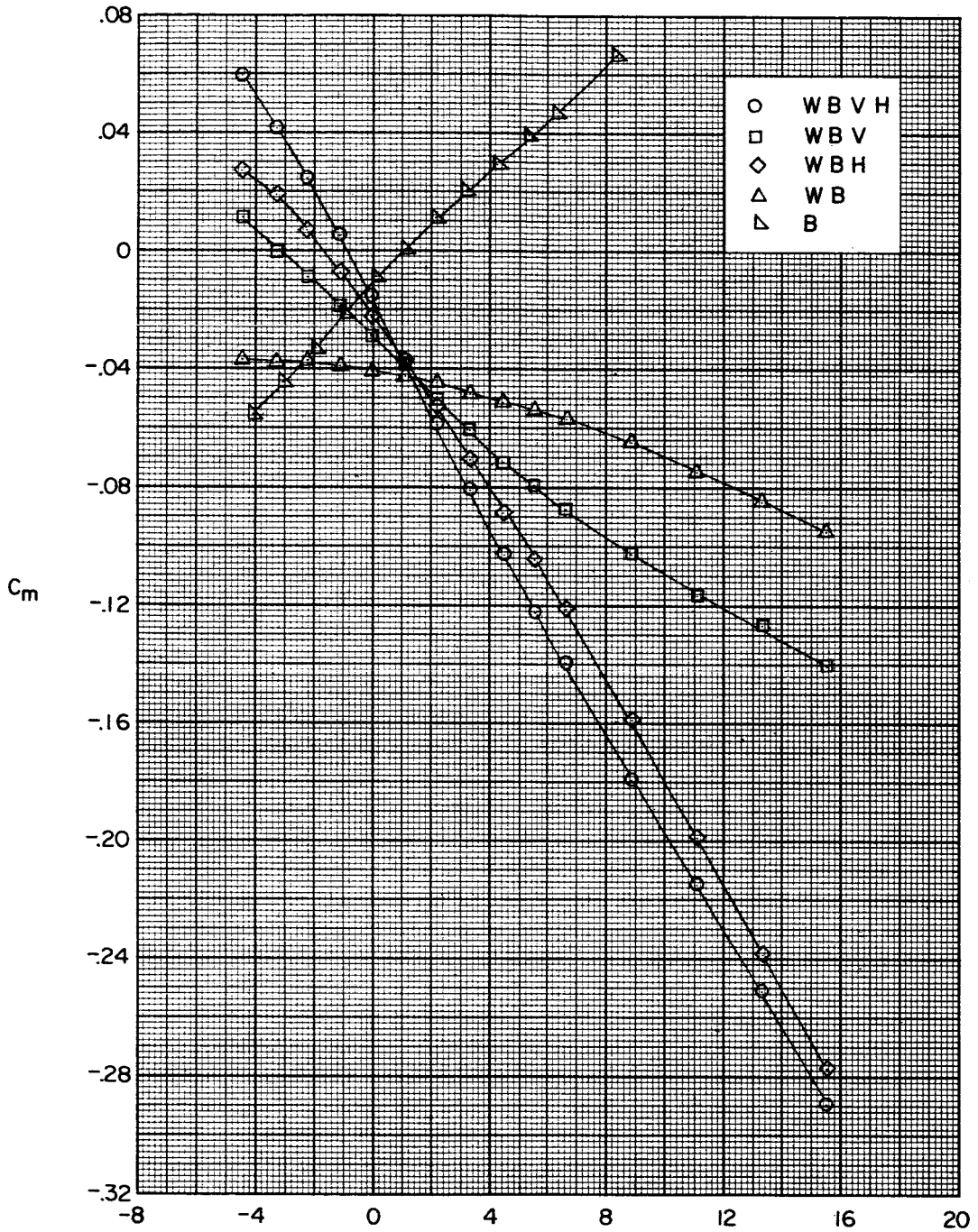

(a) Wing skew, 0°.

Figure 8.- Effects of various components on the longitudinal aerodynamic characteristics of the model. M = 2.20.

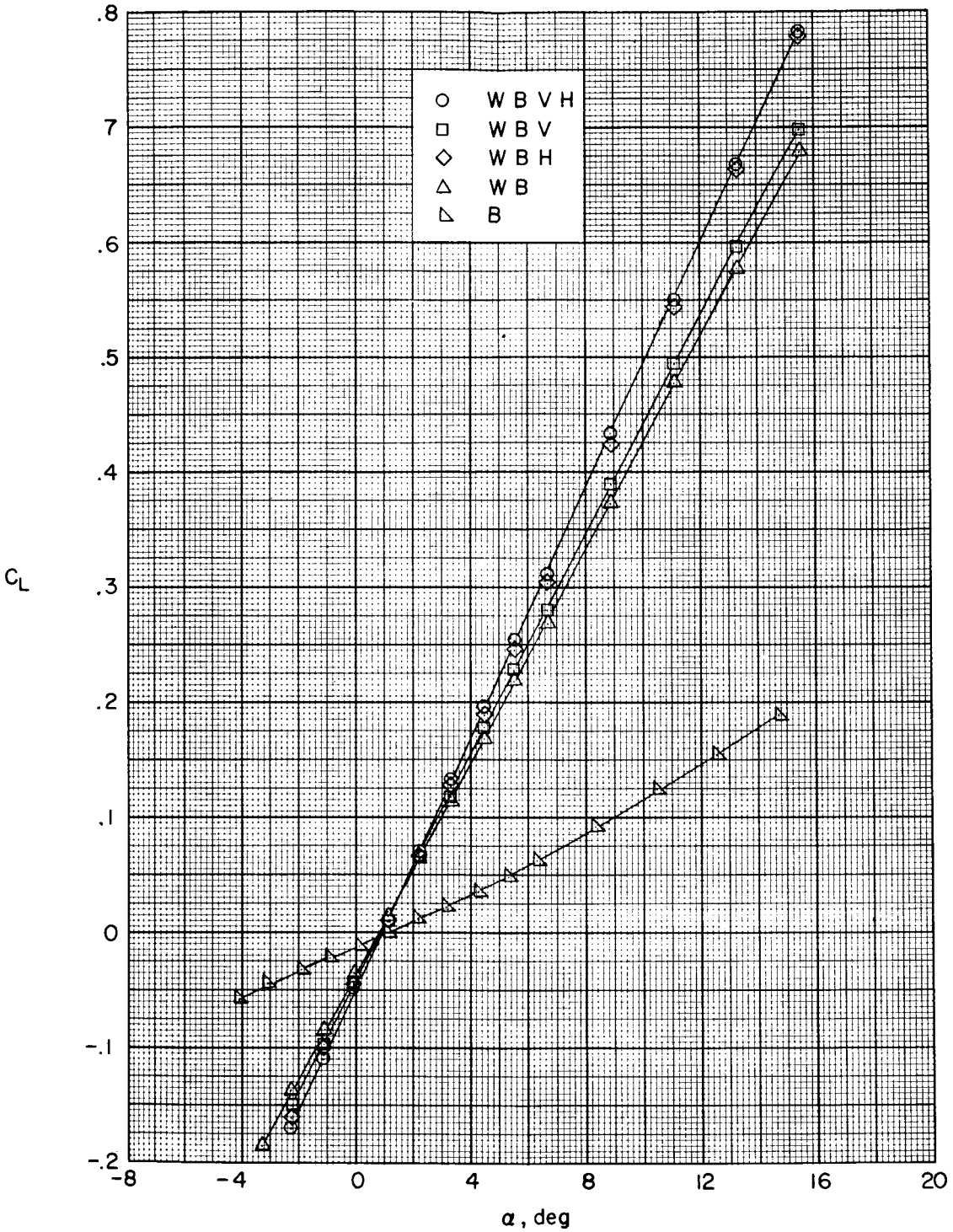

(a) Wing skew, 0°. Continued.

Figure 8.- Continued.

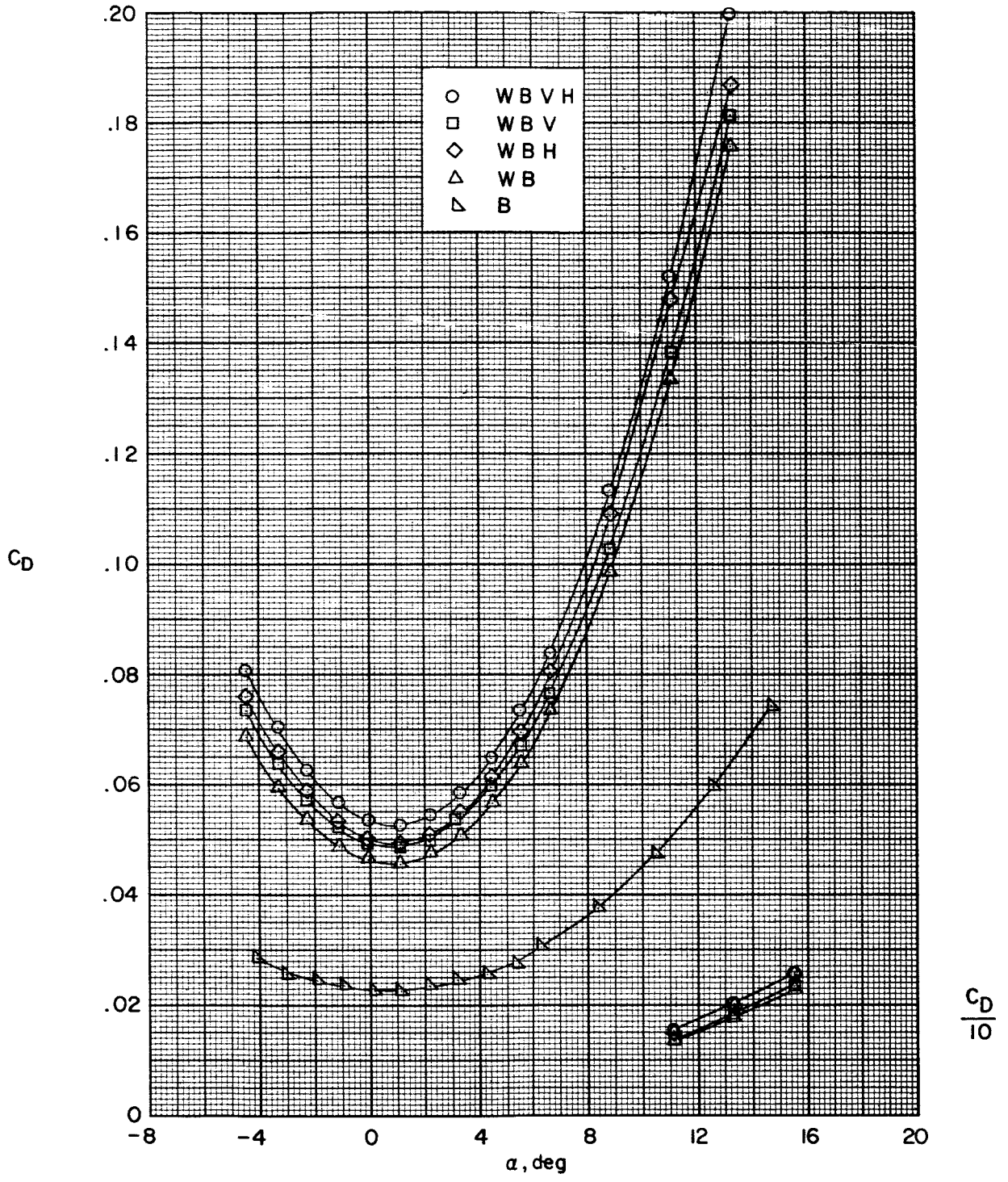

(a) Wing skew, 0°. Concluded.

Figure 8.- Continued.

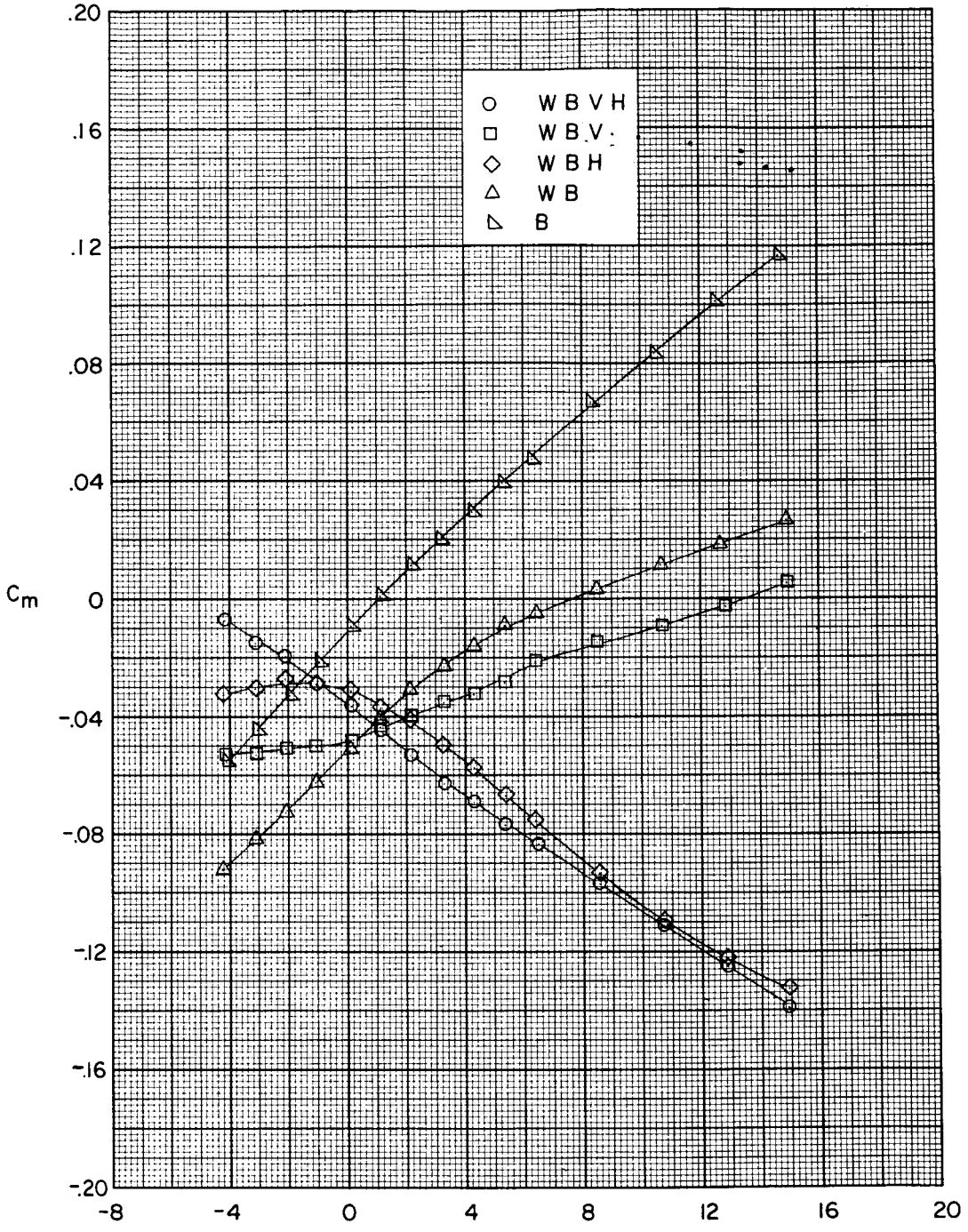

(b) Wing skew, -90°.

Figure 8.- Continued.

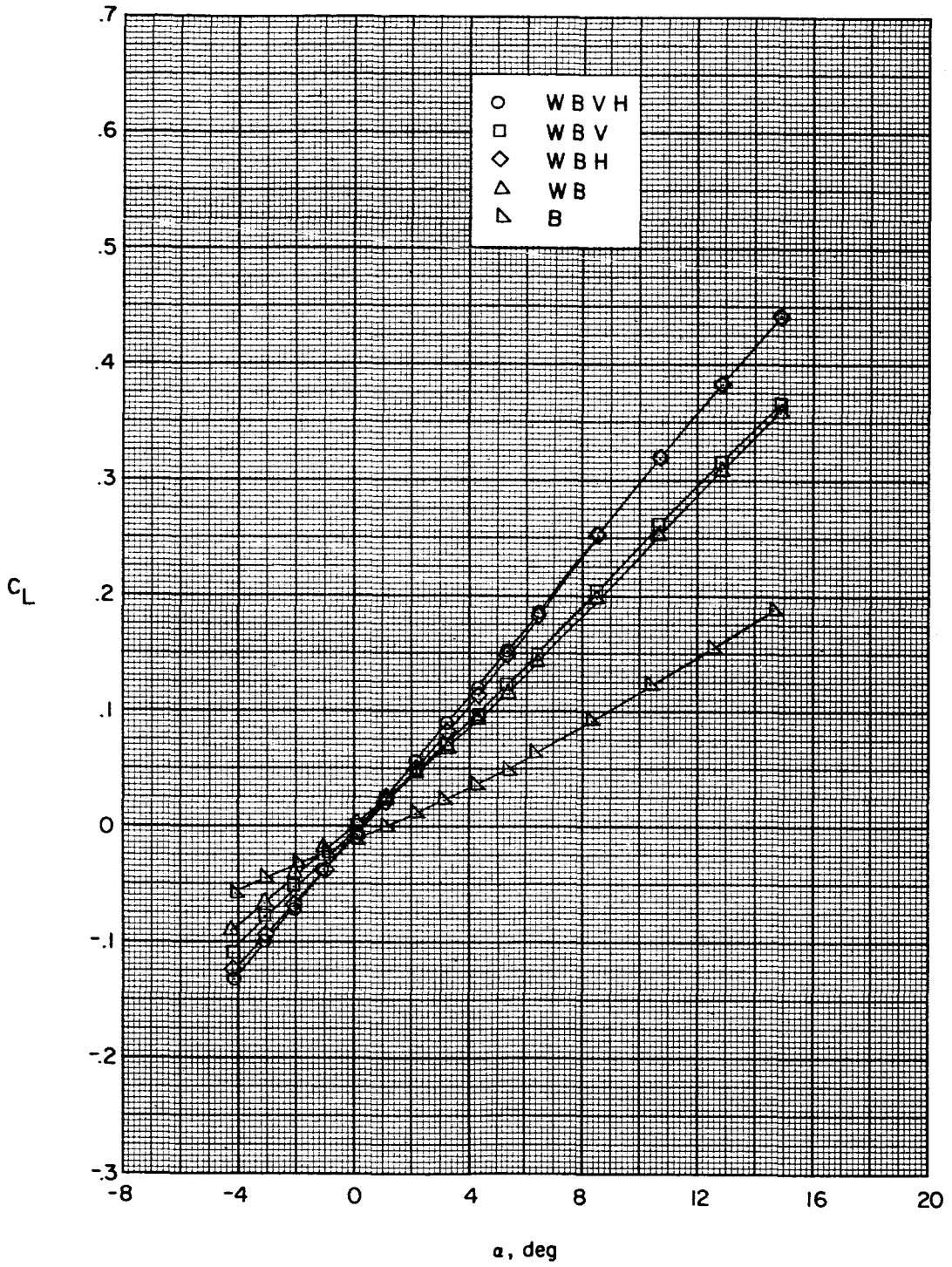

(b) Wing skew, -90°. Continued.

Figure 8.- Continued.

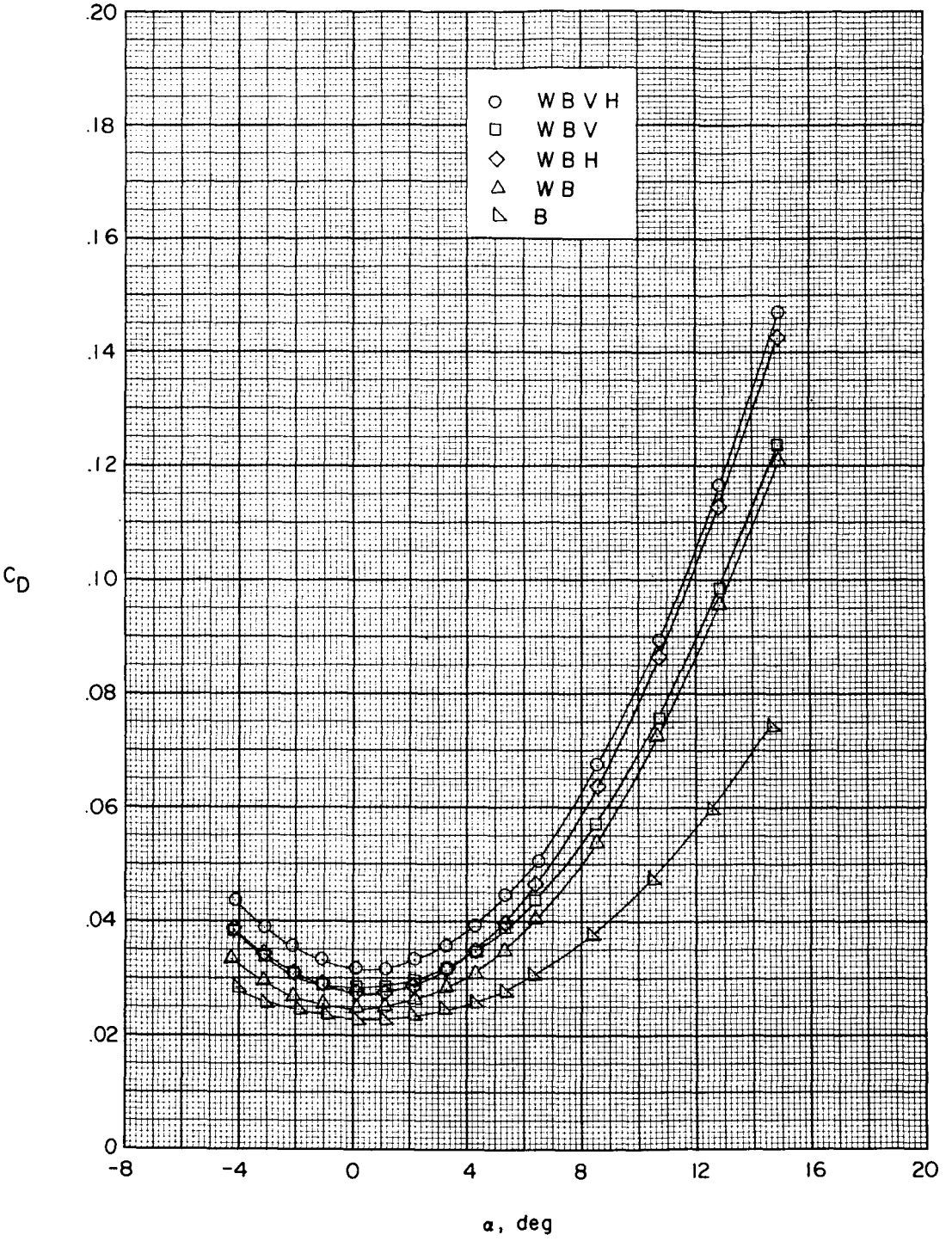

(b) Wing skew, -90°. Concluded.

Figure 8.- Concluded.

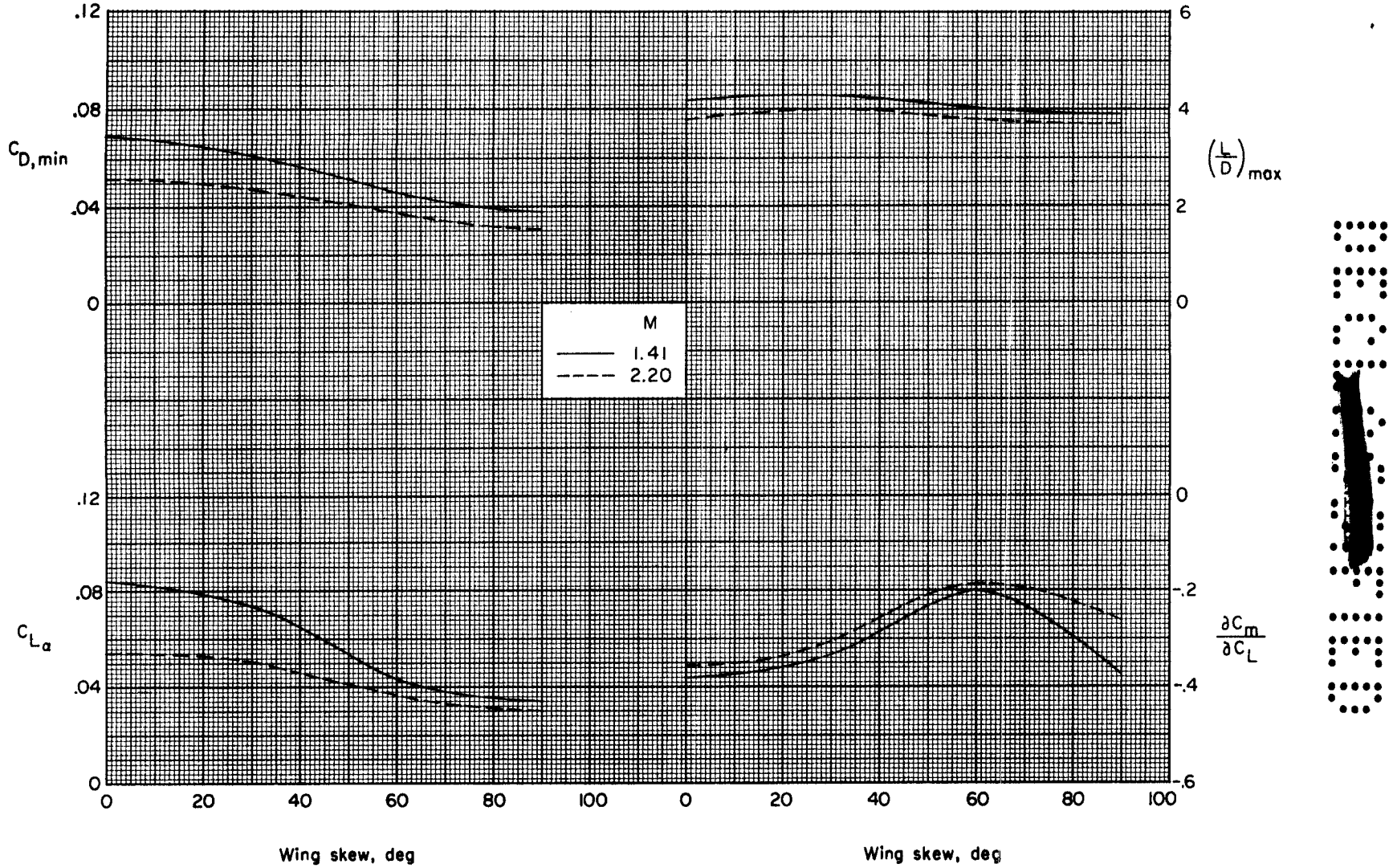

Figure 9.- Variation of longitudinal parameters with wing skew angle. Complete configuration.

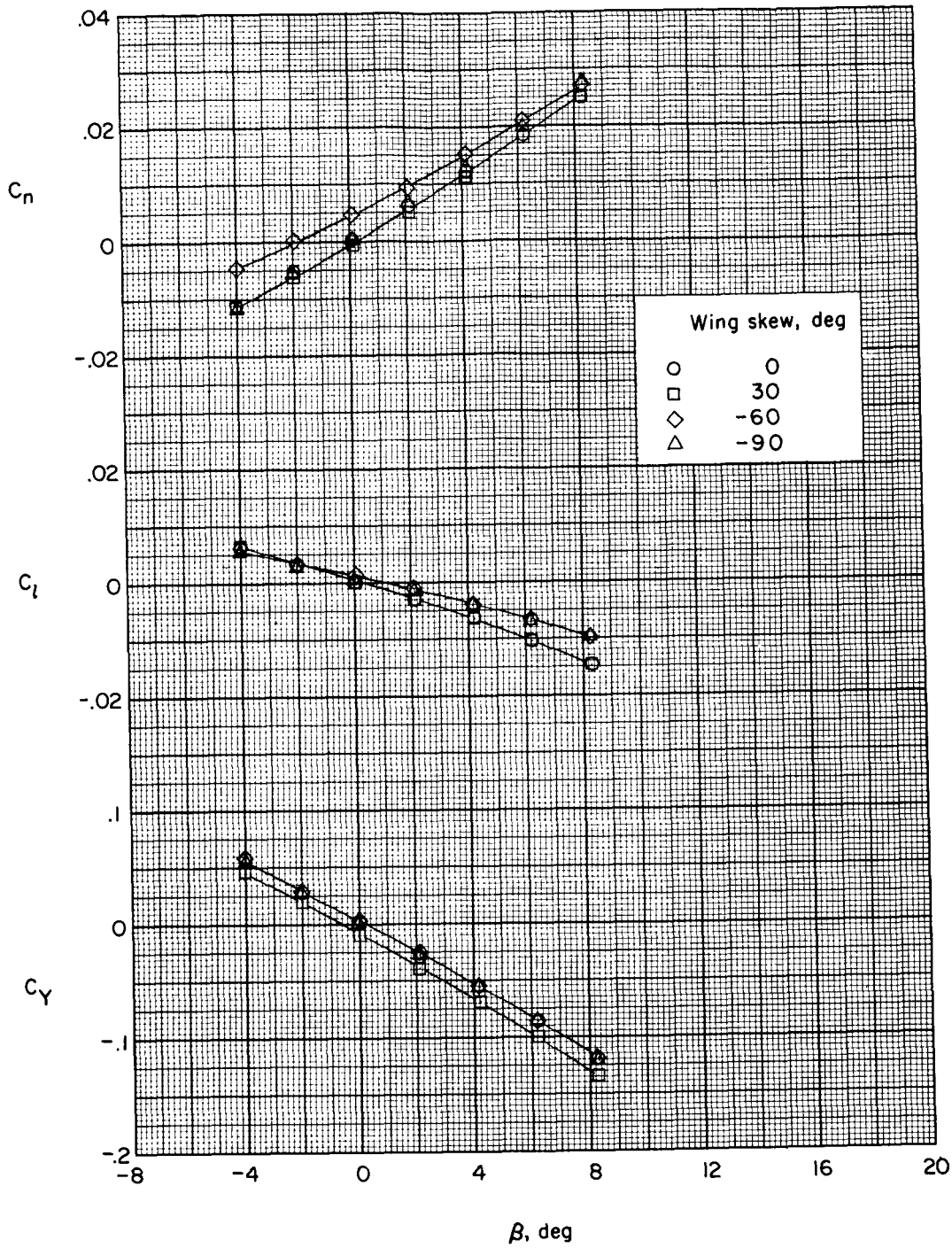

(a) $\alpha = -0.4^{\circ}$.

Figure 10.- Effect of variation of wing skew angle on the lateral aerodynamic characteristics of the complete configuration. $\delta_h = 0^{\circ}$; M = 1.41.

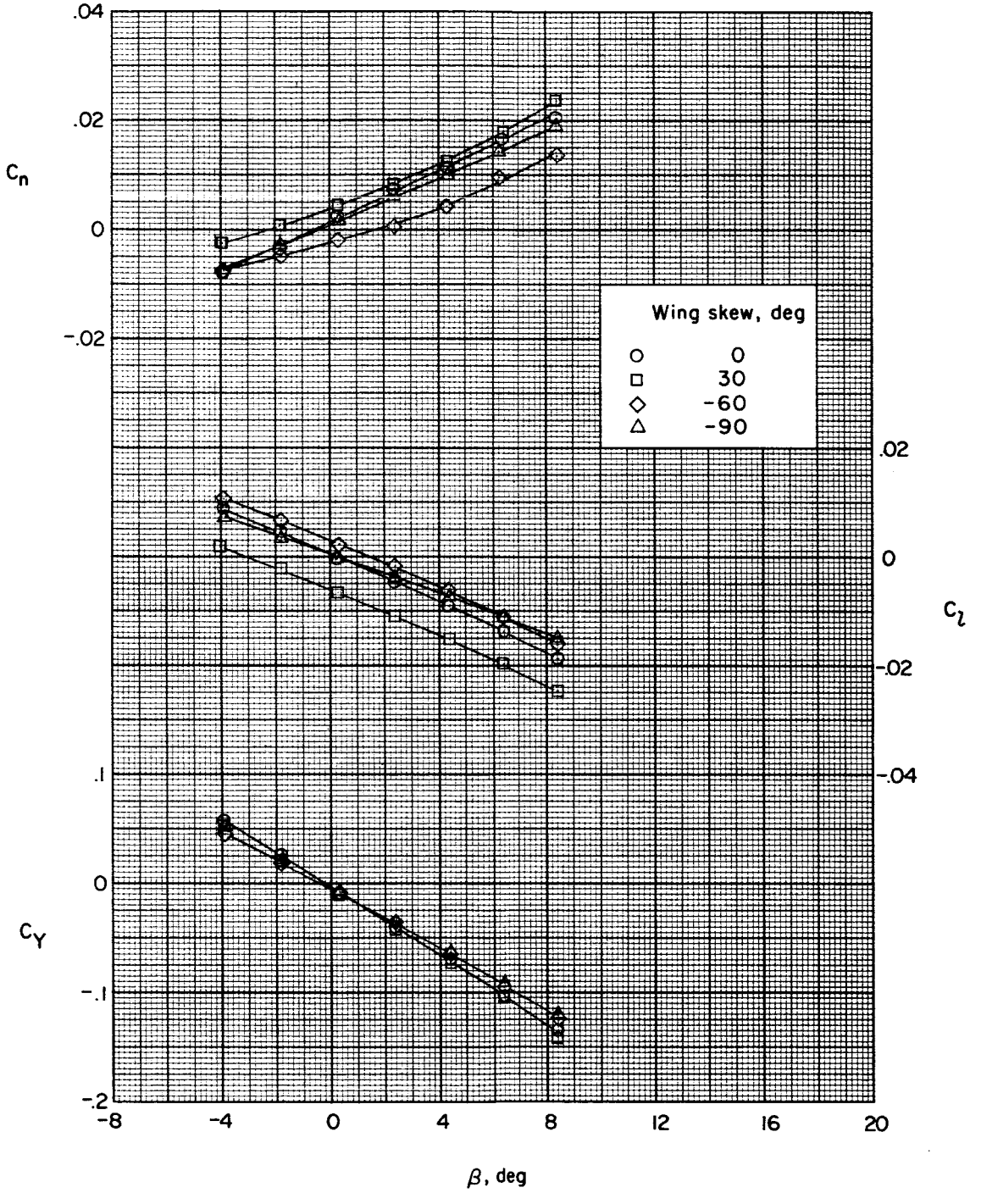

(b) $\alpha \approx 4.8°$.

Figure 10.- Continued.

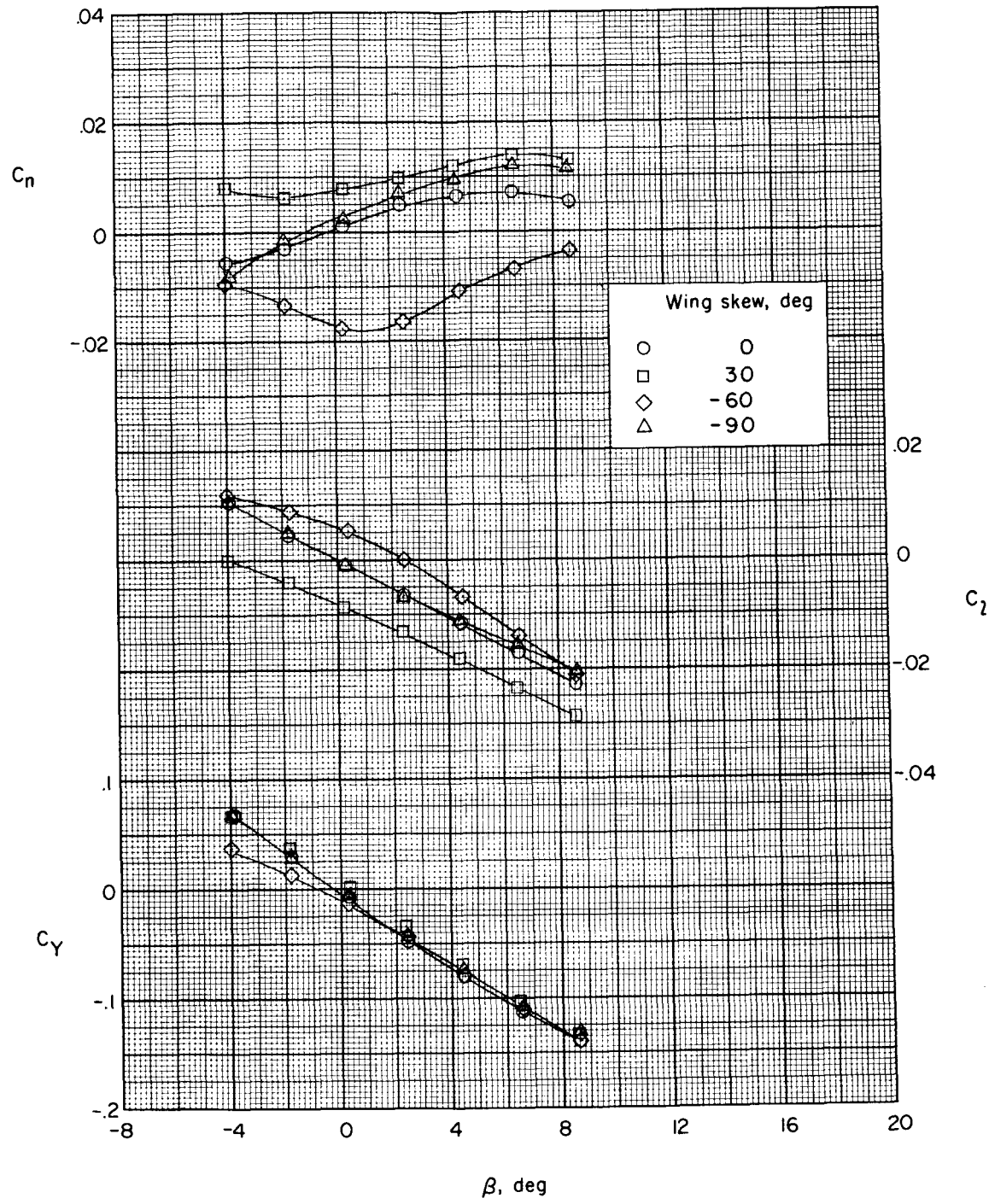

(c) $\alpha \approx 9.5°$.

Figure 10.- Concluded.

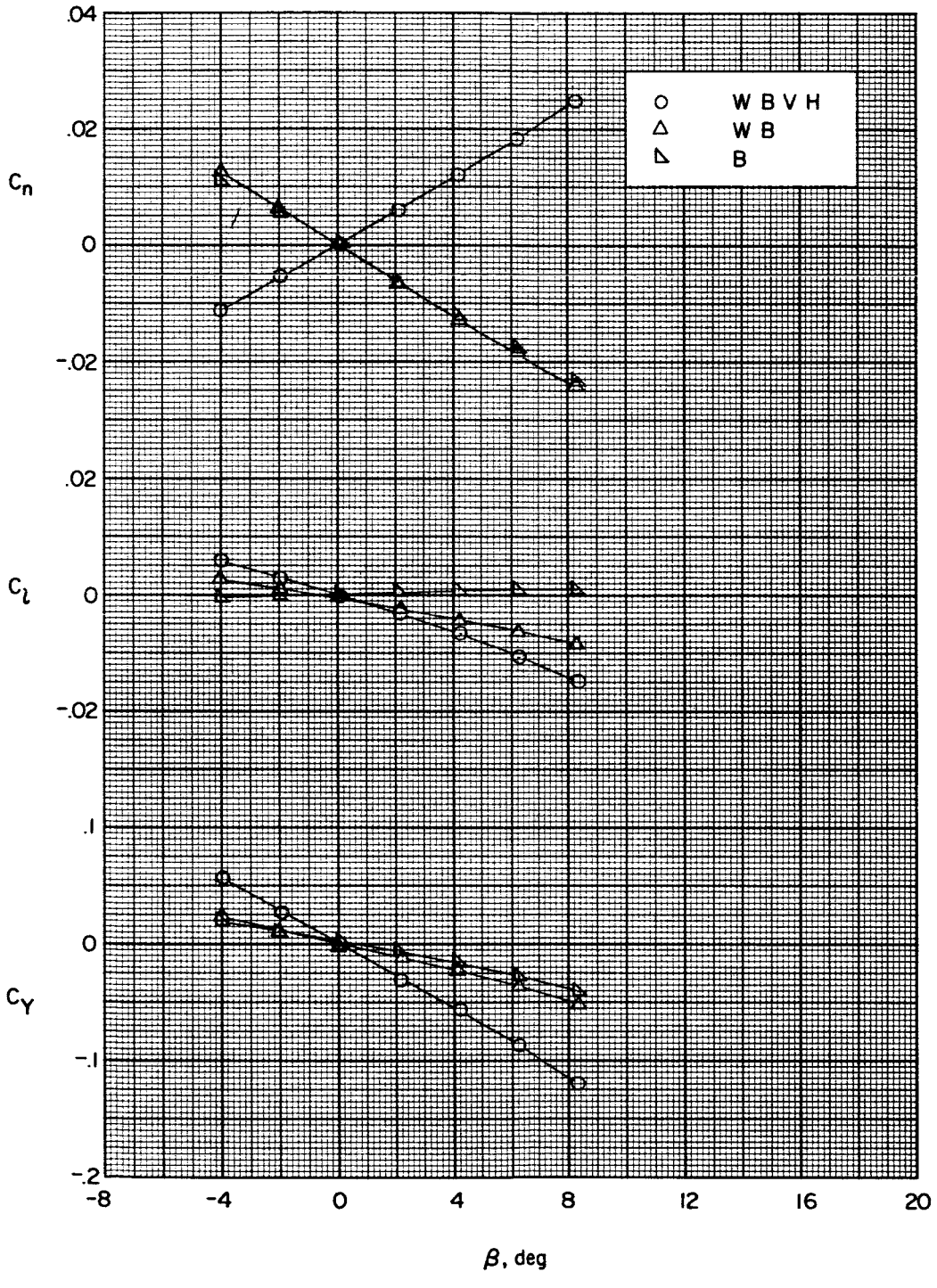

(a) $\alpha = -0.4^{\circ}$.

Figure 11.- Effect of various components on the lateral aerodynamic characteristics of the model in sideslip. Wing skew angle = 0°; M = 1.41.

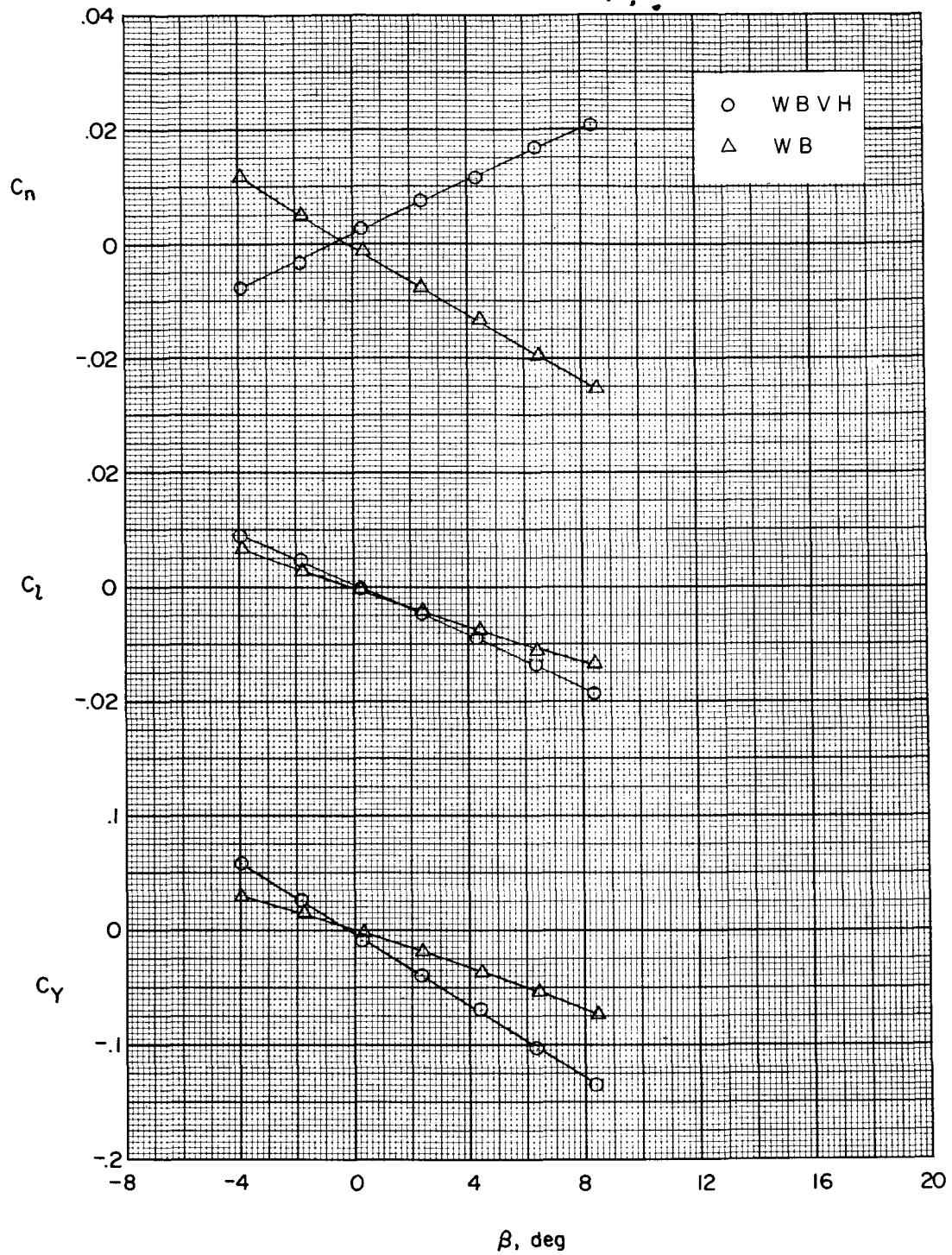

(b) $\alpha = 5.0^{\circ}$.

Figure 11.- Continued.

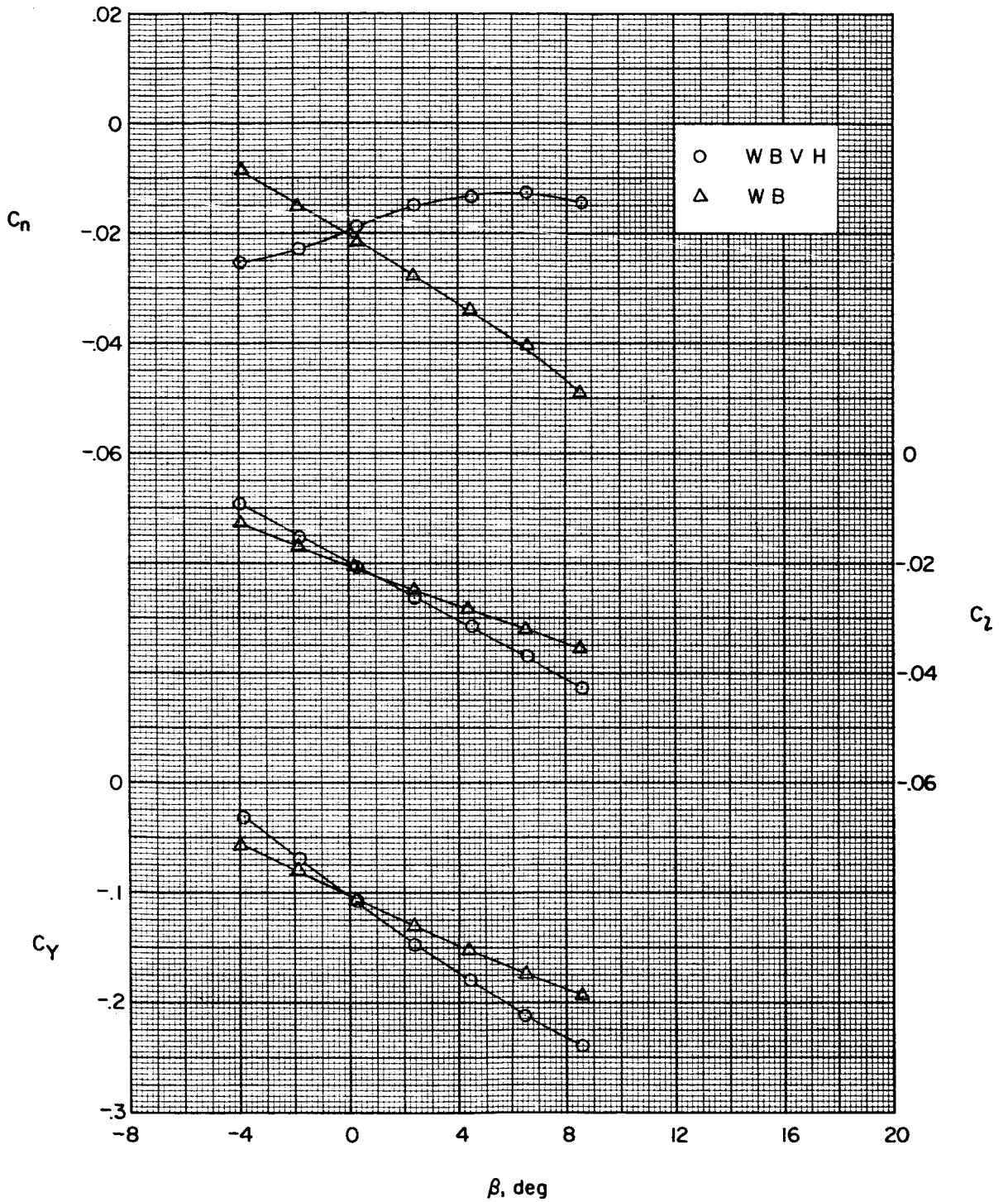

(c) $\alpha \approx 10.4^{\circ}$.

Figure 11.- Concluded.

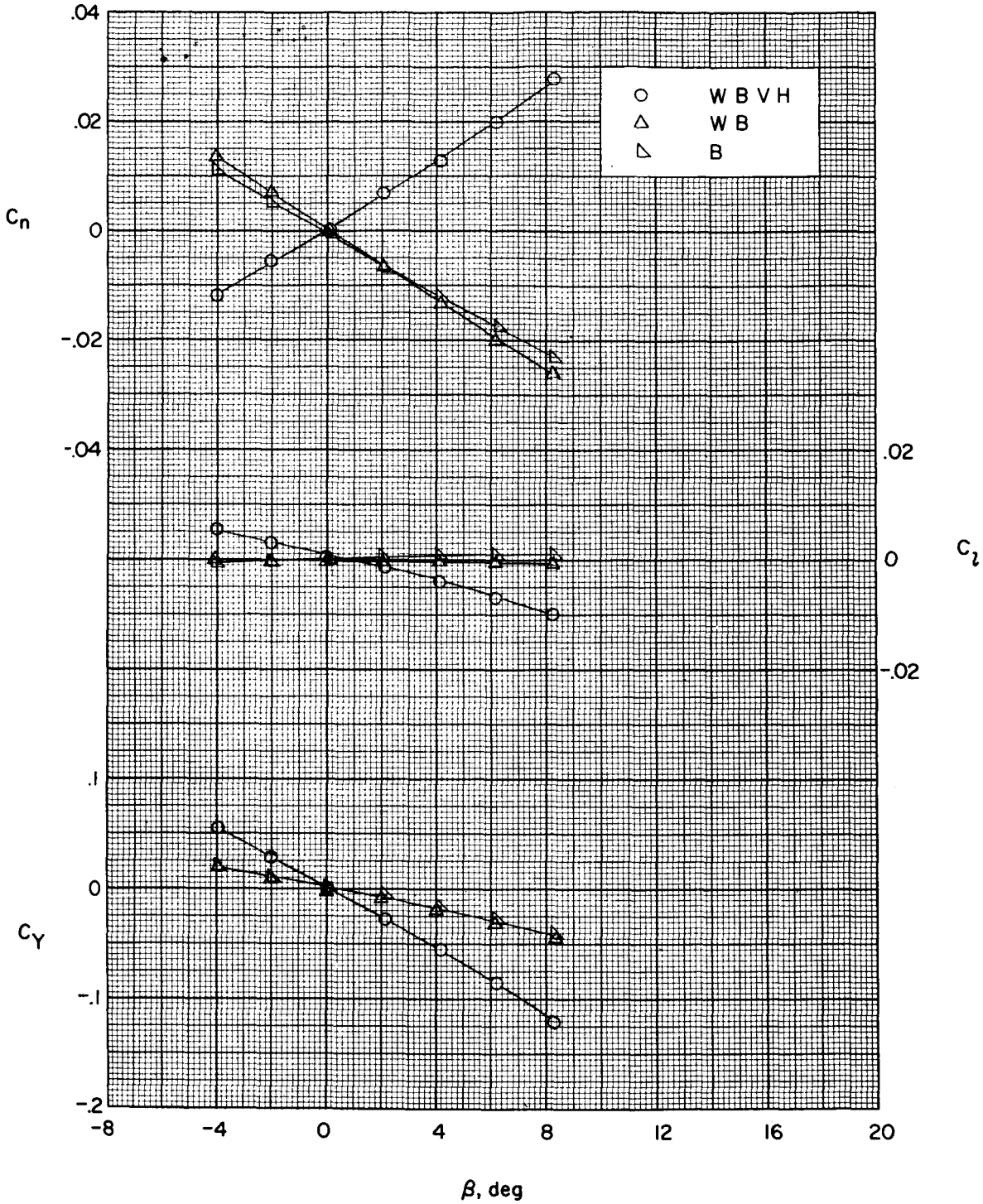

(a) $\alpha = -0.4^{\circ}$.

Figure 12.- Effect of various components on the lateral aerodynamic characteristics of the model in sideslip. Wing skew angle = -90°; M = 1.41.

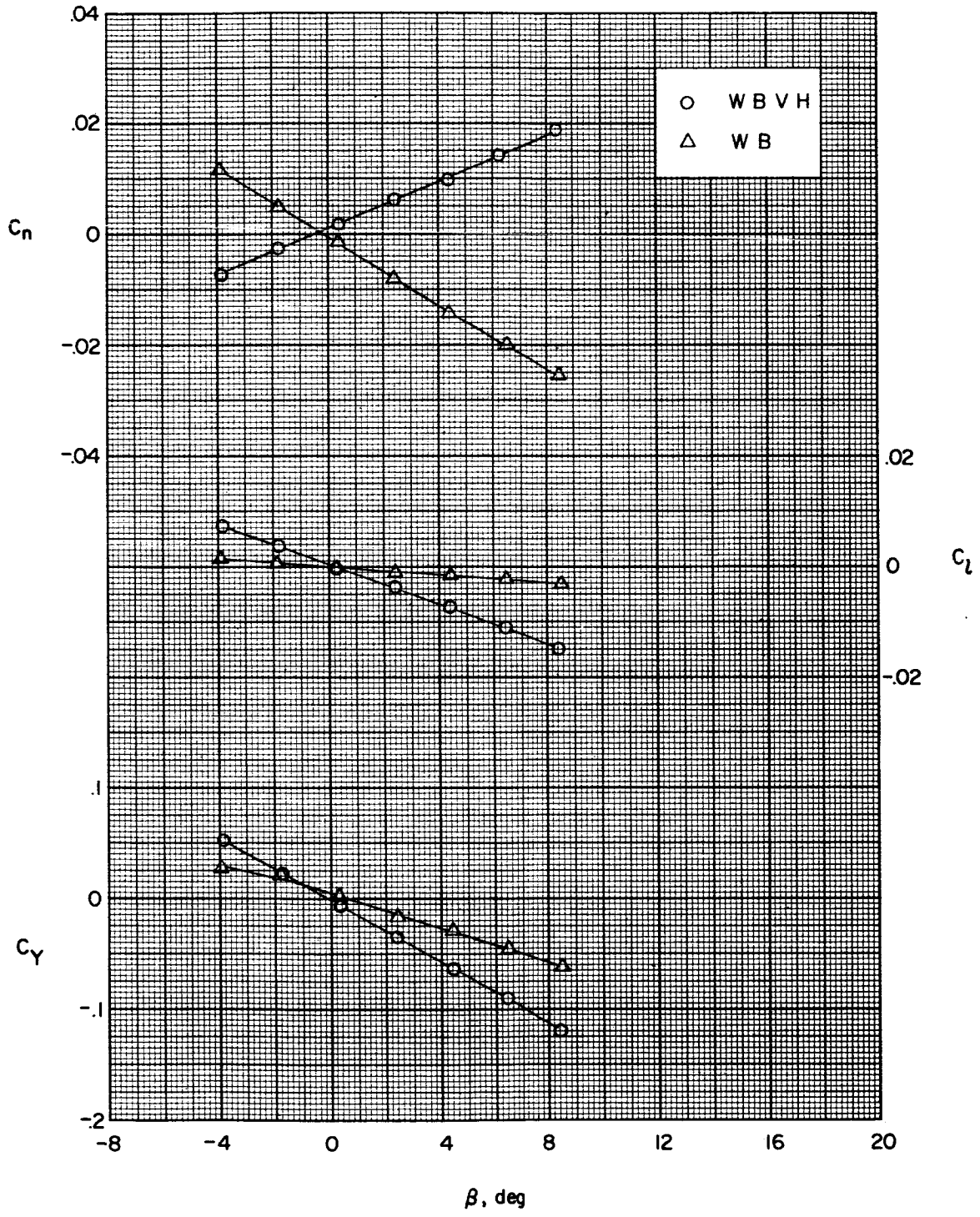

(b) $\alpha = 5.0^{\circ}$.

Figure 12.- Continued.

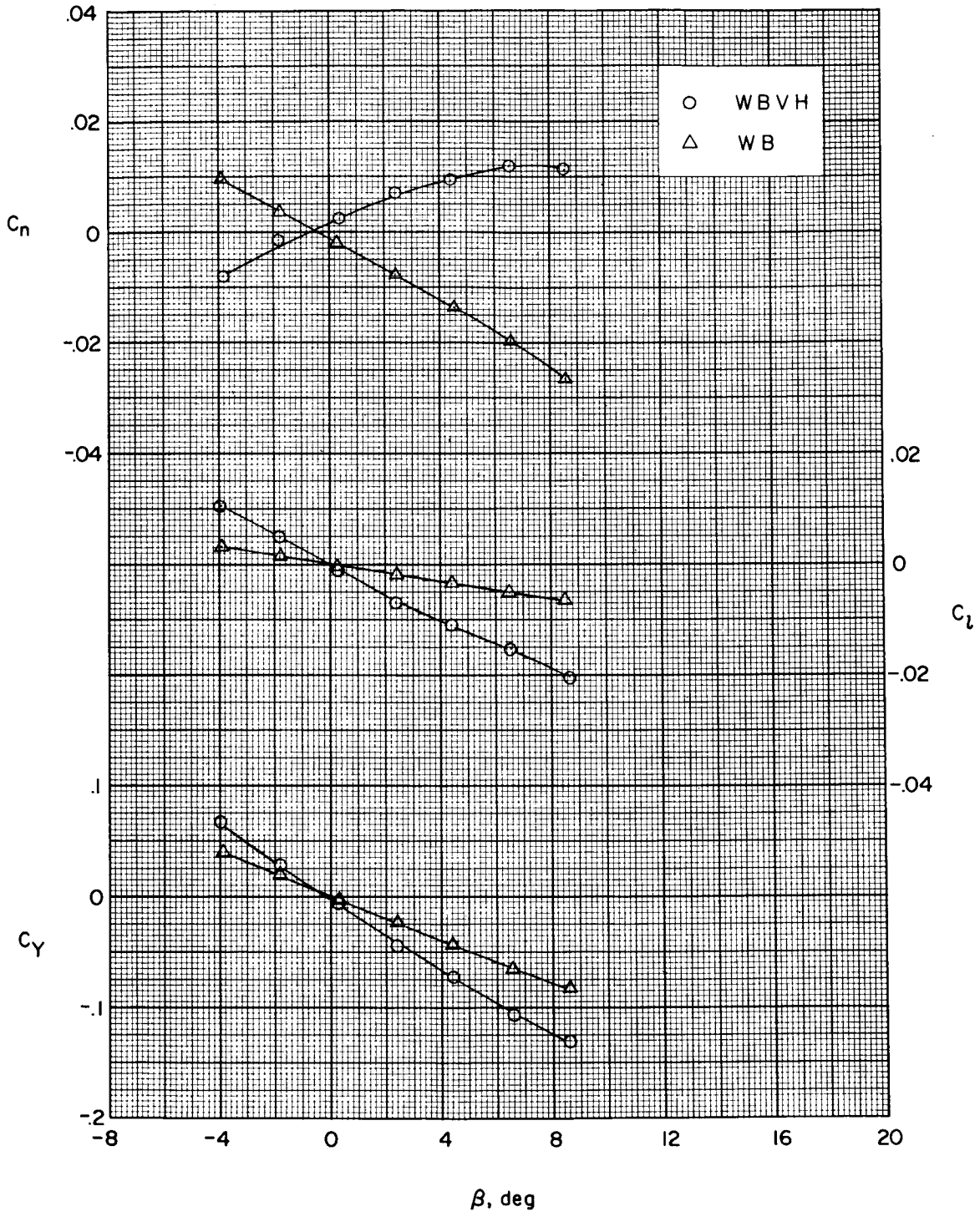

(c) $\alpha \approx 11.0^{\circ}$.

Figure 12.- Concluded.

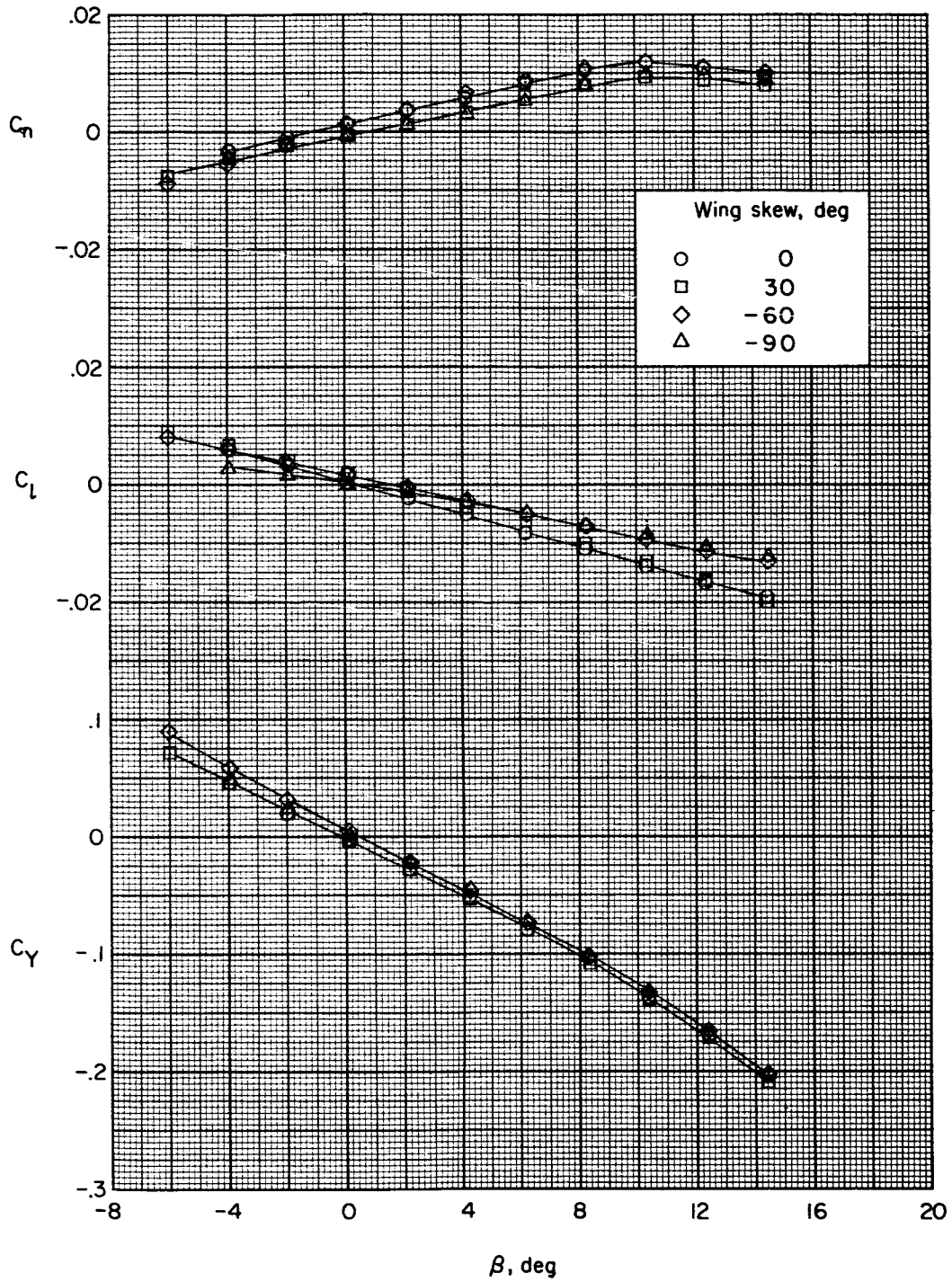

(a) $\alpha = -0.4^{\circ}$.

Figure 13.- Effect of variation of wing skew angle on the lateral aerodynamic characteristics of the complete configuration. $\delta_h = 0^{\circ}$; M = 2.20.

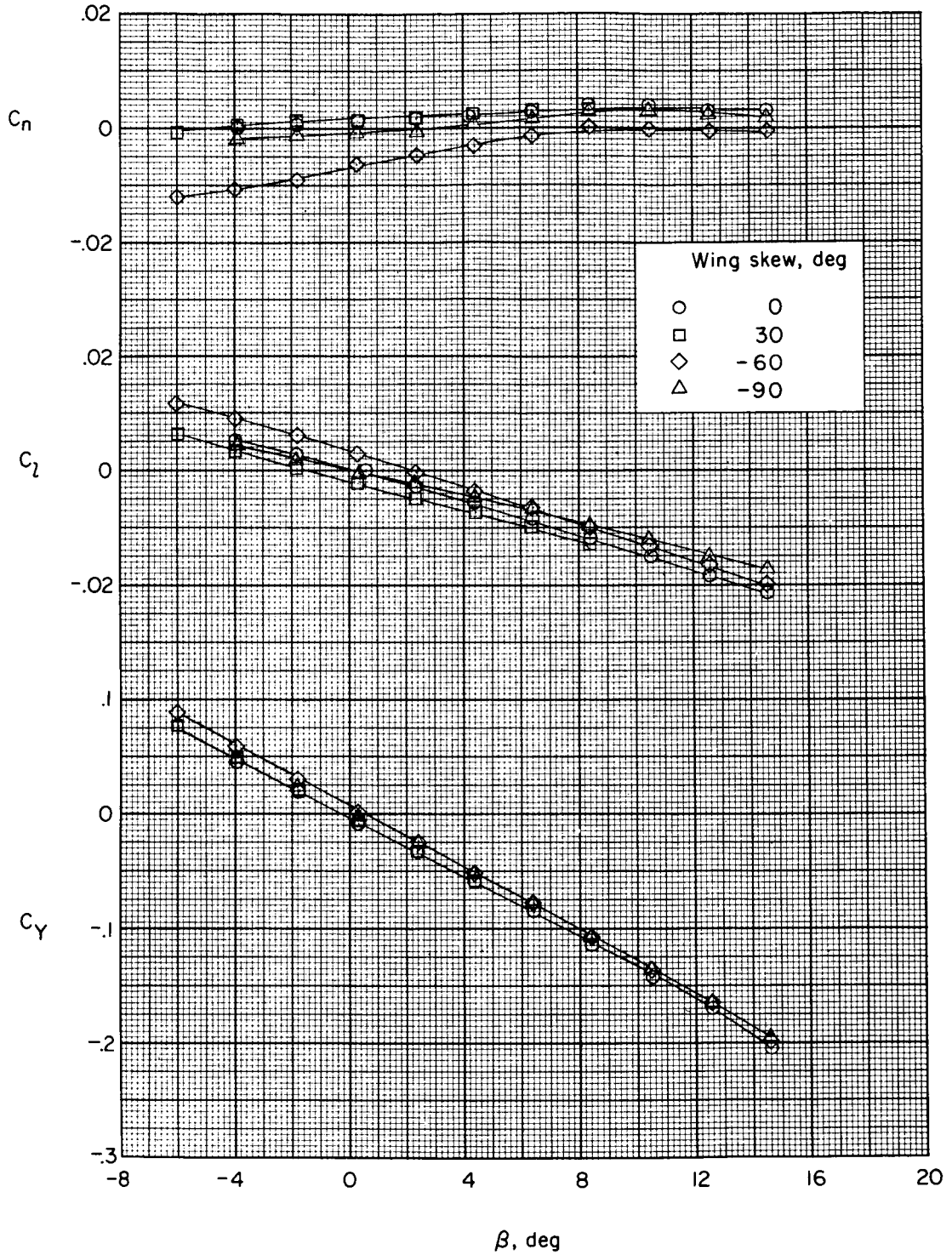

(b) $\alpha = 4.4^{\circ}$.

Figure 13.- Continued.

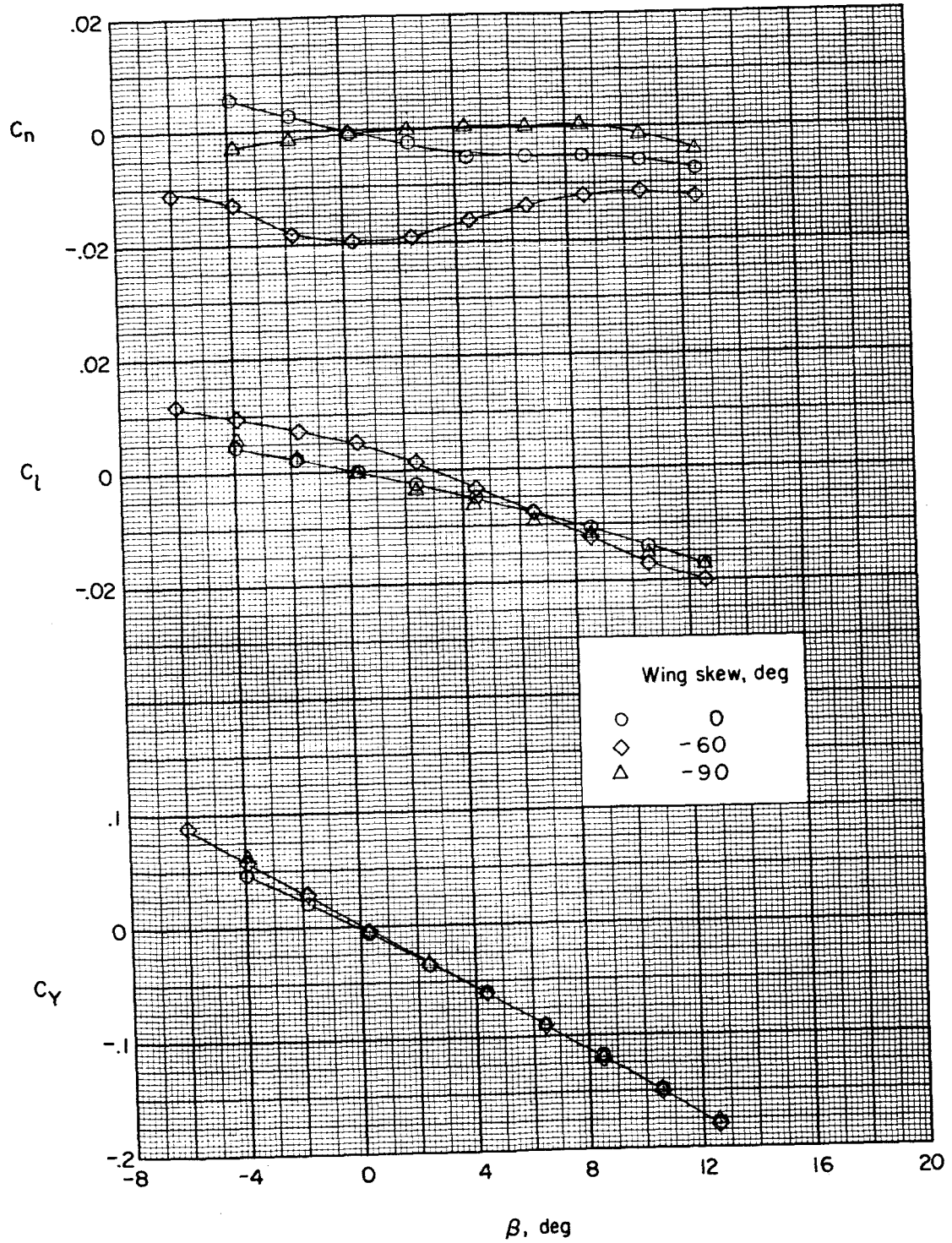

(c) $\alpha = 8.7°$.

Figure 13.- Continued.

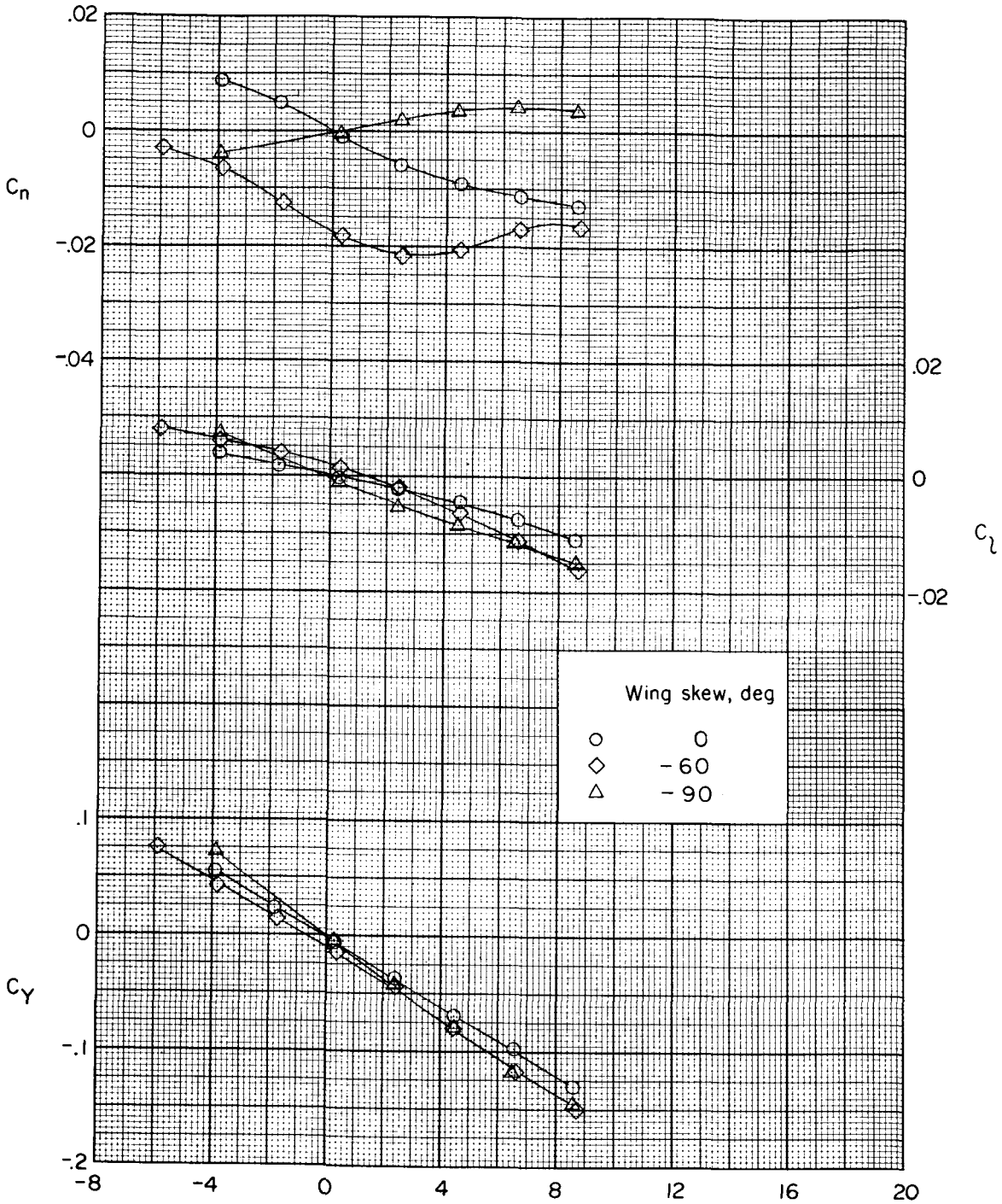

(d) $\alpha = 13.0^{\circ}$.

Figure 13.- Concluded.

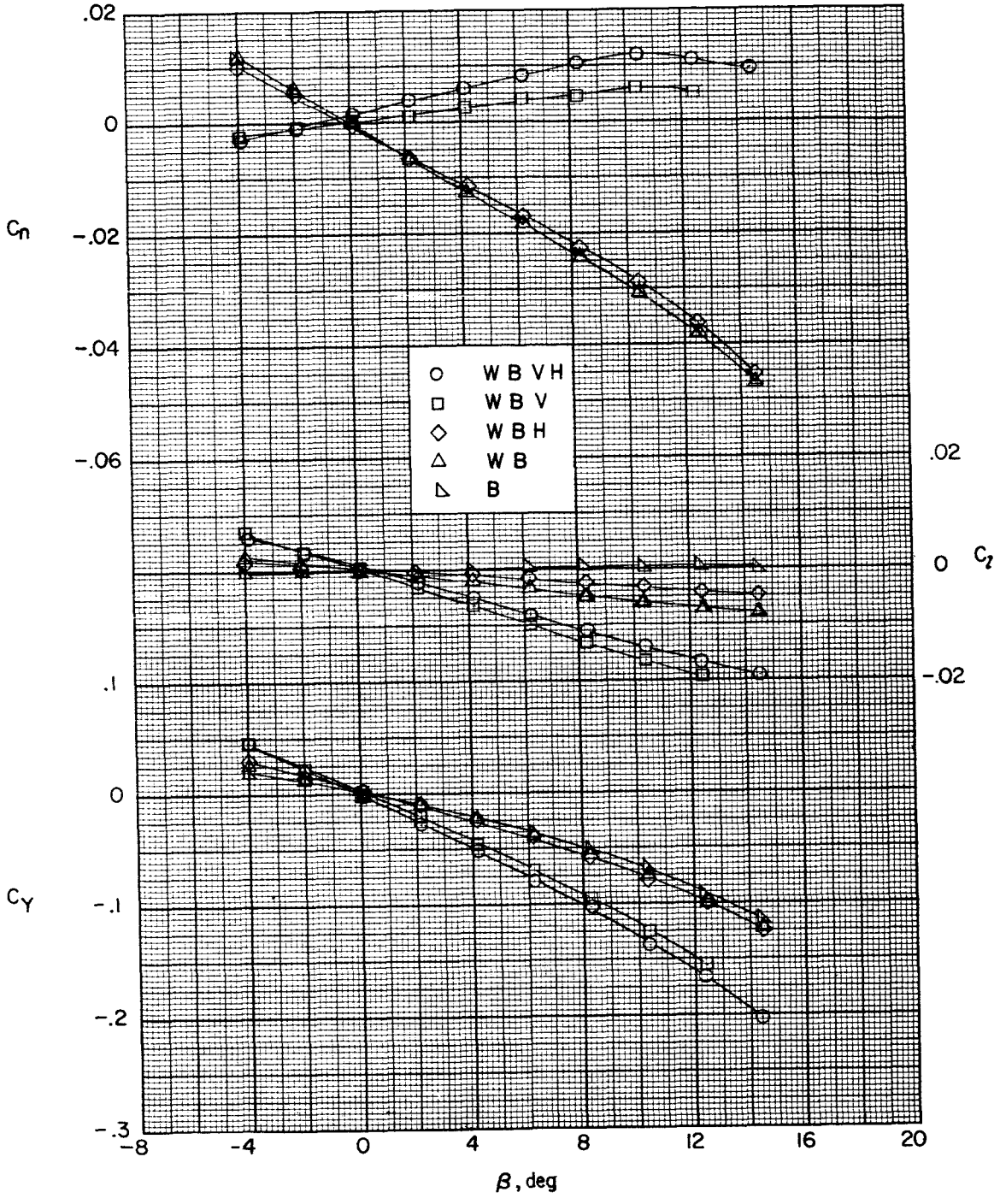

(a) $\alpha = -0.4^{\circ}$.

Figure 14.- Effect of various components on the lateral aerodynamic characteristics of the model in sideslip. Wing skew angle = 0°; M = 2.20.

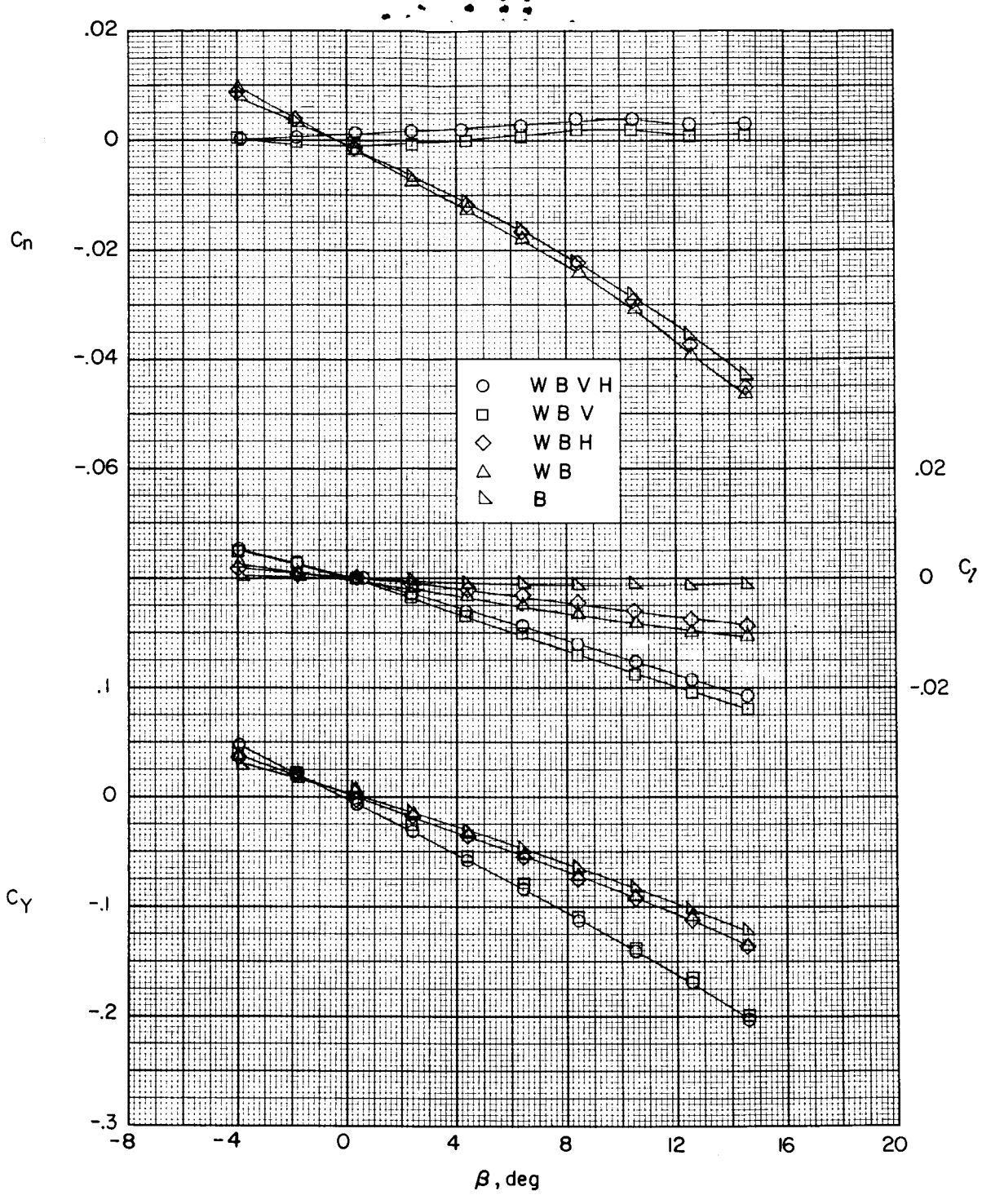

(b) $\alpha = 4.1^\circ$.

Figure 14.- Continued.

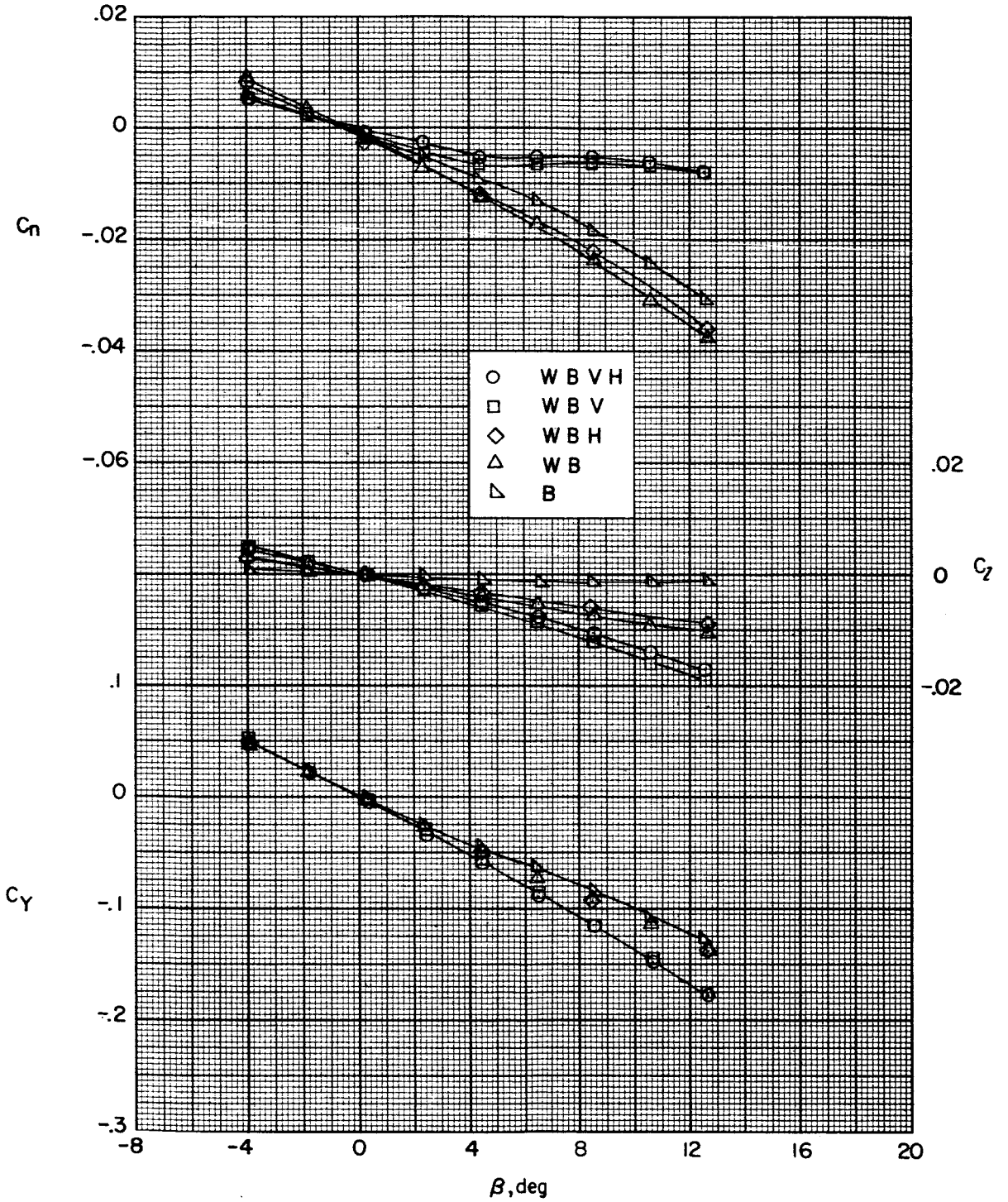

(c) $\alpha = 8.8^{\circ}$.

Figure 14.- Continued.

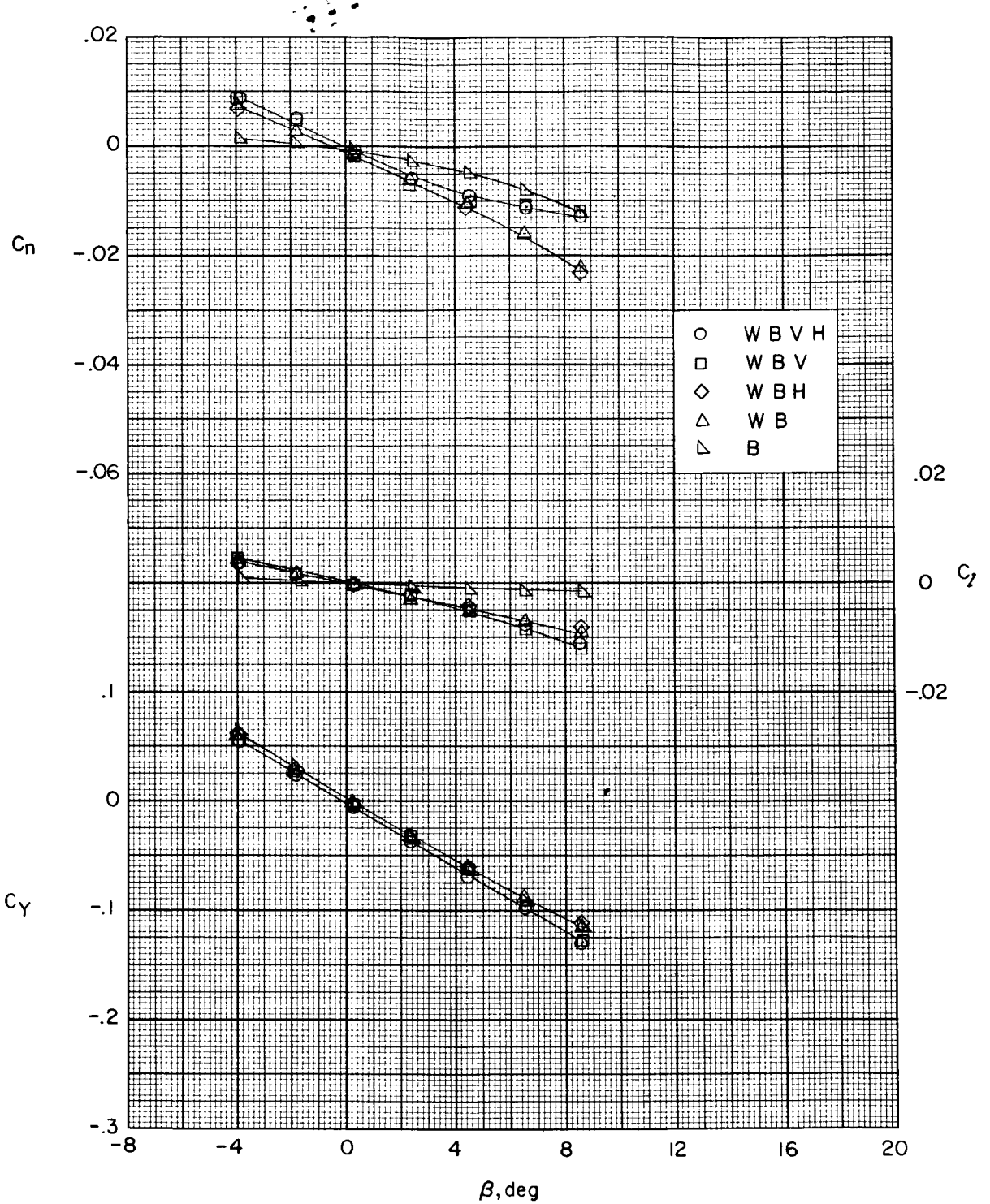

(d) $\alpha = 13.3^{\circ}$.

Figure 14.- Concluded.

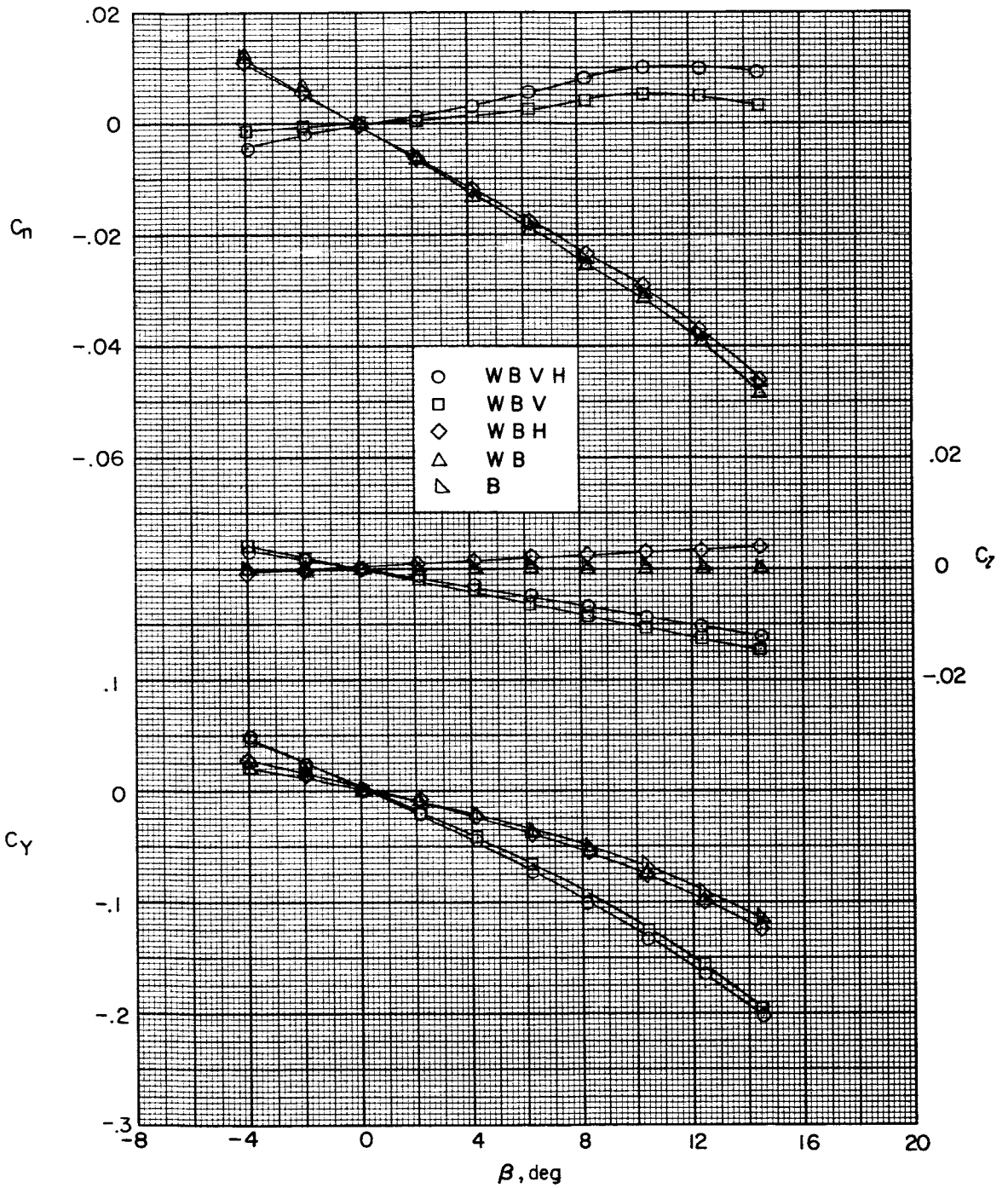

(a) $\alpha = -0.3^{\circ}$.

Figure 15.- Effect of various components on the lateral aerodynamic characteristics of the model in sideslip. Wing skew angle = -90°; M = 2.20.

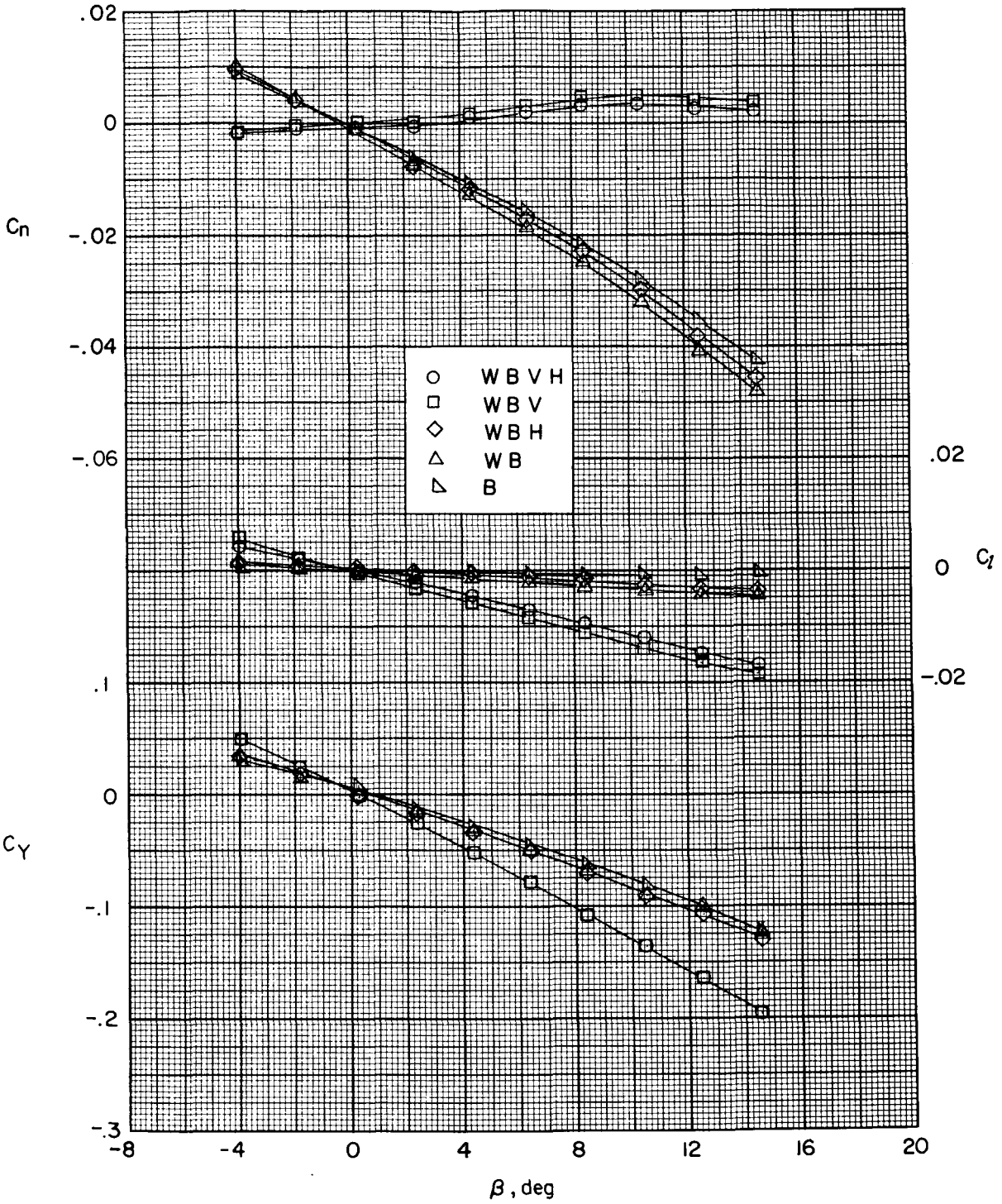

(b) $\alpha = 4.3^{\circ}$.

Figure 15.- Continued.

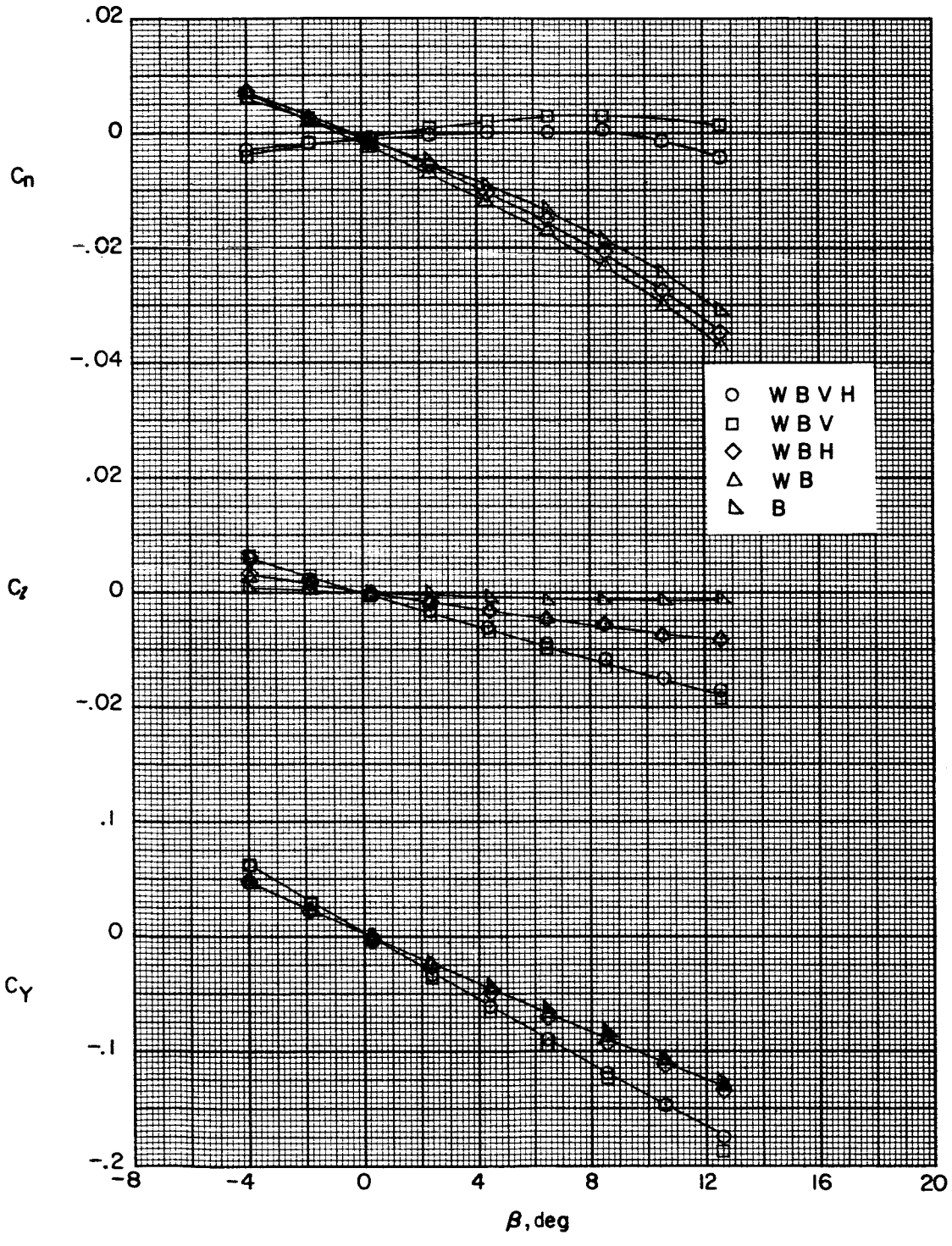

(c) $\alpha = 8.5°$.

Figure 15.- Continued.

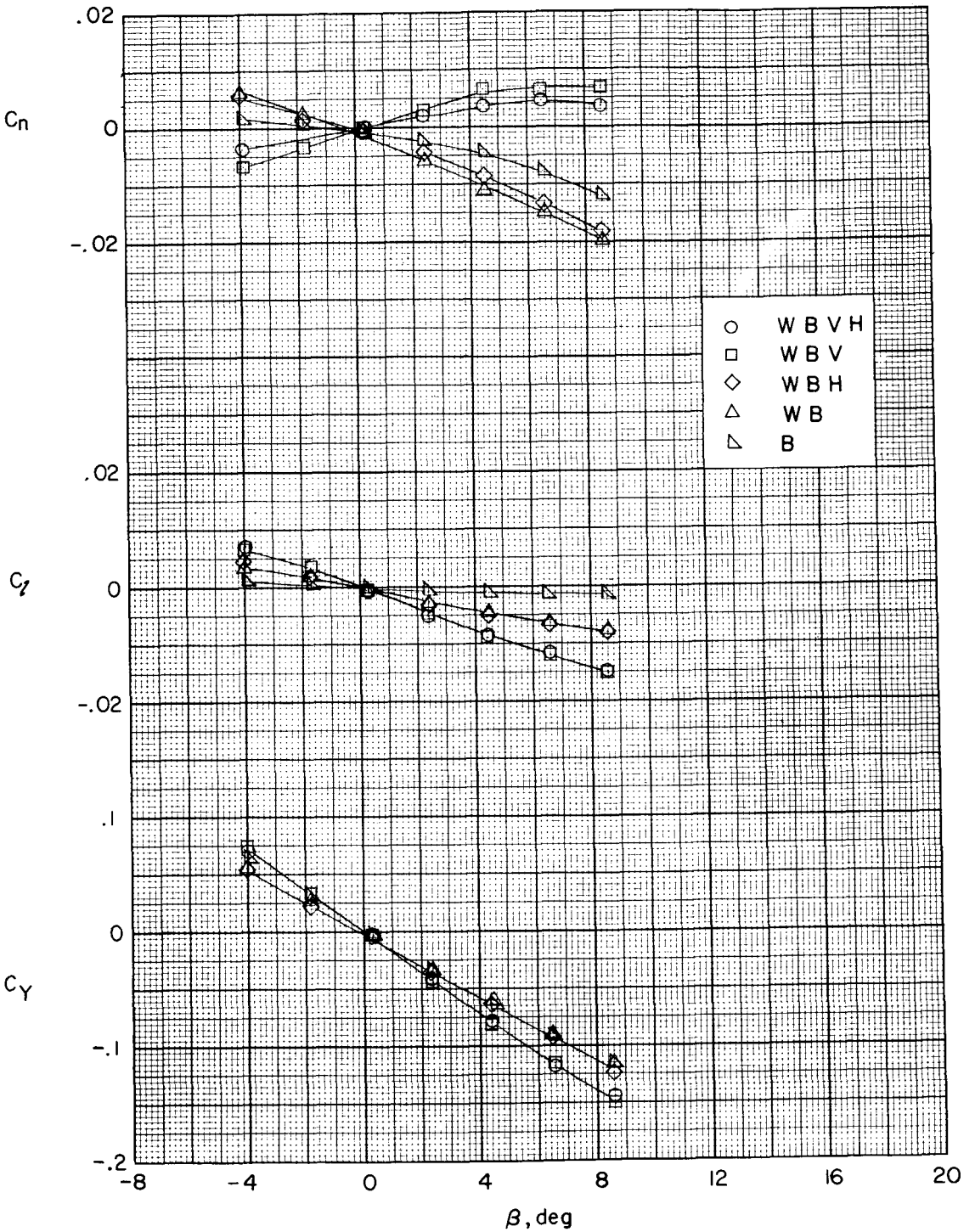

(d) $\alpha = 12.8^{\circ}$.

Figure 15.- Concluded.

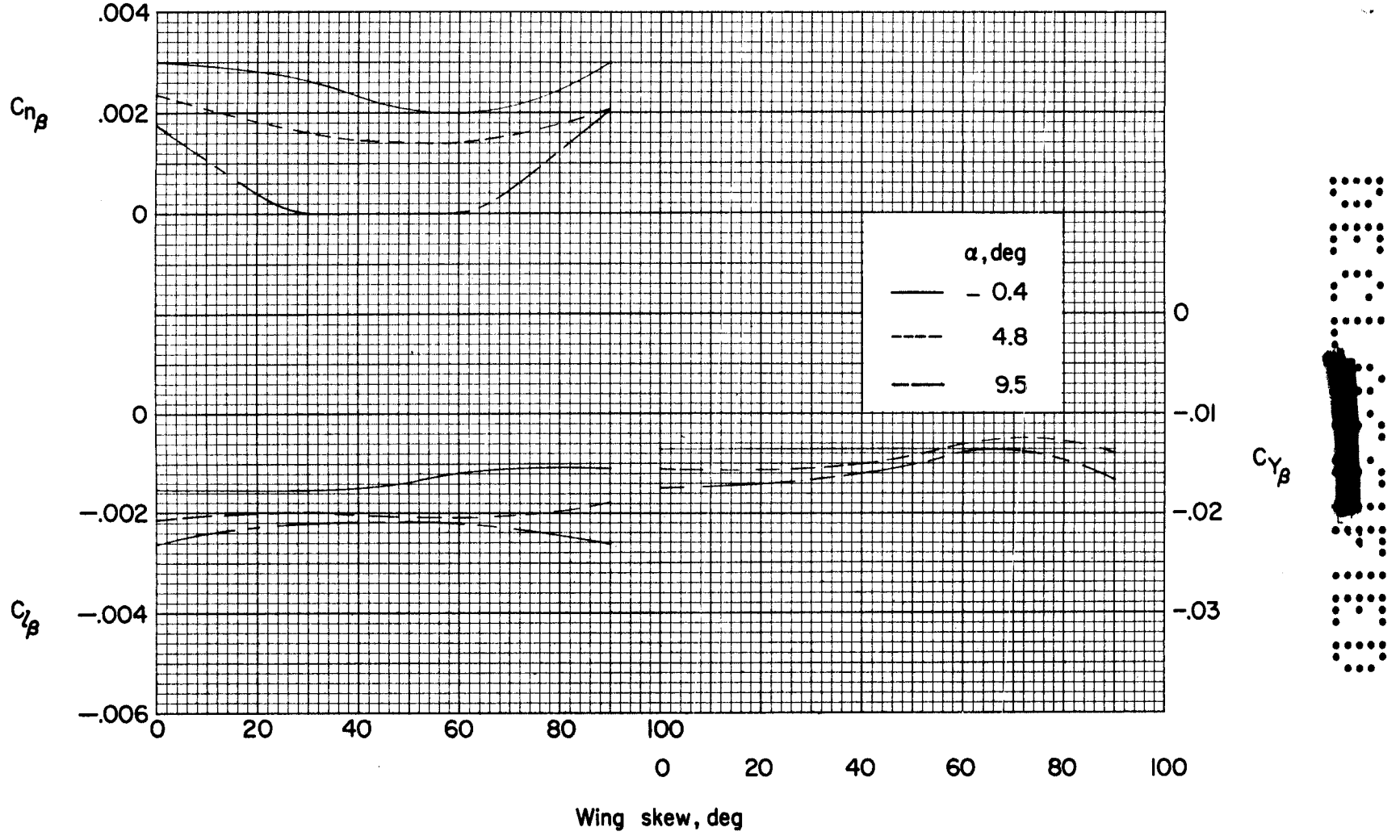

(a) M = 1.41.

Figure 16.- Variation of directional and lateral stability derivatives for various angles of attack with wing skew angle.

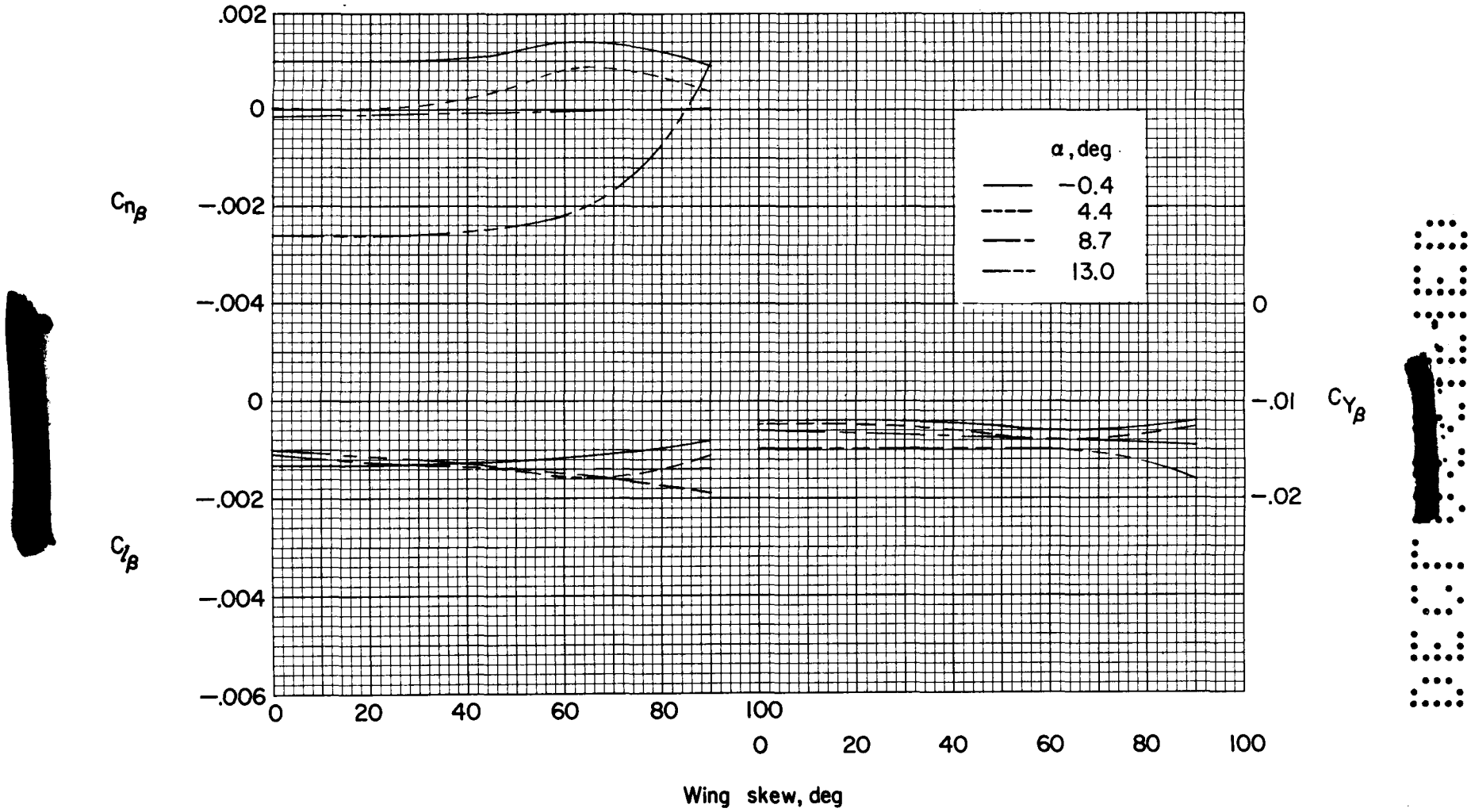

(b) M = 2.20.

Figure 16.- Concluded.

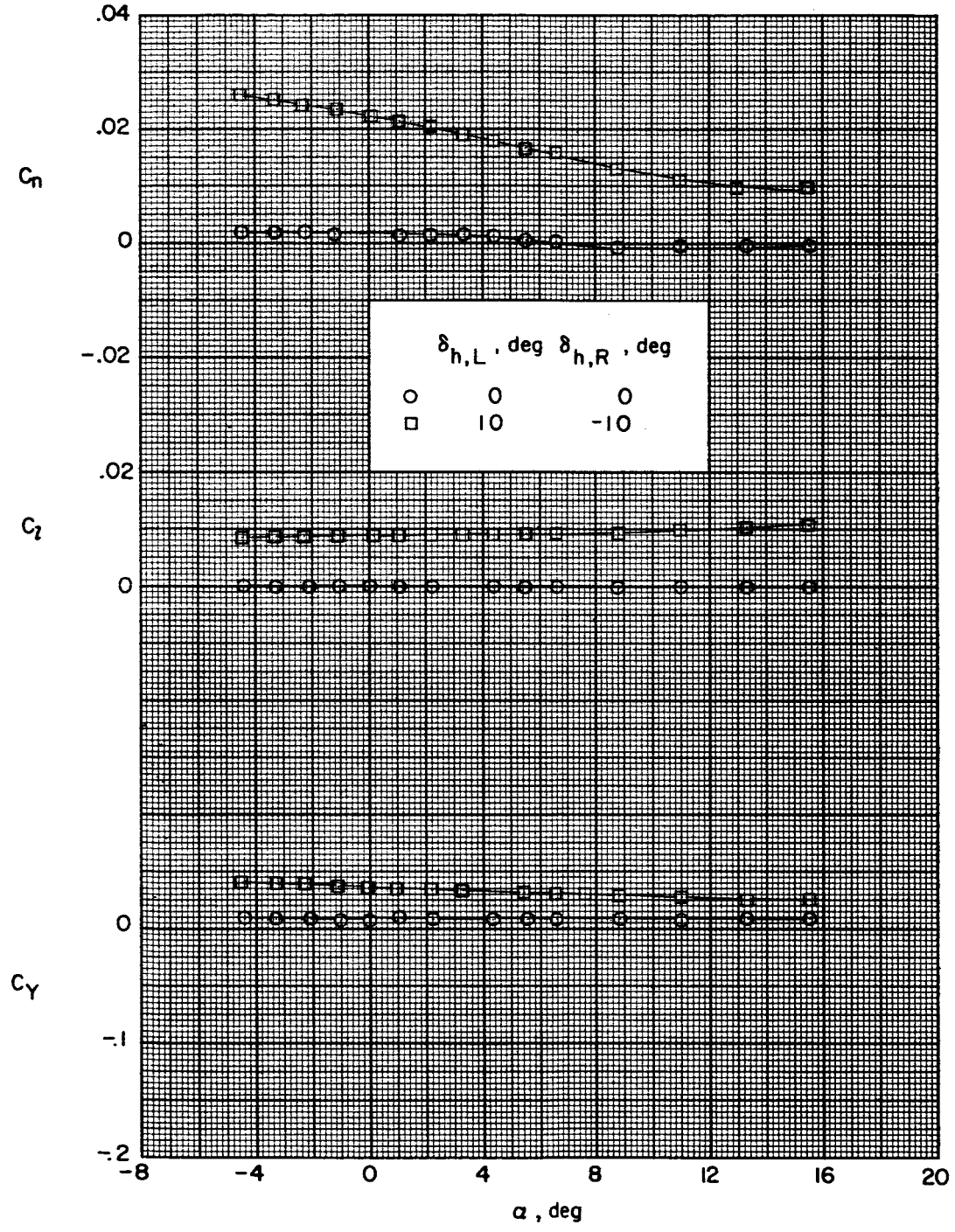

(a) $\Lambda = 0^{\circ}$.

Figure 17.- Effect of differential deflection of the horizontal tail on the lateral aerodynamic characteristics of the complete model. $\beta = 0.3^{\circ}$; $M = 2.20$.

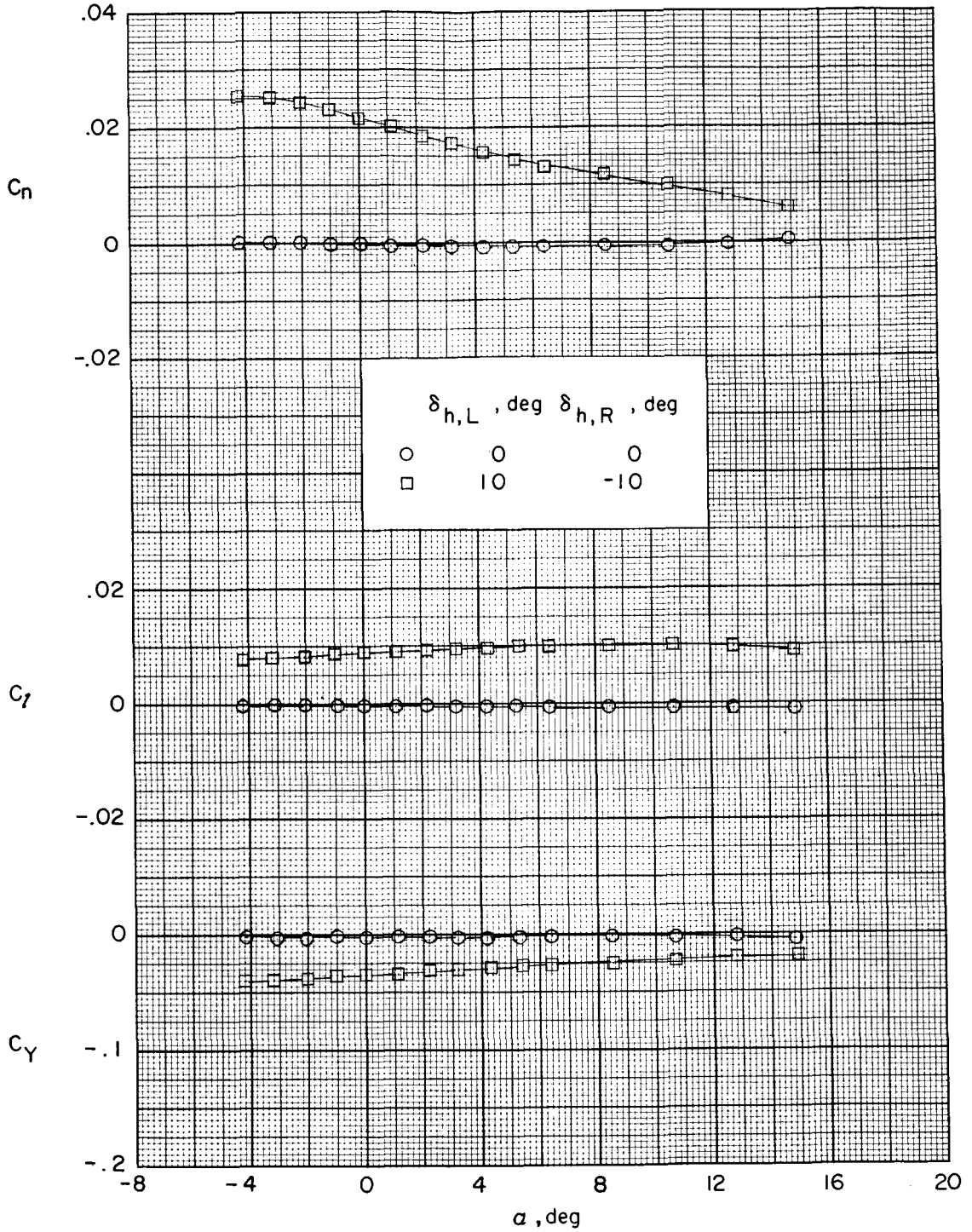

(b) $\Lambda = -90^{\circ}$.

Figure 17.- Concluded.